Multiscale study of the host control on its symbiotic microalgae

Andrea Valeria Catacora Grundy

THÈSE

Pour obtenir le grade de

DOCTEUR DE L'UNIVERSITÉ GRENOBLE ALPES

École doctorale : CSV- Chimie et Sciences du Vivant
Spécialité : Biologie Végétale
Unité de recherche : LPCV - Laboratoire de Physiologie Cellulaire Végétale

Etude multi-échelle du contrôle de l'hôte sur ses algues symbiotiques

Multiscale study of the host control on its symbiotic microalgae

Présentée par :

Andrea Valeria CATACORA GRUNDY

Direction de thèse :

Gilles CURIEN CHARGE DE RECHERCHE, CNRS	Directeur de thèse
Johan DECELLE Université Grenoble Alpes	Co-directrice de thèse

Rapporteurs :

Sonia CRUZ
ASSOCIATE PROFESSOR, Universidade de Aveiro
Christophe ROBAGLIA
PROFESSEUR DES UNIVERSITES, Aix-Marseille Université

Thèse soutenue publiquement le **6 mai 2024**, devant le jury composé de :

François LALLIER, PROFESSEUR DES UNIVERSITES, Sorbonne Université	Président
Sonia CRUZ, ASSOCIATE PROFESSOR, Universidade de Aveiro	Rapporteure
Christophe ROBAGLIA, PROFESSEUR DES UNIVERSITES, Aix-Marseille Université	Rapporteur
Rozenn LE HIR, CHARGEE DE RECHERCHE HDR, INRAE Ile-de-France-Versailles-Saclay	Examinatrice
Florence COURTOIS, MAITRESSE DE CONFERENCES HDR, Université Grenoble Alpes	Examinatrice
Annika GUSE, FULL PROFESSOR, Ludwig-Maximilians-Universität München	Examinatrice

Invités :

Benjamin BAILLEUL
CHARGE DE RECHERCHE, CNRS Paris Centre

Table of Contents

Introduction

Symbiosis: an inherent piece of life

Symbiosis, a vital aspect of life and evolution, involves close and enduring relationships between two or more species spanning from mutualistic to parasitic interactions. This phenomenon has significantly influenced biodiversity and adaptation across different environments. A notable instance of symbiosis is photosymbiosis, where a photosynthetic organism is in association with a host organism. In evolution, photosymbiosis led to the integration of a photosynthetic machinery into eukaryotic hosts. In freshwater and marine ecosystems, photosymbiosis is taxonomically and functionally very diverse. Well-known examples include associations between green algae and host ciliates in freshwater ecosystems, and dinoflagellate algae and corals in coastal marine environments. Such relationships not only shape ecological dynamics but also impact the health and resilience of aquatic ecosystems. While photosymbiosis is significant for diversity and evolution of life, there are still unresolved questions regarding the cellular and physiological mechanisms taking place in these associations.

I.1 Symbiosis

Life emerged on earth not only by combat but also by networking (Margulis and Sagan 2008). Symbiosis comes from the Greek '*together*' and '*living*' and its introduction in biology is attributed to the German Anton De Bary (1831-1888) who defined symbiosis as "*the living together of unlike organisms*" (Sanders 2001). Symbiosis could be defined as a durable association across generations with at least two different species. Despite its crucial role in the emergence of eukaryotic cells 1.8 Ga years ago, symbiosis was long considered an exception to nature's law during the 19th century (Sapp 2004). The evolutionary role of symbiosis was first formulated by the Russian biologist Mereschkowsky in 1910, but it was not recognized until 1970, when Lynn Margulis confirmed and popularized the concept of "*endosymbiosis*" as central in the evolution of life. In her book "*Origin of Eukaryotic Cells*", she postulated that eukaryotes evolved and acquired new organelles from endosymbiotic bacteria (Margulis 1996, 1998). Thereafter, symbiosis was recognized as an essential biological phenomenon for the origin of plastids and mitochondria within eukaryotic cells (López-García, Eme, and Moreira 2017). During evolution, different symbiosis events led to plastid acquisition in different eukaryotic lineages. Primary endosymbiosis involves the engulfment of a photosynthetic prokaryote (cyanobacterium) by a eukaryotic host with a mitochondrion. This event was the origin of all plastids and resulted in the red, green, and glaucophyte algae lineages (Matsuzaki et al. 2004; Moreira, Le Guyader, and Philippe 2000; Puerta 2004; Stibitz, Keeling, and Bhattacharya 2000). Secondary endosymbiosis (internalization of a eukaryotic alga with its primary plastid), led to "complex" plastids with three/four membranes (Fig. 1). This secondary endosymbiosis gave rise to modern phytoplankton taxa (diatom, haptophytes) that dominate the oceans. Dinoflagellates lost their secondary plastid but some species reacquired another plastid through tertiary endosymbiosis by engulfing an alga containing a secondary plastid (Bhattacharya, Yoon, and Hackett 2004) (Fig. 1).

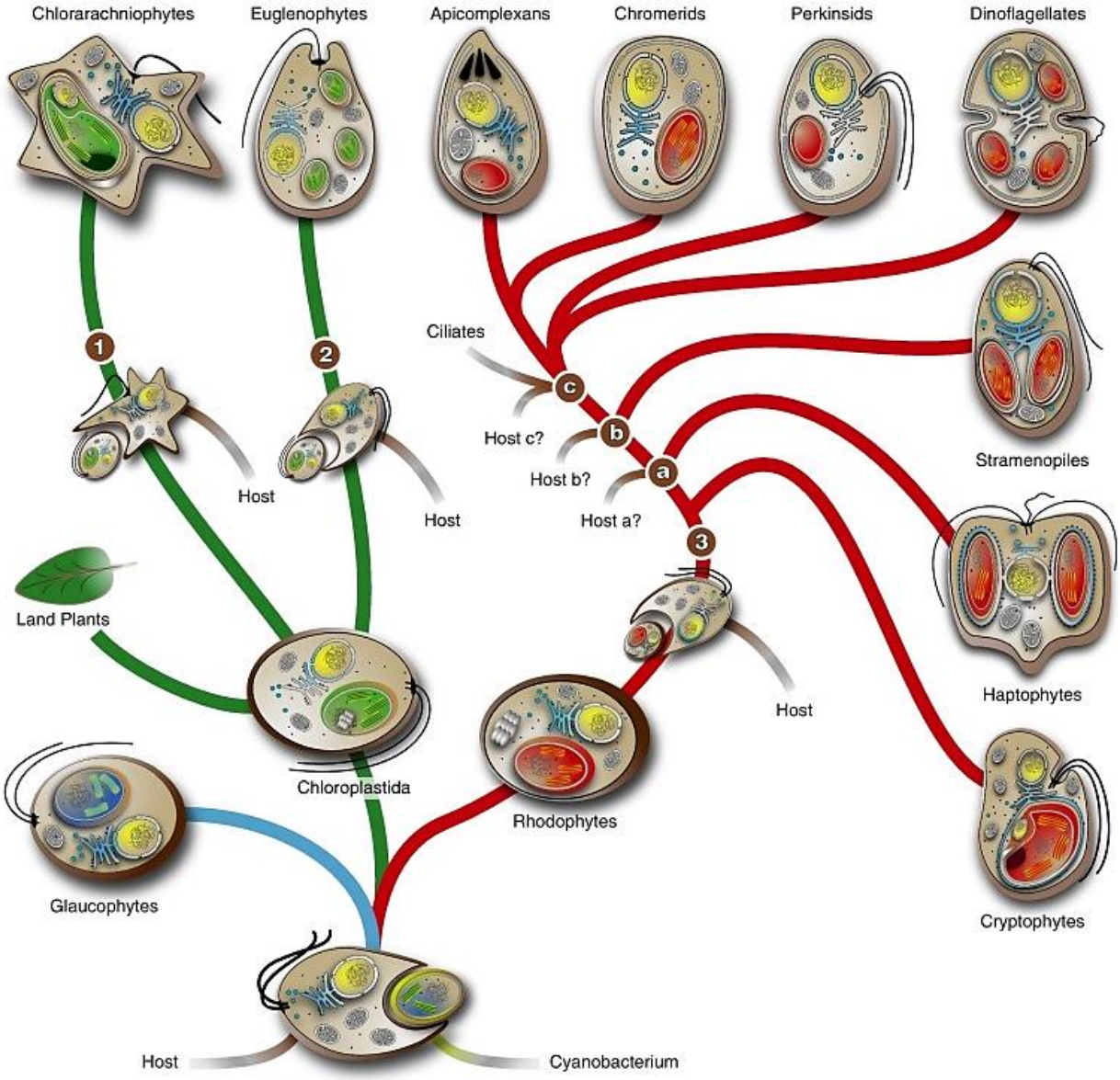

Figure 1. Plastid evolution. The introduction of a cyanobacterium into a heterotrophic host initiates the divergence into three distinct lineages: Glaucophytes, Chloroplastida, and Rhodophytes. Following this, two subsequent secondary endosymbiotic events occur involving algae from the Chloroplastida lineage and two heterotrophic hosts of unidentified origin, resulting in the emergence of Chlorarachniophytes (symbiosis 1) and Euglenophytes (symbiosis 2). The evolutionary trajectory of secondary red plastids is not entirely elucidated, yet the initial phase appears to be monophyletic (symbiosis 3). Although evidence suggests that the initial secondary plastid originates from a monophyletic source, uncertainty persists regarding the number of subsequent hosts involved (potentially additional symbioses a–c). In certain lineages, red complex plastids may originate from tertiary endosymbiotic events (Zimorski et al. 2014).

Symbioses are facultative or obligate (e.g. one or both partners are unable to live or complete their life cycle without the other) and symbionts can be physically integrated inside (endosymbiosis) or outside

the host (ectosymbiosis) (Grube, Seckbach, and Muggia 2017). The impact of symbiosis can be assessed based on the fitness (indicator of reproductive success) of the partners involved (e.g. mutualism= fitness increase for both partners, commensalism= no fitness change; parasitism= fitness decrease in one partner) (López-García et al. 2017). Yet, measuring the fitness in microbial symbioses is a difficult task, so the nature of many symbioses remains unknown. Symbiotic interactions are a source of new metabolic capacities, where the host and symbionts combine and integrate their metabolic functions (e.g. photosynthesis, nitrogen fixation and recycling, methanogenesis, and sulfide oxidation). Typically, symbionts benefit from a nutrient-rich microenvironment, and also protection from grazers or parasites (Dziallas et al. 2012). Symbiosis is also a major source of genetic innovation (endosymbiotic gene transfer) and can eventually lead to symbiogenesis and speciation (Margulis 1998). In today's ecosystems, symbiosis is integral to life, and there is a large diversity of symbiotic associations, encompassing various partners and different configurations (McKenna et al. 2021) (Fig. 2).

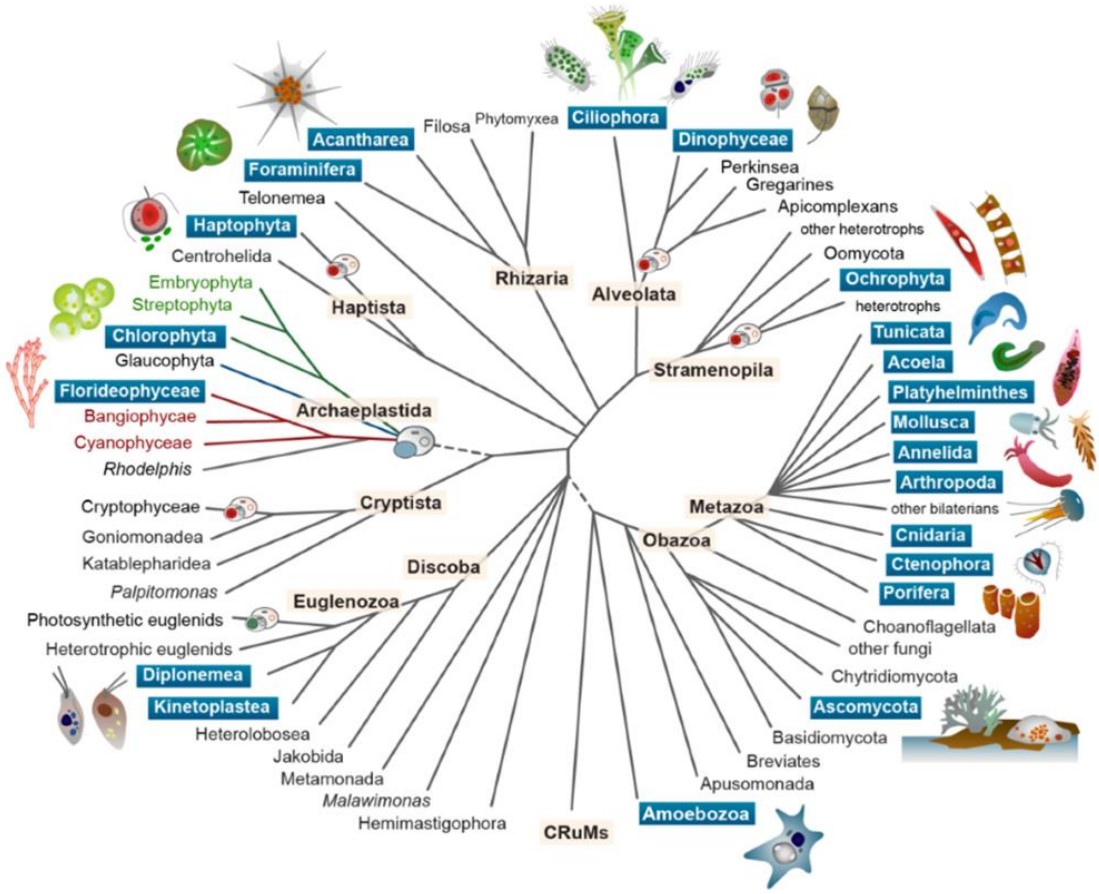

Figure 2. Diversity of eukaryotes and acquisition of chloroplasts in the evolution. On the branches of the tree, the small cartoons indicate the major event of plastid acquisition through endosymbiosis with a cyanobacterium (in the Archaeplastida; engulfed blue cell) and the several events of secondary and tertiary plastid acquisition in other lineages (engulfed red cell) (McKenna et al. 2021).

I.2 Photosymbiosis in aquatic ecosystems

Photosymbioses involving a multicellular or unicellular heterotrophic host and one or more photosynthetic partners are abundant and widespread in aquatic ecosystems (Davy, Allemand, and Weis 2012; Decelle, Colin, and Foster 2015). One of the first observations of photosymbiotic consortia in plankton dates back to the 1850s, credited to the English naturalist Thomas Henry Huxley, who documented the presence of yellow cells of unknown nature within colonies of Radiolaria (Decelle et al. 2015). Physiological experiments then demonstrated that these yellow cells are not parasites but beneficial algae (Brandt 1881; Geddes 1878). Yet, naturalists tended to pay more attention to terrestrial photosymbioses such as lichens, resulting in a comparatively limited understanding of aquatic photosymbiosis (Rohde 2005). In aquatic ecosystems, photosymbioses play different functional and ecological roles and involve a wide taxonomic diversity of microbial partners (Grube et al. 2017). Photosymbiotic associations are often found in oligotrophic waters (where nutrients are poorly available), but such associations can also be found in more productive waters. Photosynthetic partners can supply organic carbon (e.g. sugars, lipids) produced by photosynthesis as cellular energy to support energetic needs of the host (Adams et al. 2020). In return, the host can provide diverse organic and inorganic compounds (e.g. amino acids and carbohydrates) and/or a physical shelter against predators and pathogens (Davy et al. 2012; Quevarec et al. 2023).

Many photosymbioses in marine ecosystems involve the dinoflagellates *Symbiodiniaceae* as photosynthetic symbionts (commonly referred to as zooxanthellae) (Nitschke et al. 2022), while in freshwater ecosystems, most symbiotic microalgae correspond to the class Trebouxiophyceae. Cyanobacteria are also known photosynthetic symbionts in both marine and freshwater ecosystems (Table 1).

The most emblematic photosymbioses in benthic coastal ecosystems are between members of the phylum Cnidaria (e.g. hard and soft corals, sea anemones, jellyfish, and hydrocorals) and the

Table 1. Diversity of Symbiotic organisms in marine ecosystems modified and extracted from (Grube et al. 2017).

Marine ecosystems	
Host	**Symbiotic microalgae**
Rhizaria: Acantharia - Foraminifera - Radiolaria	Dinophyta: *Symbiodiniceae*, *Scrippsiella sp.* Haptophyta: *Phaeocystis*
Alveolata: Ciliata	Cyanobacteria. Dinophyta: *Symbiodiniceae*
Alveolata: Dinoflagellates	Cyanobacteria, eukaryotic algae
Porifera	Cyanobacteria: *Synechococcus sp.*
Cnidaria	Dinophyta: *Symbiodiniaceae* Rarely Trebouxiophyceae
Acoelomorpha: *Symsagittifera sp.*	Prasinophyceae: *Tetraselmis*
Acoelomoprha: *Convoluta sp.*	Bacillariophyceae: *Licmophora*
Annelida: Echiuroidea	Cyanobacteria
Mollusca: Bivalvia	Dinophyta: *Symbiodiniaceae*
Urochordata: Ascidia	Cyanobacteria: *Prochloron*

Symbiodiniceae (Davy et al. 2012). Dinoflagellate symbionts support the host coral metabolism, growth, and reproduction in reef waters (Wang and Douglas 1997). Furthermore, these dinoflagellates also have a high impact on the recycling of essential nutrients in the ecosystem. The loss of dinoflagellate symbionts and/or their photosynthetic pigments from corals (bleaching event) due to abiotic or biotic stress can ultimately result in the death of the coral and the destruction of the reef (Hughes, Kerry, et al. 2017). In the host, dinoflagellates typically reside within the cells of the cnidarian's gastrodermis (i.e. the innermost tissue layer that borders the gastrovascular cavity) (Davy et al. 2012; Hoegh-Guldberg 1999). The sea anemone *Aiptasia* became a model to study cnidarian-*Symbiodiniaceae* interactions (*sensu Exaiptasia pallida*) (Grajales and Rodríguez 2014; Wolfowicz et al. 2016). One of the advantages

of this model is the access to clonal lines, enabling the study of processes in the absence of biological variation, as well as the possibility of having symbiont-free anemones in culture and re-establishing symbiosis.

In the oceanic single-celled plankton, photosymbiosis is also ubiquitous in surface waters, especially within protistan hosts like Foraminifera and Radiolaria (eukaryotic supergroup Rhizaria). These host organisms can harbor diverse symbiotic microalgae, including dinoflagellates (*Brandtodinium*), haptophytes (*Phaeocystis*), and prasinophytes (Decelle et al. 2012; Gast and Caron 2001; Shaked and De Vargas 2006). Planktonic photosymbioses are ecologically important because they contribute to planktonic biomass, carbon fixation (through photosynthesis of the algal symbionts), carbon export to the deep ocean, and biogeochemical cycles of different elements (Biard et al. 2016; Brierley 2017; Decelle et al. 2019).

I.3 Photosymbiosis in freshwater ecosystems

First identified by the Dutch microbiologist Martinus Willem Beijerinck in 1890 (Krienitz, Huss, and Bock 2015), photosymbiotic relationships in freshwater ecosystems predominantly involve green algae, previously referred to as *Zoochorella*. Now classified as the class Trebouxiophyceae, they constitute a polyphyletic group encompassing diverse examples of symbiotic associations with various hosts (Pröschold et al. 2011). For example, endosymbiotic microalgae can belong to independent lineages of the Trebouxiophyceae (Choricystis-, Elliptochloris-, Auxeno*Chlorella*- and *Chlorella*-clades) (Pröschold et al. 2011) (Table 2).

Table 2. Diversity of Symbiotic organisms in freshwater ecosystems modified and extracted from (Grube et al. 2017).

Freshwater ecosystems	
Host	**Symbiont**
Rhizaria: testate amoeba	Trebouxiophyceae: *Chlorella spp.*
Alveolata: Ciliata: *Paramecium bursaria, Stentor spp. Oophyra*	Trebouxiophyceae : *Chlorella*-clade *Chlorella spp., Micractinium conductrix*

Amoebozoa: testate and non-testate amoebae	Trebouxiophyceae: *Chlorella spp.*
Porifera: *Spongilla*	Trebouxiophyceae: *Chlorella spp.*
Cnidaria: Hydrozoa	Chlorophyceae, Trebouxiophyceae: *Chlorella*-clade, *Chlorella variabilis, Nannochloris sp., Chlorella vulgaris*
Acoelomoprha: *Dalvella*	Trebouxiophyceae: *Chlorella spp.*
Mollusca: Bivalvia	Trebouxiophyceae: *Chlorella spp.*
Chordata: Amphibia	Trebouxiophyceae

Chlorella-clade includes four species: *C. vulgaris* in symbiosis with the ciliates *Climatostomum virens, Coleps, Euplotes daidaleos,* and *Paramecium bursaria. C. variabilis* and the new species *Micractinium conductrix* (Pröschold et al. 2011) can be endosymbionts of *P. bursaria* depending on their geographic distribution. The endosymbiotic lifestyle in the green algae of Trebouxiophyceae likely emerged multiple times. The underlying factors that make microalgae from Trebouxiophyceae more susceptible to establishing symbiotic associations are not yet fully elucidated. Potential factors favoring symbiotic interactions could include co-occurrence in similar ecological niches, such as lakes and ponds. Additionally, such associations may serve as a strategy to mitigate viral infections, particularly relevant for *Chlorella* algae susceptible to *Chlorella* virus (Fujishima 2009). In freshwater ecosystems, a diverse array of symbiotic associations can be found including unicellular planktonic photosymbiosis like ciliates, Euplotes, heliozoan and certain invertebrates (Grube et al. 2017; Pröschold et al. 2011). The host *Hydra viridissima* became a freshwater symbiotic model that improved our understanding of photosymbiosis (Fig 3c). This small animal has been reported to be in symbiosis with green microalgae belonging to the class Trebouxiophyceae (order *Chlorella*les, genus *Chlorella*) and Chlorophyceae (order Sphaeropleales, genus Desmodesmus) (Rajević et al. 2015). This photosymbiosis is obligatory, as the host Hydra cannot live without its symbiotic microalgae. Inside the host, the symbionts are enclosed in the host endodermal epithelial cells within the symbiosome (Hamada et al. 2018). This association has been described as mainly driven by metabolic exchanges: the algae depend on nutrients from the

host, and in return, the host receives a significant amount of photosynthetically-fixed organic carbon from the algae (Hamada et al. 2018). Another instance of multicellular photosymbiosis in freshwater ecosystems involves the sponge *Spongilla lacustris* with Trebouxiophyceae (Fig. 3b). In this symbiotic system, microalgae that are exposed to low-light are digested by the sponge. Consequently, a single symbiotic sponge can exhibit both green and white areas, depending on variations in light availability over space and time (Skelton and Strand 2013). Among vertebrates, a unique photosymbiosis was reported involving an amphibian host: the spotted salamander *Ambystoma maculatum* and the green algae *Oophila amblystomatis*. This symbiosis encompasses both ectosymbiotic colonization of the egg capsule and intracellular infiltration of salamander tissues and cells (Burns, Kerney, and Duhamel 2020) (Fig 3a).

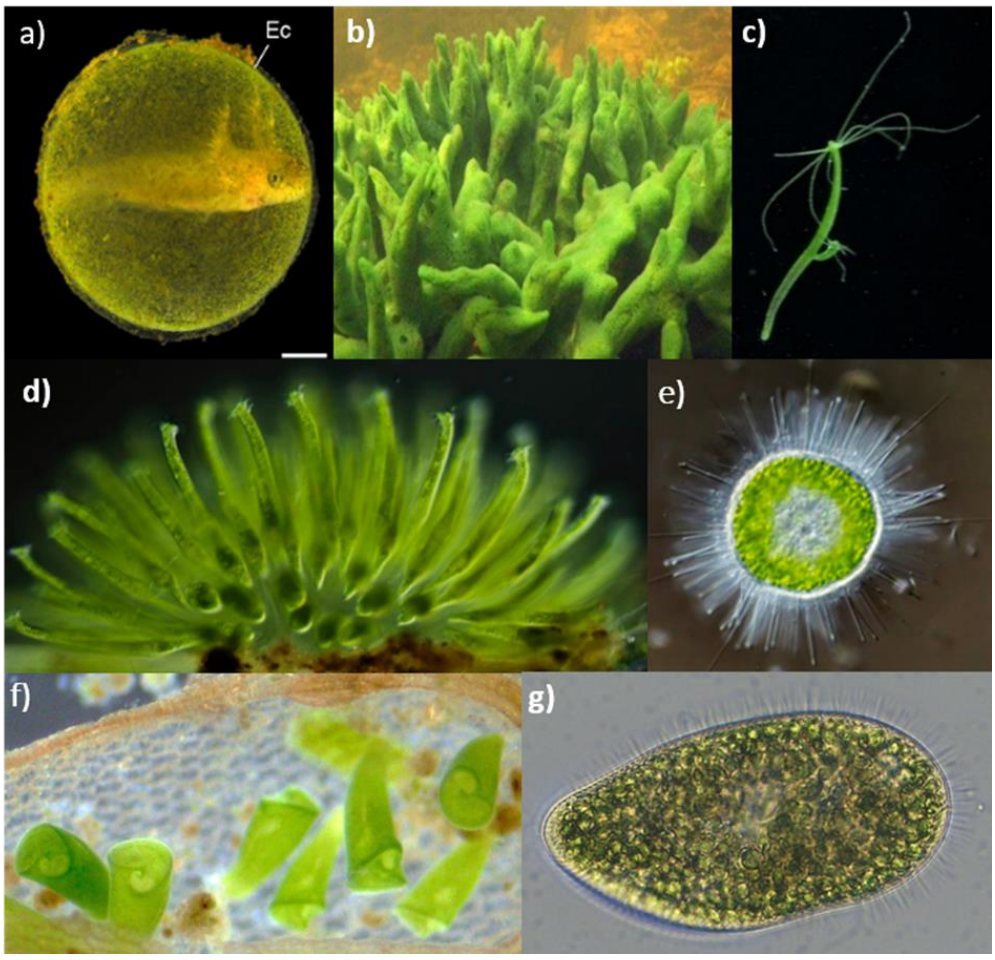

Figure 3. Examples of well-known freshwater hosts in symbiosis with green algae: **a)** Embryo of the spotted salamander (*Ambystoma maculatum*) and green algae *Oophila amblystomatis* (Kerney et al., 2011). **b)** Sponge Spongilla *lacustris.* Copy right: Kirillow O. **c)** Hydra *Hydra viridissima*. Copy right: Peter Schuchert **d)** Ciliate *Ophrydium versatile* colony. Copy right: Bewie 's Mikrowelt, **e)** Heliozoan *Acanthocystis turfacea*. Copy right: Bewie 's Mikrowelt **f)** Ciliate *Stentor pyriformis* (Hoshina et al. 2021)**, g)** Ciliate *Paramecium bursaria* (CCAP1660/18) Copy right: Photosymbiosis Team.

I.3.1 Ciliate hosts

Ciliates, found in various aquatic environments (e.g. coastal waters, hydrothermal vents, anoxic sediments, muddy zones, and both oxygenic and anoxic water columns) can host prokaryotic or eukaryotic symbionts (Dziallas et al. 2012) including microalgae (Fig. 4). For instance, it has been reported that 25% of aquatic ciliates contain internal "foreign" symbiotically-acquired chloroplasts via photosymbiosis with microalgae or kleptoplastidy (i.e. the process by which a host organism sequesters and retains algal chloroplasts) (Cruz and Cartaxana 2022). The main function of endosymbiotic microalgae or stolen chloroplasts is very likely photosynthesis and the production of energy-carrying carbohydrates (Foissner, Berger, and Schaumburg 1999; Nowack and Melkonian 2010).

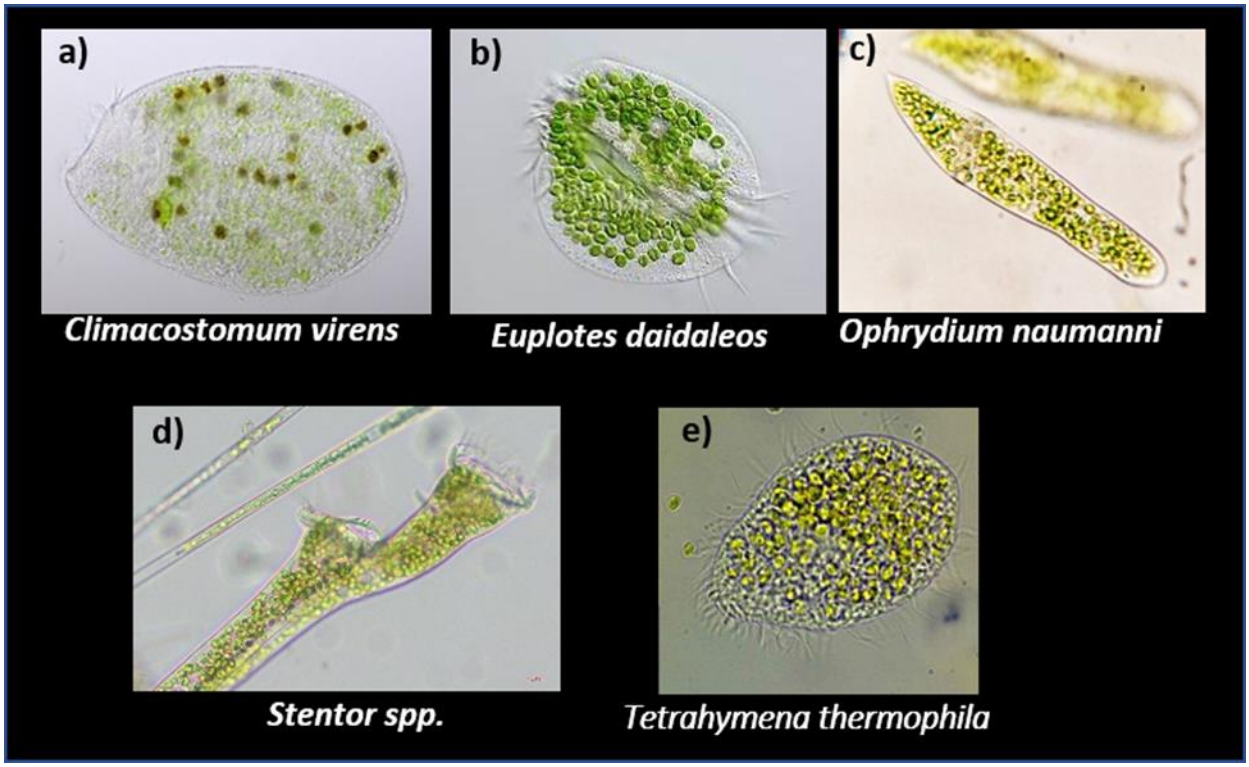

Figure 4. Ciliates in symbiosis with green microalgae of the class Trebouxiophyceae a) Ciliate *Climacostomum virens* and symbiotic *Chlorella* in its cytoplasm (Karajan et al. 2007) **b)** Another ciliate from freshwater *Euplotes daidaleos* **c)** *Ophrydium naumanni,* in symbiosis with *Chlorella* observed in an oligotrophic South Andean lake in Argentina (Queimalinos 1999) **d)** Endosymbiotic *Chlorella* are known to be present also in other freshwater protozoa, such as *Stentor spp.,* and **e)** *Tetrahymena thermophila* (Kodama and Fujishima 2005).

I.4 Photosymbiosis in the ciliate *Paramecium bursaria*

The *Paramecium-Chlorella* symbiosis has been a model to study unicellular photosymbiosis for many years. This model is particularly advantageous due to its ease of culture and presence in ecosystems. It provides valuable insights into mutualistic and endosymbiotic relationships, uncovering the evolution of ciliates (Kodama et al., 2014; Sheng et al., 2020). The host *Paramecium bursaria,* known as the "Green ciliate" lives in symbiotic association with green algae from the Trebouxiophyceae class (Pröschold et al. 2011). Initially classified in the subgenus *Chloroparamecium* (Ehrenberg, 1833), it was later referred to as *Paramecium bursaria* Focke (1836). "Bursaria" comes from the Latin word "*bursa*," which means "purse" or "pouch", given the size of its contractile vacuoles. The green ciliates have an oblong/slipper shape of ~150 microns in length and harbor hundreds of symbiotic microalgae (*Chlorella sp* or *Micractinium sp*) within their cytoplasm (black arrows) (Fig. 5).

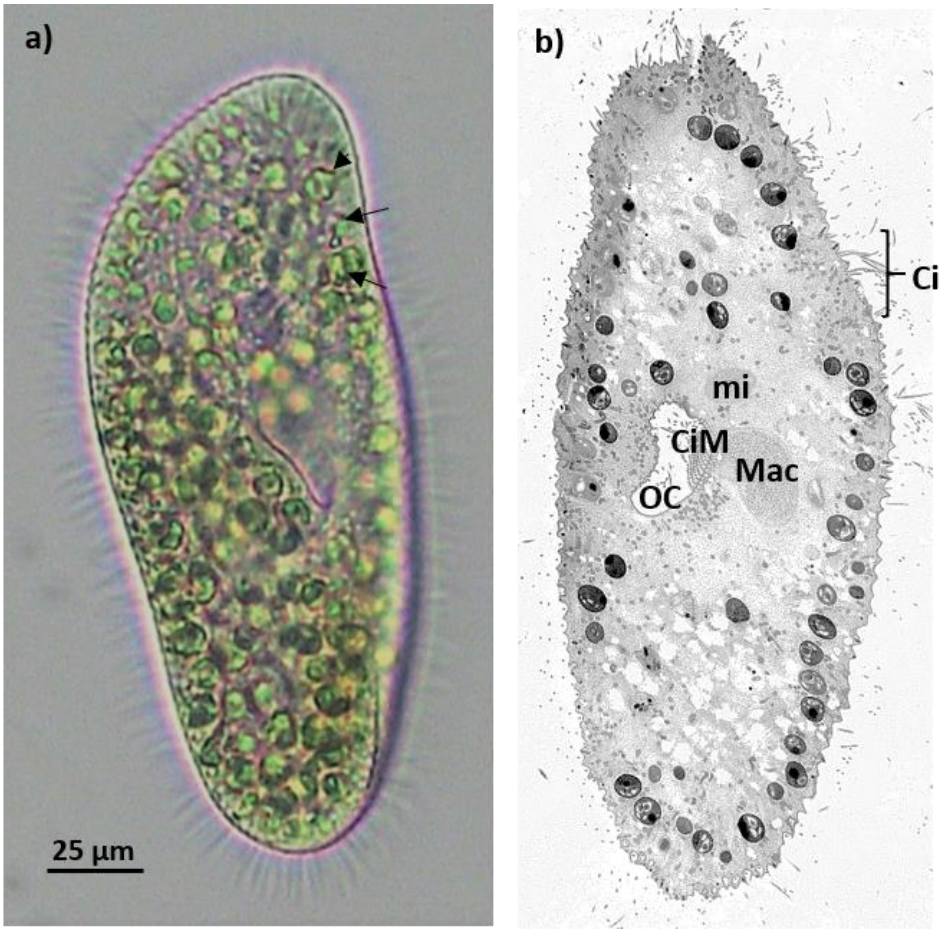

Figure 5. SEM micrography of *Parameium bursaria* a) The ciliate *Paramecium bursaria* (CCAP1660/18) with symbiotic microalgae unveiled by light microscopy. Symbiotic microalgae *Micractinium conductrix* (only three cells are indicated with black arrows). **b)** Transmission electron microscopy micrograph of *Paramecium bursaria,* showing major cellular components: cilia covering all the surface of the cell (Ci), a section of the micronucleus and macronucleus (mi; Mac), the oral cavity (OC) covered by cilia membranelles (CiM). SEM micrography: A. Catacora-Grundy, P.H. Jouneau.

At the surface of *Paramecium*, cilia (Ci) are involved in motility (Valentine and Van Houten 2022). The basal bodies of the cilia are located in the cell cortex (periphery of the *Paramecium* cell), where the symbiotic microalgae are also found. Another important structure in the ciliate *Paramecium* is the oral cavity (OC) positioned ventrally for predation. This cavity is fully covered by ciliary membranelles (CiM) and serves to capture prey and endosymbionts (Hausmann and Allen 2010). *Paramecium bursaria* contains one macronucleus (Mac) and one micronucleus (mi). The copy number of the macronucleus in the ciliate cells is generally several hundreds or thousands of times higher than the micronucleus (He et al. 2019**).** The Mac is responsible for gene expression and the micronucleus (mi) is

involved in the gene transmission through sexual processes (conjugation) (Rautian and Potekhin 2002). When conjugation does not take place, the ciliate undergoes binary division. For *P. bursaria*, five syngens (reproductively isolated mating types) have been described so far (He et al. 2019; Spanner et al. 2022).

During *P. bursaria's* cell cycle, the host and microalgae synchronously go through cell division: the number of algae doubles before or during the division of the host cells and the algal population in the two daughter cells is maintained at a constant level (Kadono et al. 2004; Kodama and Fujishima 2012). In this case, endosymbionts are inherited by vertical transmission (inheritance of the photosynthetic partner, directly into the daughter cells) but horizontal transmission might also take place in the natural environment (a phenomenon that remains to be described) (Takahashi 2017).

In the natural environment, the aposymbiotic form of the ciliate *P. bursaria* and the non-symbiotic *C. variabilis* have never been reported (Hoshina and Imamura 2008; Ogura et al. 2022). **Under laboratory conditions, both host and symbiotic microalgae can be separated and cultured independently.** The alga-less form of the ciliate can be obtained by the use of herbicides (e.g. paraquat). The symbiotic microalgae can be mechanically removed from the host and be cultivated in nutrient-enriched media, and then grown in its free-living form (Kodama and Fujishima 2012, 2016; Tanaka et al. 2002). **The flexibility behind this association makes this system a promising experimental model for understanding essential phenomena and mechanisms in photosymbiosis.**

I.4.1 Diversity, specificity, and geographic distribution of *Paramecium-Chlorella* symbiosis

Symbiotic algae isolated from different *Paramecium bursaria* are generally represented by *Chlorella*-like species belonging to two genetically distinct "European" and "American" populations (Hoshina and Imamura 2008). In the "European" population, phylogenetic analyses confirmed the occurrence of two algal groups: *Micractinium conductrix* and *Chlorella vulgaris* (Pröschold et al. 2011). The "American" population is mainly represented by the species *Chlorella variabilis* and has been found in *Paramecium bursaria* strains from the USA. An evolutionary scenario for *P. bursaria* presented by (Hoshina and Imamura 2008) concerning algal acquisition and subsequent switching suggests the coexistence of both species belonging to the "American" and "European" endosymbiont groups in one cell of ancestral *P. bursaria*. Recently, a new geographic distribution of *P. bursaria* and its symbiotic microalgae was revisited (Table 3). The five distinct genetic varieties (syngen) have specific geographic distributions (Spanner et al. 2022). With this new phylogenetic analysis, the relationship between symbiotic species and geographic distribution described previously is under revision.

Syngen Paramecium bursaria	Geographic distribution	Symbiotic microalgae
R1	Europe	*C. variabilis, M. conductrix*
R2	Europe	*C. variabilis, M. conductrix*
R3	Europe, Asia, North America, South America and Australia	*C. variabilis*
R4	Europe, North America and South America	*C. vulgaris, C. variabilis, M. conductrix*
R5	Europe	*C. variabilis, M. conductrix*

Table 3. List of the geographic distribution of *Paramecium bursaria* based on syngen type and the identified symbiotic microalgae. Extracted from (Spanner et al. 2022).

I.4.2 Establishment of the photosymbiosis

To establish photosymbiosis, *P. bursaria* cell phagocytes "*Chlorella*" cells by the oral cavity (Karakashian 1975). Through an unidentified mechanism referred as "membrane-membrane reaction", some of the engulfed microalgae resist to phagocytosis and digestion (Dolan 1992). A single symbiotic *Chlorella* is then enclosed into a symbiosome (Perialgal Vacuole - PV) derived from the host Digestive Vacuole (DV), where it is protected from digestion (Fujishima 2009; Gu et al. 2002; Takeda et al. 1998). The timing and differentiation through the host's digestive vacuoles, acidosomal and lysosomal fusions have been extensively described in (Kodama and Fujishima 2005, 2007, 2008) (Fig. 6). The authors observed that some microalgae acquire temporal resistance to lysosomal enzymes after phagocytosis in the DVs. To establish endosymbiosis, *Chlorella* microalgae must be localized beneath the host cell cortex after budding from the host DV (Kodama and Fujishima 2007) (Fig.6)

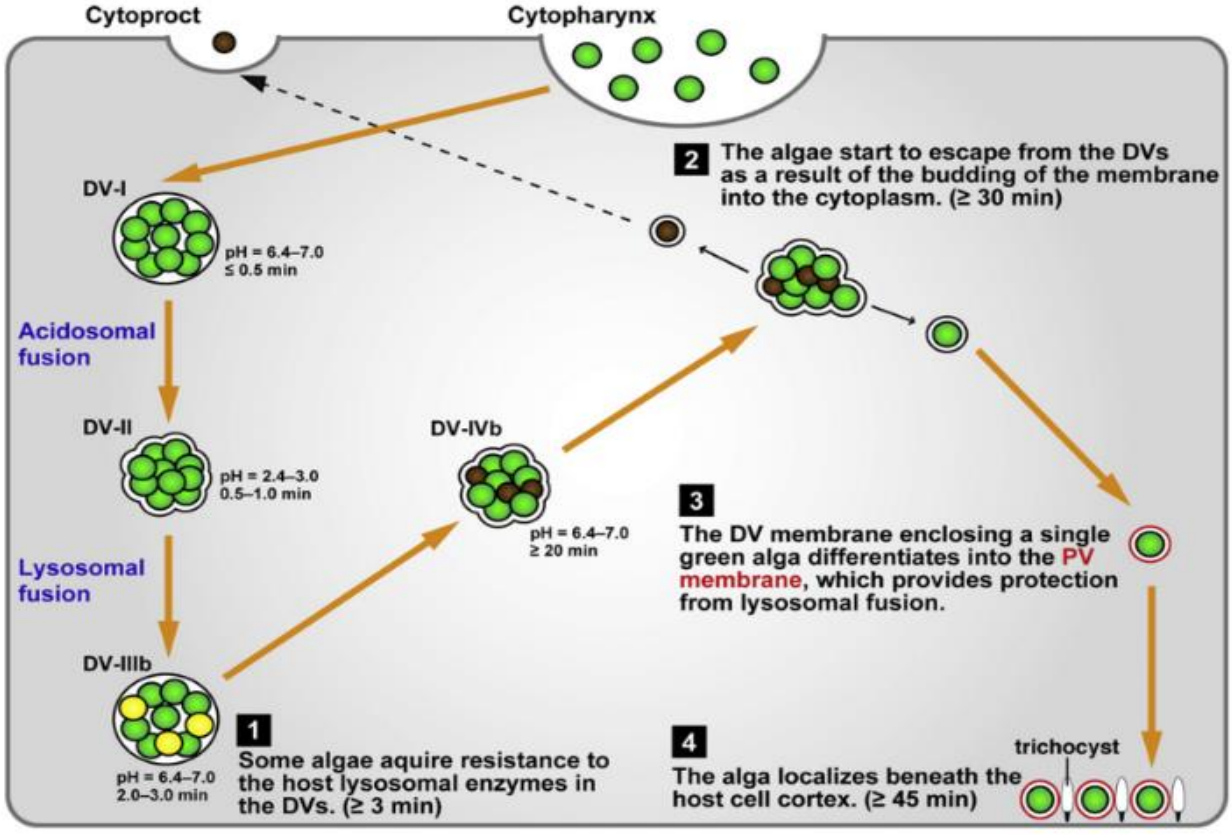

Figure 6. Schematic representation of the endosymbiosis establishment between the microalgae *Chlorella* spp. and their host *Paramecium bursaria*. DV: digestive vacuole, PV: perialgal vacuole. From: (Fujishima 2009).

The membrane-limited surrounding symbionts of host-origin was first described as "symbiosome" by Roth et al. (1988). The term was used to define a "membrane-bound compartment containing one or more symbionts and certain metabolic components and located in the cytoplasm of eukaryotic cells" (Mohd Noor, Day, and Smith 2015). In *Paramecium-Chlorella* association, the symbiosome corresponds to the perialgal vacuole membrane (PV) surrounding a single algal cell (Gu et al. 2002). The symbiosome is hardly observable under light microscope (Fujishima 2009; Reisser and Wiessner 1984). By electron microscopy, it has been reported that 25-180 nm is the average distance between symbiont microalga cell wall and the host-symbiosome suggesting a breach small enough to allow direct molecular interactions of the host and symbiotic microalgae (Song, Murata, and Suzaki 2017). In the host cell, symbiotic microalgae are surrounded by extrusive host-organelles named trichocysts (involved in cell defense against predators) and numerous mitochondria of the host (Fig. 7) (Song et al. 2017).

Symbiotic microalgae are maintained in the host symbiosome. The lysosomal and acidic characteristic (low pH) of the symbiosome, due to its phagocytic origin, has been linked to play a role in the metabolic crosstalk of photosymbiotic partners in the marine photosymbiosis *Tridacna maxima* giant clam and corals *Acropora yongei* and *Stylophora pistillata* (Armstrong et al. 2018; Barott et al. 2015; Dorling, McAuley, and Hodge 1997a, 1997b). In the symbiosome of *Acropora yongei* and *Stylophora pistillata,* VHA (vacuolar-type H^+-ATPase enzyme) may also be involved in the acidification of the compartment and the enhancement of photosynthesis via carbon concentrating mechanism (CCM) as suggested by (Barott et al. 2015; Tresguerres 2016). VHA utilizes energy from ATP hydrolysis to transport H^+ across biological membranes, so creating local acidification. The speciation of inorganic carbon (Ci) into CO_2, is therefore more efficiently facilitated, to provide CO_2 over O_2 to the dinoflagellate ribulose-1,5-bisphosphate carboxylase/oxygenase (RuBisCo), the terminal enzyme for carbon fixation (Leggat et al. 2002). A chemical approach using monensin (a carboxylic ionophore, known to induce cell-wall acidification) showed *Paramecium bursaria* symbiosome increased in size, indicating that the symbiosome membrane could contain an active proton pump (SchluBler and Schnepf 1992).

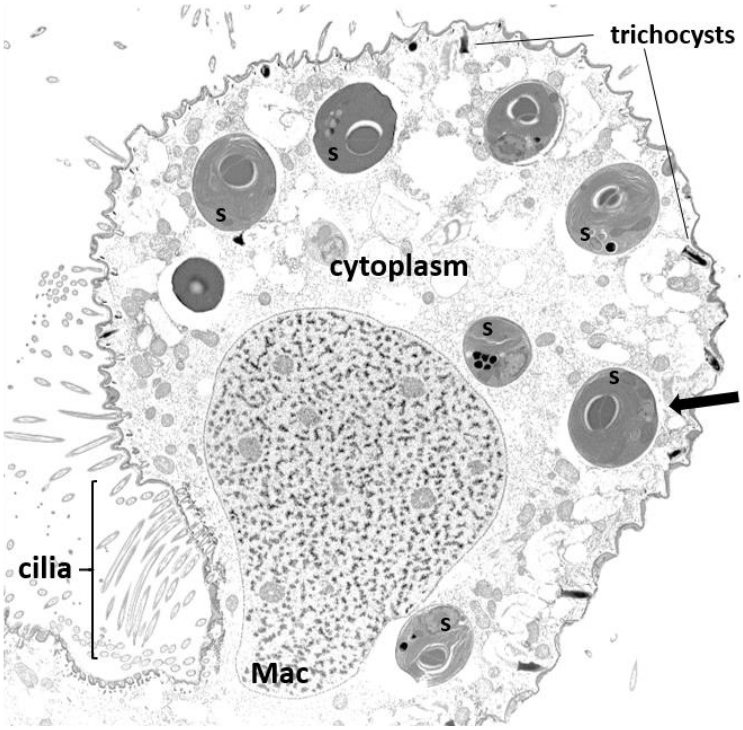

Figure 7. Ultrastructural organization of the host *Paramecium bursaria* and its microalgae *Micractinium conductrix*. SEM micrograph showing closer distribution of symbiotic microalgae in the host *P. bursaria*. The black arrow indicates the gap between the microalga cell membrane and the host symbiosome vacuole. S: symbiotic microalgae, Mac: macronucleus. Focused Ion Beam Scanning Electron Microscope (FIB-SEM) micrograph from A. Catacora-Grundy, PH Jouneau.

I.4.3 Physiology and metabolism of the symbiotic microalgae

Within photosymbiotic associations, the host likely exerts an influence on the overall physiology and metabolism of its microalgae. For instance, it has been noted that in *Paramecium bursaria*, the growth of symbiotic microalgae is closely linked to the growth of their host (Kadono et al. 2004). In addition, it has been reported that the host are thought to regulate symbionts by limiting metabolite exchange, non-photosynthesizing symbionts, and acquiring new symbionts from the environment, although the precise mechanisms are not fully understood (Lowe et al. 2016).

The German biologist Werner Reisser described some physiological parameters of symbiotic microalgae in *Paramecium bursaria*. Notably, he observed that the host may support the carbon dioxide requirements of the symbiotic microalgae in low-CO_2 environments favoring a high photosynthetic activity (Reisser 1980). However, when comparing photosynthetic efficiency to their free-living forms, symbiotic microalgae showed a reduced photosynthetic efficiency in terms of Fv/Fm (the intrinsic

efficiency of photosystem II [PSII]) in normal conditions. This observed decline in Fv/Fm is suggested to be linked with potential nutrient stress (i.e. host limited nutrient supply) (Lowe et al. 2016). Under environmental fluctuations (e.g. light intensity and temperature), symbiotic microalgae residing within the host exhibit different responses. Under high light, symbiotic microalgae are reported to better dissipate excess light energy as heat without compromising photosynthetic efficiency (Sørensen et al. 2020). Temperature variation impacts the photosynthetic efficiency (Fv/Fm) of *P. bursaria* symbionts, leading to a decreased Fv/Fm in cells not acclimated to low temperatures (Możdżeń et al. 2018). **Despite the research conducted since the 1980s on the symbiotic microalgae of *P. bursaria*, further investigation is needed to gain deeper insights into the physiological capabilities of these symbiotic microalgae, particularly compared to their free-living forms.**

In unicellular marine plankton, some morphological changes in symbiotic microalgae have been observed, including expansion of chloroplast volume and higher carbon fixation capability (Decelle et al. 2019, 2021a; Uwizeye et al. 2021). **Whether this phenomenon is shared across other photosymbioses from marine and freshwater ecosystems remains unknown.**

The photosynthetic abilities of symbiotic microalgae are closely tied to their carbon metabolism, with starch acting as the primary carbon reservoir (Ran et al. 2019). During the day, in green microalgae like *Chlorella*, organic carbon produced by photosynthesis is stored as starch in the chloroplast. At night, this stored starch is mainly used to support cellular processes and growth (Busi et al. 2014). Under stress conditions (i.e. nitrogen/phosphorus limitation) organic carbon is stored in neutral lipids (e.g. triacylglycerols (TAG), lipid droplets) in the cytoplasm (León-Saiki et al. 2017; Ran et al. 2019). So far, little attention has been paid to the dynamics of the allocation and turnover of photosynthates within the symbiotic microalgae (carbon homeostasis). In the symbiotic dinoflagellate of *Pocillopora damicornis*, ^{13}C-bicarbonate accumulation in subcellular compartments known as 'C reserves' (e.g. starch granules and lipid droplets) was systematically recorded (Kopp et al. 2015). 'C reserves' of symbiotic dinoflagellates follow a diurnal dynamic with the formation (during light) and utilization (under dark) of lipid droplets and starch compounds (Kopp et al. 2015). In photosymbiosis, the **influence of the host on carbon fixation and carbon metabolism of its microalgae remains unclear. To comprehensively understand the host effect, it is essential to investigate the dynamics of carbon metabolism in symbiotic algae in comparison to their free-living forms.**

I.4.4 Metabolic connectivity: from the microalga to the host

In the realm of photosymbiosis, photosynthates such as sugars (i.e. glucose, maltose, glycogen) are hypothesized as the primary metabolic currency exchanged from the symbiotic microalgae to the host. It has been shown that the growth rate of *P. bursaria* is influenced by the abundance of endosymbiotic microalgae (Karakashian and Karakashian 1965). These observations underscore the potential significance of photosynthates (e.g., maltose/glucose) as an energy source for supporting host growth.

The ability of certain *Chlorella* microalgae species to establish symbiotic associations with various host species could be linked to their capacity to release photosynthetically-derived small organic carbon compounds, such as maltose and glucose, and potentially transfer it to the host (Kessler, Kauer, and Rahat 1991). The release of these carbon compounds has been primarily identified under acidic conditions. *Chlorella variabilis* and *Micractinium reisseri*, both symbiotic algae, can release about 40-50% of their photosynthetically fixed carbon such as maltose or glucose under acidic conditions (Muscatine, Karakashian, and Karakashian 1967), a capability not observed in *Chlorella* species that are unable to do symbiosis (Arriola et al. 2018a; Kamako et al. 2005; Shibata et al. 2021). Symbiotic *Chlorella* of *Stentor polymorphus*, *Acanthocystis turfacea*, and *Hydra viridissima* are also known to excrete photosynthetic products (e.g. maltose) (Hoshina et al. 2013; Matzke, Schwarzmeier, and Loos 1990; Schüßler and Schnepf 1992). Inside the host, the capability to release photosynthates is attributed to the acidic environment of the symbiosome. (Schüßler and Schnepf 1992) proposed that the host *Paramecium* triggers the release of maltose from endosymbiotic *Chlorella* through symbiosome acidification facilitated by an active proton pump. However, this remains a hypothesis requiring further experimental investigation.

Carbon fixation and carbon storage of the symbiotic microalgae are likely linked to the transfer of photosynthates to the host. (Ziesenisz, Reisser, and Wiessner 1981) proposed that endosymbiotic *Chlorella* photosynthetically synthesized maltose under light conditions, but that maltose was produced via starch degradation under dark conditions. **Yet, despite the numerous studies on the release of maltose by symbiotic algae (many of them date back the 70s and 80s), there is still limited information on how symbiosis impacts the carbon metabolism of the symbiont prior to the translocation of sugar compounds to the host.** A broader understanding of the cellular mechanisms

within symbiotic microalgae is pivotal, with particular emphasis on the spatial context, such as the microenvironment in the host.

In the symbiotic relationship between *Paramecium* and *Chlorella*, the sugar-release capacity of symbiotic microalgae is predominantly assessed in the extracellular environment rather than within the host. Thus, the mechanisms governing carbon translocation to the host remain to be addressed. Within the cellular environment, membrane transporters serve as primary facilitators for the movement of compounds across cell membranes (Lizák et al. 2019). Numerous studies have explored the translocation and exchange of organic molecules supporting symbiotic interactions (Burriesci, Raab, and Pringle 2012; Davy et al. 2012; Hofmann and Kremer 1981; Kopp et al. 2015). **However, despite its recognized importance, the molecular mechanisms underlying this transfer remain poorly understood.**

Sugar transporters facilitate or allow the movement of sugars across cell membranes, for nutrient uptake, energy production, and cellular signaling in various biological interactions, including symbiotic relationships (Carbó and Rodríguez 2023). Key sugar transporters involved in symbiotic associations include MSTs (monosaccharide transporters), SUTs (sucrose transporters), and SWEETs (Sugar Will Eventually be Exported Transporter) (Chen 2014; Eom et al. 2015). More particularly, SWEET transporters have been described as pivotal in various cellular interactions, like plant-pathogen, plant-rhizobia (Sugiyama et al. 2017), and plant-mycorrhizal symbioses, showing different transcriptional regulation (Bezrutczyk et al. 2018; Manck-Götzenberger and Requena 2016). Of note, SWEETs have been reported to be involved in facilitating sugar exchange in photosymbiosis contributing to the translocation of organic carbon produced through photosynthesis (Maor-Landaw et al. 2023). Another category of sugar transporter involved in photosymbiotic interactions is the Glucose membrane transporters (GLUT-type) within the major facilitator superfamily (MFS). Phylogenetic analysis in cnidarians identified two classes of GLUT transporters, emphasizing their role in transporting symbiont photosynthates (Sproles et al., 2020). *In silico* predictions suggest that GLUT transporters are likely located within the symbiosome. Higher transcription of GLUT transporters was reported in the medusa *Cassiopea andromeda* (Carabantes et al., 2024), *Hydra viridissima*, as seen in anemone *Aiptasia* (Lehnert et al., 2014; Sproles et al., 2018).

I.4.5 Metabolic connectivity: from the host to the microalga

The association between *Paramecium* and the symbiotic microalgae *Chlorella* is likely supported by a nutritional and metabolic exchange. The growth and metabolism of algae must rely on essential nutrients supplied by the host (e.g. nitrogen). Previous research identified Ammonium and L-glutamine as nitrogen sources transported from the host (Albers, Reisser, and Wiessner 1982). In a more detailed study comparing the impact of various nitrogen sources on symbiotic (from the Japanese strain *P. bursaria*) *versus* free-living *Chlorella*, the symbiotic form exhibited a growth increase in culture when specific amino acids (e.g., Asparagine or Serine) were added to the culture media, in contrast to the free-living form (Quispe et al. 2016). The absence of nitrate reductase further implies that the symbiotic microalgae may depend on its host to supply ammonium or amino acids. A pH-dependent proton symport was described as a potential system for general amino acid transport in symbiotic microalgae (Kamako et al. 2005). Additionally, a differential expression analysis based on transcriptomics in symbiotic microalgae *Chlorella variabilis* confirmed the presence of amino acid transporters (Hoshina and Imamura 2008). Of note, a ^{15}N enrichment metabolomic approach highlighted that in "American" symbiotic *Chlorella*, the transfer of nitrogen from the host to the symbiotic microalgae is more likely to occur through amino acid and purine pathways (i.e. arginine)(Sørensen et al. 2020). The host may also regulate nitrogen service to its symbionts through digestion to reduce its total investment in nitrogen provisioning (Lowe et al. 2016).

I.5 PhD Objectives

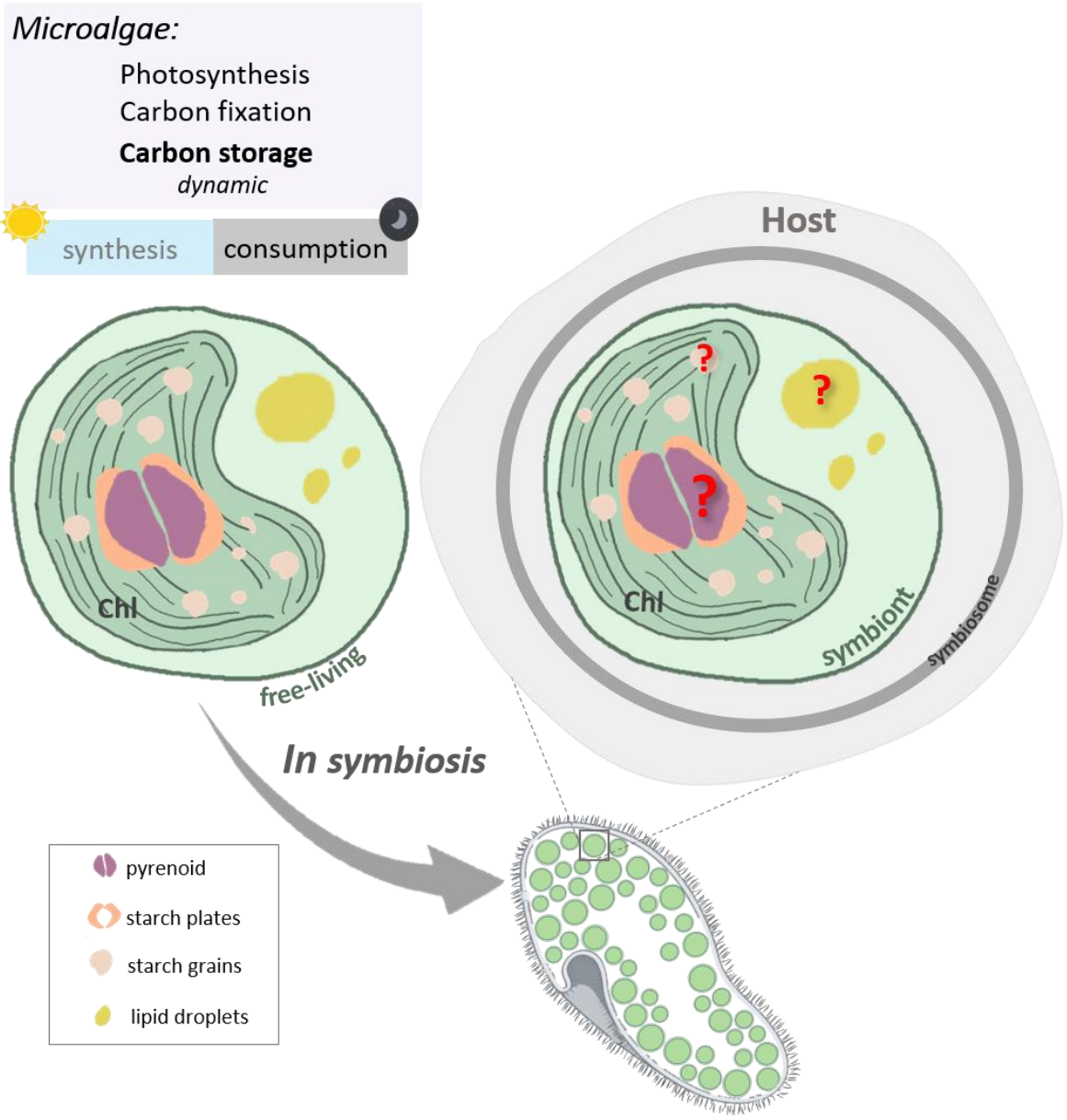

General scheme 1 presenting the objectives of this PhD thesis. In plants and microalgae, photosynthesis takes place in chloroplasts (Chl), where carbon fixation enables the conversion of atmospheric carbon dioxide into organic molecules, that can be stored for cell growth and cellular processes. The carbon metabolism of microalgae is known to be dynamic, following a diurnal rhythm for carbon synthesis (e.g. starch) during the day and carbon consumption during the night. Long-term storage compound (e.g. neutral lipids/ lipid droplets) are generally accumulated in the cell under stress conditions. In symbiosis, photosynthetic carbon is the main currency of exchange. Yet, little is known about the influence of the host on the carbon metabolism of the symbiotic microalgae before the translocation of carbon to the host (e.g. sugars).

The *Paramecium-Chlorella* freshwater model is a valuable system for investigating potential morphological and physiological changes of symbiotic microalgae. This cellular model is easy to maintain in culture and the non-symbiotic form for both, the microalgae and the host can be obtained in laboratory conditions. Photosynthesis and carbon metabolism play central roles in photosymbiotic interactions, yet the host's influence on microalgae carbon dynamics in symbiosis remains uncharacterized, despite being pivotal for carbon exchanges with the host. So far, key questions regarding the carbon metabolism of the symbiotic algae have not been addressed:

Question 1. What is the impact of symbiosis on the central carbon metabolism of the microalgae?
Question 2. What is the impact of symbiosis on the morphology/cellular architecture of the microalgae (chloroplast)?
Question 3. What is the metabolic connectivity between host and algae and what are the sugar transporters expressed in symbiotic versus free-living forms?

Chapter I.

Chapter I of my Ph.D. project will study the subcellular architecture and the central carbon metabolism of symbiotic microalgae and unveil the dynamics of carbon partitioning compared with the free-living form.

In this work, a multiscale study combining 3D subcellular imaging (e.g. Focused Ion Beam Scanning Electron Microscope) will allow us to visualize and obtain morphometrics information from free-living and symbiotic microalgae focusing on their major organelles such as chloroplast and mitochondrion. Another objective of this study is to provide new insights into the quantity and temporal dynamics of carbon storage (e.g. starch and lipid droplets in the morning *versus* the afternoon) in both stages. Additionally, I aim to integrate photophysiological measurements with subcellular imaging. This combination aims to establish a comprehensive link between subcellular information and functional aspects, providing a more thorough understanding of the carbon metabolism of microalgae in symbiotic relationships.

Objectives of Chapter I.

- Unveil subcellular architecture and morphometrics of symbiotic and free-living microalgae focusing on chloroplast and mitochondrion.
- Measure over time (morning *versus* afternoon) the carbon storage (lipid and starch) of symbiotic and free-living microalgae by FIB-SEM (Focused Ion Beam Scanning Electron Microscope) and bulk quantification (e.g. Enzymatic quantification and spectrophotometry)
- Measure physiological parameters related to carbon uptake and carbon fixation of both living forms (e.g. Carbon uptake, Rubisco quantification, oxygen production).

Chapter II.

Light is a major factor influencing photosynthesis and carbon production. For instance, in benthic corals symbiotic microalgae are kept in distinct microniches within host tissues exhibiting significant diversity in light patterns. Thus, the integration of spatial distribution of symbionts could serve to gain a holistic understanding of coral ecophysiology and unveil heterogeneity among the symbiont population.

Chapter II of my Ph.D. project study aims to unveil morphometric changes of symbiotic dinoflagellates from the same multicellular host using FIB-SEM. I aim to unveil the 3D cellular organization and morphometrics of symbiotic microalgae localized in the top (canopy) and bottom part of the host, exposed to different light within the host.

Objectives of Chapter II.

- Unveil subcellular architecture and morphometrics of symbiotic microalgae collected from the top and bottom region of a multicellular host (Cnidarian).
- 3D reconstruction and morphometrics of the cell, chloroplast, and starch compartments of the symbiotic microalgae.

Chapter III.

In photosymbiotic interactions, the ability of symbiotic microalgae to release or deliver sugars from their photosynthesis is largely discussed. The symbiotic microalgae residing in the host *Paramecium* is known to release sugars (e.g. maltose, glucose). Yet, the mechanisms (e.g. active/

versus passive transport) by which the transfer of the photosynthates occurs in cells are still poorly understood.

Chapter III of my PhD aims to unveil potential transporters of the host and the microalgae involved in the exchange of sugars in symbiosis using a transcriptomic approach.

Objectives of Chapter III.

- Investigate potential candidate sugar transporters of the **microalga** involved in symbiosis
- Investigate potential candidate sugar transporters of the **host** involved in symbiosis

I.6 A subcellular 3D microscopy approach to better understand the physiology and metabolism of a microalga

The integration of structure and function in biology is fundamental to better understanding biological processes. 2D imaging provides a limited understanding of the ultrastructure of organelles, their interactions, and the overall cellular architecture. In addition, only partial quantitative information and a view of the cellular organization can be extracted from such 2D imaging data since it depends strongly on the section of the cell observed, providing a partial view of the cellular organization. Focused Ion Beam Scanning Electron Microscope (FIB-SEM) enables high-resolution three-dimensional imaging of intricate cellular structures. FIB-SEM not only provides spatial resolution at a nanometric scale, but it also provides important morphometric data (e.g. quantitative measurements of volume and surface).
The first example of FIB-SEM technology applied to 3D imaging of biological specimens was reported by (Heymann et al. 2006), who demonstrated the application of this iterative milling and imaging approach to a variety of biological specimens. FIB-SEM application was extended to mammalian cells (Bennett et al. 2009), then including microalgae: for instance, a study in diatoms revealed new architectural features associated with cell division (Hildebrand et al. 2009). Additionally, FIB-SEM has been used to reveal the 3D ultrastructure of several microalgal cells with high resolution (4–10 nm) to investigate and compare their subcellular architecture (Uwizeye et al. 2020). In the field of

photosymbiosis, 3D electron microscopy was an important tool to unveil the morphological transformation that undergoes in the microalga *Phaeocystis* in symbiosis within the host Acantharia, a non-cultivable unicellular marine photosymbiotic association (Uwizeye et al. 2021). This work underscored the significance of incorporating a subcellular context to disclose the plasticity of cellular structures in photosymbiosis.).

I.6.1 Cryofixation: first step before subcellular imaging

Sample preparation is a key step in electron microscopy. Conventional methods at room temperature involve chemical fixation, dehydration, and resin embedding. The primary limitation associated with chemical fixation is the significant modification of cellular structures. High-pressure freezing and freeze substitution, show a better preservation of cells and reduce the artifacts of conventional EM specimen preparation (McDonald and Auer 2006).

High-pressure freezing (HPF) is based on using high pressure (about 2000 atmospheres or bar) to freeze cells. This allows for immobilizing all molecules/structures in a cell within milliseconds without forming ice crystals. By HPF, water molecules in the cells form amorphous (i.e. non-crystalline) ice limiting ultrastructural artifacts. Hence, the sample is preserved close to its native form (e.g. no alteration of the cellular architecture). This technique is powerful for structural cell biology (McDonald and Auer 2006; Moor 1987). Following HPF, freeze substitution takes place and involves chemical fixation and resin embedding at low temperatures. At this stage, cellular water is replaced by acetone, and cells are chemically fixed and stained (e.g. using osmium) (i.e. between (- 90 °C to - 30 °C). This process carried out at low temperatures prevents proteins and lipid molecules from moving, avoiding distortions in the sample, often observed at room temperature. Then embedding with epoxy resin at low temperatures takes place for several days to have a block with cells at room temperature.

I.6.2 FIB-SEM: Focused Ion Beam Scanning Electron Microscope

The Focused Ion Beam (FIB) often uses Gallium (Ga^+) to ablate the surface of a specimen resin block with a nanoscale resolution (e.g. a resin block containing HPF biological samples embedded in resin[2]). When paired with a Scanning Electron Microscope (SEM), FIB-SEM turns into a practical microscopy tool for 3D imaging (Fig. 8).

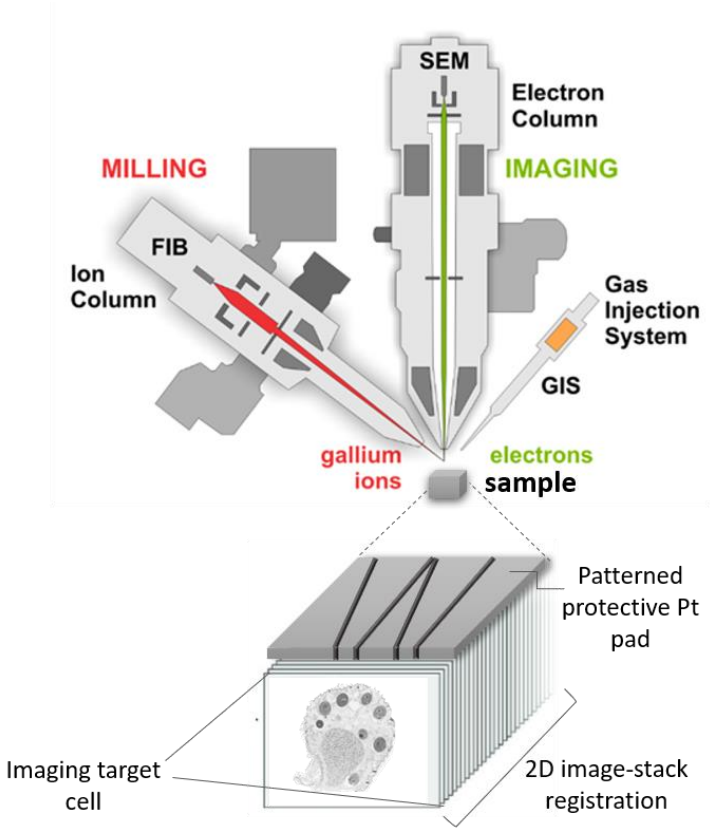

Figure 8. Schematic representation of FIB-SEM microscope and sample registration. The gallium ion beam is produced by a liquid metal ion source at the top of the ion column. The beam is focused onto the sample (embedded cells)). The electron beam is used to monitor the milling process and acquire micrograph. A gas injection system (GIS) is used prior to milling to apply a thick protective platinum coating onto the sample. Principle of ion beam milling: a selected region of the sample undergoes trenching to expose the area of interest, followed by a repetitive process of resin milling using the FIB (red beam) and subsequent SEM (green beam) imaging of the exposed surface to generate a stack of 2D images. The platinum (Pt) pad patterned on the sample surface enables automated beam adjustment and control over slice thickness. The stack of 2D images is then digitally transformed into a 3D volume, aligned, and segmented to unveil the desired 3D structure. Adapted from (Kuba et al. 2021) and (Narayan and Subramaniam 2015).

Upon insertion into the FIB-SEM chamber, a protective layer of platinum or carbon is initially deposited via a Ga+ beam to safeguard the target region for imaging. Subsequently, an iterative process ensues, wherein resin milling by the FIB alternates with Scanning Electron Microscope (SEM) imaging to unveil a series of 2D images at each milling step of few nanometers of distance. The iterative process repeats until obtain, for example an entire cell acquired. Once the cycle is finished, registration of the 2D image stack occurs. The 3D volume is then obtained by slice images alignment through a computational process (Narayan and Subramaniam 2015).

I.6.3 Image processing and segmentation

3D-based electron microscopy allows us to access a more complete view of the subcellular architecture of a cell. An image stack registration of a cell comprises between 300 and 600 high-resolution SEM images depending on the specimen volume. A dataset may comprise between 60 to 100 gigabytes (GB). Before initiating 3D reconstruction, a critical initial step is to convert the data into a compatible format and reduce its size for compatibility with available software. Image processing involves pre-processing images by enhancing the contrast of specific subcellular features, including stack registration and noise reduction to facilitate identification and characterization of Regions of Interest (ROIs). Fiji offers plugins for displaying image features, enhancing resolution, and performing stack registration. Following data processing, 3D reconstruction is conducted based on pixel classification, with various techniques reviewed by "(Zhao et al. 2024)".

Chapter I

Assessing the carbon dynamics in microalgae within a host through a multiscale study

Authors: A. Catacora-Grundy[1], F. Chevalier[1], D. Yee [1,2], C. LeKieffre[1], N. L. Schieber[2], Y. Schwab[2], B. Gallet[3], P.H. Jouneau[4], G. Curien[1], J. Decelle[1*]

[1] Cell and Plant Physiology Laboratory, CNRS, CEA, INRAE, IRIG, Université Grenoble Alpes, 38054 Grenoble, France
[2] Cell Biology and Biophysics Unit, European Molecular Biology Laboratory, 69117 Heidelberg, Germany
[3] Université Grenoble Alpes, CEA, CNRS, Institut de Biologie Structurale (IBS) UMR 5075, 38044 Grenoble cedex 9, France
[4] Institut Nanosciences et Cryogénie, Université Grenoble Alpes, CEA, 38054 Grenoble, France

* To whom correspondence may be addressed. Email: johan.decelle@univ-grenoble-alpes.fr

Symbiotic interactions between a heterotrophic host and intracellular microalgae are widespread in aquatic ecosystems and are considered to be energized by photosynthetically-derived carbon energy. However, little is known about the impact of symbiosis on algal symbiont bioenergetics (e.g. carbon production and storage). This study reveals time-resolved morphological and physiological changes of a microalga inside a host at the subcellular scale. We show that the photosynthetic machinery expands and carbon fixation and storage are boosted in symbiotic microalgae beyond their growth needs. Photosynthetic production is very likely enhanced by the energetic demands of the host. These findings advance our basic understanding of photosymbiosis and provide new insights into the mechanisms and drivers of metabolic exchange between partners.

Keywords: symbiosis, carbon metabolism, symbiotic microalgae, chloroplast, subcellular imaging

Abstract

Symbiosis between a host and intracellular eukaryotic microalgae is a widespread life strategy in aquatic ecosystems. This partnership is considered to be mainly energized by the photosynthetically-derived carbon energy of microalgal symbionts. A major question is whether microalgae increase their photosynthetic production and decrease carbon storage in order to maximize carbon translocation to their host. By combining three-dimensional subcellular imaging and physiological analyses, we show that the photosynthetic machinery (chloroplast and CO_2-fixing pyrenoid) of the symbiotic microalga *Micractinium conductrix* significantly expands inside their host (the ciliate *Paramecium bursaria*) compared to the free-living state. This is accompanied by a 13-fold higher quantity of Rubisco enzymes and 16-fold higher carbon fixation rate. Time-resolved subcellular imaging revealed that photosynthetically-derived carbon is first allocated to starch during the day, with five times higher production in symbiosis despite low growth. Nearly half of the carbon stored in starch is consumed overnight and some accumulates in lipid droplets, which are 20-fold more voluminous in symbiotic microalgae. We also show that carbon is transferred to the host and hypothesize that much of this is respired by the high density of surrounding host mitochondria. We provide evidence that photosynthetic production of symbiotic microalgae is likely boosted in response to the energetic demands of the host. Overall, this study provides an unprecedented view of the subcellular remodeling and dynamics of carbon metabolism of microalgae inside a host, highlighting the potentially key role of the source-sink relationship in aquatic photosymbiosis.

I.1 Introduction

Symbiotic associations encompass a broad spectrum of interactions, many of which rely on metabolic exchanges between partners. Photosymbiosis (the association between a heterotrophic host and photosynthetic symbionts) is ubiquitous in aquatic ecosystems. While the most emblematic example of photosymbiosis is the association between corals and microalgae (e.g. Symbiodiniaceae) (Hughes, Barnes, et al. 2017; Sukumaran and TR Keerthi. 2023), photosymbiotic interactions with marine and freshwater protists, such as radiolarians, ciliates, dinoflagellates, as hosts are also widespread (Decelle et al. 2015; Stoecker et al. 2009). Although it remains challenging to quantify the benefits for the host and

the microalgal symbionts, it is widely considered that photosymbiosis is mutually beneficial, i.e. the host acquires new metabolic capabilities (production of photosynthesis-derived carbohydrates, nitrogen recycling) and symbiotic microalgae benefit from a nutrient-rich environment and protection against predators and viruses (Decelle et al. 2015; Dziallas et al. 2012; Johnson 2011; Yellowlees, Rees, and Leggat 2008). Nevertheless, our mechanistic understanding of this metabolic crosstalk between host and symbiont, particularly the impact of symbiosis on the bioenergetics of microalgae, remains in its infancy. Physiological and morphological changes in symbiotic microalgae have previously been described in unicellular marine plankton photosymbiosis, including expansion of chloroplast volume and higher carbon fixation capability (Decelle et al. 2019, 2021a; Uwizeye et al. 2021). This algal transformation strongly suggests an enhanced primary production of the algae within their hosts, with possible impact of photosymbiosis in global carbon cycles. However, given the wide diversity of taxonomic partners and habitats, it is not known whether this is a common phenomenon in photosymbioses from marine and freshwater ecosystems.

The remodeling of the photosynthetic apparatus in oceanic photosymbiosis raises the question of how microalgae manage their photosynthetically-derived carbon energy within hosts, and more particularly what is the fate of this carbon? In microalgae, carbohydrates (e.g. sugars) produced by photosynthesis are typically used for respiration and growth, or partitioned into storage compounds such as starch (or other glucose polymers) and triacylglycerols (TAG) in lipid droplets (Busi et al. 2014; León-Saiki et al. 2017). Synthesis and degradation of starch and lipids are dynamic (Jouhet et al. 2022; Kong et al. 2018) and depend on cell growth, the time of the day and environmental conditions (León-Saiki et al. 2017; Ran et al. 2019). We speculate that starch and lipid storage in symbiotic microalgae is limited compared to the free-living condition since it has been shown that most (90%) of the organic carbon produced by microalgae is transferred to coral hosts, mainly as glucose and lipids (Davy et al. 2012; Falkowski et al. 1984). Starch and lipids have been observed in microalgae living within corals, Foraminifera and Radiolaria (Decelle et al. 2021b; Gibbin et al. 2020; Krueger et al. 2018), but their diel dynamics inside and outside the host has never been addressed. This knowledge gap prevents us from understanding the impact of the host on the bioenergetics of their symbiotic microalgae, and therefore, the mechanisms and drivers of carbon exchange.

Studying the metabolisms of symbiotic microorganisms is challenging because it requires disentangling the metabolism of both partners with sufficient spatial and temporal resolution. Transcriptomics can provide insights into potentially active metabolic pathways, but do not provide quantitative information (for example about the quantity of carbon that is stored). In this study, we therefore conducted time-resolved 3D ultrastructural imaging to reveal the subcellular architecture of microalgae outside and inside a host over time, quantifying volumes of organelles and compartments that produce and store carbon energy. Combined with physiological measurements, this imaging approach is essential to obtain a full understanding of the metabolic status of a symbiont within a host. We used a single-celled photosymbiotic system, *Paramecium bursaria* (host ciliate) and *Chlorella spp.* (green microalgae, Chlorophyta), that is widely distributed in freshwater ecosystems (Pröschold et al. 2011; Reisser 1980). The ciliate has the capacity to establish a symbiosis with 100-800 algal cells, individually localized in a symbiosome vacuole. These symbiotic microalgae can belong to the genera *Chlorella* and *Micractinium*, which are also able to be cultured in the free-living state (Fujishima 2009). We demonstrate that symbiotic microalgae undergo a major expansion of their chloroplast, including the CO_2-fixing pyrenoid, which lead to higher carbon fixation compared to the free-living stage. By tracking the fate of this photosynthetically-produced carbon in symbiosis, we show that there is a higher starch production during the day, a higher consumption overnight, carbon accumulation in lipid droplets, and carbon transfer to the host. Our study provides experimental evidence that this high primary productivity could be linked to the energetic demands of the host. Therefore, this study provides new insights into the carbon metabolism of symbiotic microalgae and on potential host processes that engineer carbon energy in photosymbiosis.

I.2 Results and Discussion

Expanded photosynthetic machinery and higher carbon fixation uptake in symbiotic microalgae

Using the volume electron microscopy technique FIB-SEM (Focused Ion Beam Scanning Electron Microscope), we compared the subcellular architecture of two free-living microalgae (*Chlorella vulgaris* and *Micractinium conductrix*, both known to be symbionts of the ciliate *Paramecium bursaria*) with that of symbiotic cells (identified here as *M. conductrix*) (Fig. 1). In total, 80 algal cells have been

analyzed, representing more than 40,000 electron microscopy images. We focused on 3D reconstruction and quantitative volumetrics of the main algal organelles (i.e. chloroplasts, mitochondria and the nucleus). The two free-living microalgae which are known to engage in symbiosis with *P. bursaria* exhibited similar cellular architecture, with organelles having comparable volumes (Fig. 1B). Having two free-living representatives provides additional evidence on the effect of symbiosis regardless the symbiont taxonomy and culture conditions. By contrast, symbiotic microalgae exhibited significant morphological differences (Fig. 1). Cell volume was 5.6-fold higher than the free-living stage (43.55 ± 12.97 μm^3 *vs* 7.79 ± 1.94 μm^3). The most important differences involved the energy-producing organelles, with the volume of the chloroplast and mitochondrion increasing 6.4 and 7.3-fold in symbiotic microalgae, respectively (22.92 ± 7.97 μm^3 *vs* 3.59 ± 1.02 μm^3 and 1.55 ± 0.52 μm^3 *vs* 0.21 ± 0.05 μm^3, respectively) (Fig. 1B). Volume occupancy of the mitochondrion and chloroplast in the cell (organelle/cell volume ratio) tended to be higher in symbiosis (3.52% ± 0.35% in symbiosis *vs* 2.77 ± 0.34% in free-living and 51.68% ± 4.27% in symbiosis *vs* 45.78% ± 2.18% in free-living, respectively). In contrast, cell volume occupancy of the nucleus was 2-fold lower in symbiosis (5.41 ± 1.14% *vs* 11.18 ± 1.50%) (Fig. 1C). Symbiotic cells exhibited a larger variability of organelle volumes compared to the free-living condition, suggesting different physiological states inside the host. The morphological changes that we observed in this symbiotic microalga share similarities with those reported for some marine planktonic photosymbioses (Decelle et al. 2021a; Uwizeye et al. 2021), suggesting that common cellular processes are involved when photosynthetic production is enhanced within a host.

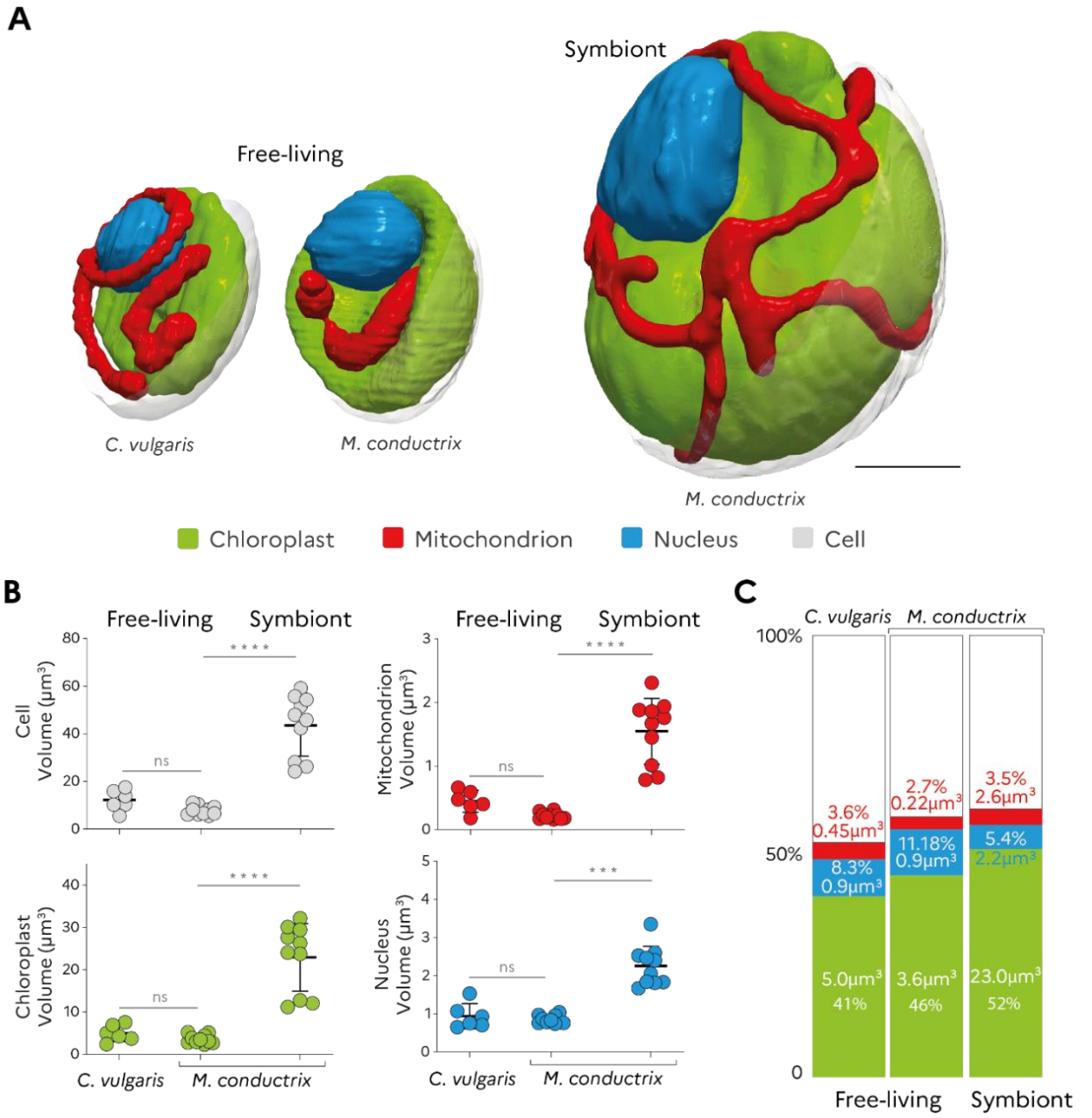

Figure 1. Subcellular architecture of free-living and symbiotic microalgae unveiled by FIB-SEM imaging. A) 3D reconstruction of the free-living microalgal cells (*Chlorella vulgaris*; and *Micractinium conductrix*) and the symbiotic microalgal cells (identified as *M. conductrix*) in the host ciliate *Paramecium bursaria* (CCAP1660/18) with chloroplast (green), mitochondrion (red) and the nucleus (blue). Scale bar: 1µm. **B)** FIB-SEM-derived volumes of the cell, chloroplast, mitochondrion and nucleus from the free-living microalgae (*C. vulgaris*; n=6 and *M. conductrix* n=10) and symbiotic microalgae (*M. conductrix*; n=10). Scatter plots present the mean volume of organelles (µm³) ± SD. Non-parametric ANOVA unpaired test: ****p < 0.0001 ***p < 0.001; ns, no significant difference. **C)** Relative volume occupancy of the chloroplast, mitochondrion and nucleus in the cell as % (organelle volume/cell volume ratio) in free-living and symbiotic microalgal cells. Volumes (µm³) of organelles are given within respective bar segments and summarized in Table S1 to S4. (Grey bar segments represent the remaining volume of the cell).

To investigate the photosynthetic capacities of symbiotic microalgae, we analyzed the structural organization and quantified the volume of the pyrenoid, the CO_2-fixing liquid-like compartment inside the chloroplast (He, Crans, and Jonikas 2023; Meyer, Whittaker, and Griffiths 2017). 3D reconstruction showed that the pyrenoid matrix of free-living and symbiotic microalgae was traversed by membrane tubules extending from the thylakoids, as previously described in other green microalgae (*Chlorella* and *Chlamydomonas*) (Engel et al. 2015; Fujishima 2009) (Fig. 2A). Compared to free-living cells, the pyrenoid was 8.8-fold larger in symbiosis (1.14 ± 0.27 μm^3 *vs* 0.13 ± 0.04 μm^3). It also tended to occupy even more space within the enlarged chloroplast (5.35 ± 1.56% in symbiosis *vs* 3.63 ± 0.70% in free-living) (Fig. 2B). The increased volume of the pyrenoid could contribute to higher carbon fixation by the cell. In order to establish the connection between morphology and function of this key compartment, we quantified carbon fixation (time-resolved incubation with ^{13}C-bicarbonate stable isotope) and the content of the CO_2-fixing enzyme Rubisco (Ribulose-1,5-bisphosphate carboxylase/oxygenase) in free-living and symbiotic microalgae (Fig. 2C-E). Carbon fixation per cell in symbiotic microalgae was 16-fold higher than in free-living cells (0.0192 ± 0.0125 pg of ^{13}C.cell-1 and 0.0012 ± 0.0002 pg of ^{13}C.cell-1, respectively) after 1h of incubation with ^{13}C-bicarbonate.

When normalized per carbon, carbon uptake was 2-fold higher in symbiosis (0.0022 ± 0.00022 pg. $^{13}C.cell^{-1}$ *vs* 0.0011 ± 0.00030 pg. $^{13}C.cell^{-1}$) (Fig. 2C-D, Table S5). Using quantitative western blot, we found that symbiotic cells possess ~13 times more Rubisco compared to free-living cells ($5.77.10^{-10}$ ± $1.32.10^{-10}$ pmol.cell^{-1} in free-living *vs* $7.75.10^{-09}$ ± $4.16.10^{-09}$ pmol.cell^{-1} in symbiosis) (Fig. 2E-Fig. S1, Table S6), corroborating the increase in pyrenoid volume. This demonstrates that pyrenoid volume assessed by 3D electron microscopy is correlated to Rubisco content, a relationship that has not previously been explored. Higher carbon fixation could also be explained by higher CO_2 availability surrounding symbiotic microalgae, partly due to the acidification of the symbiosome (Kodama and Fujishima 2005). Overall, the increase in pyrenoid volume and Rubisco content, as well as higher carbon fixation, clearly illustrate significant remodeling of the photosynthetic machinery and enhancement of photosynthetic production by microalgae in symbiosis.

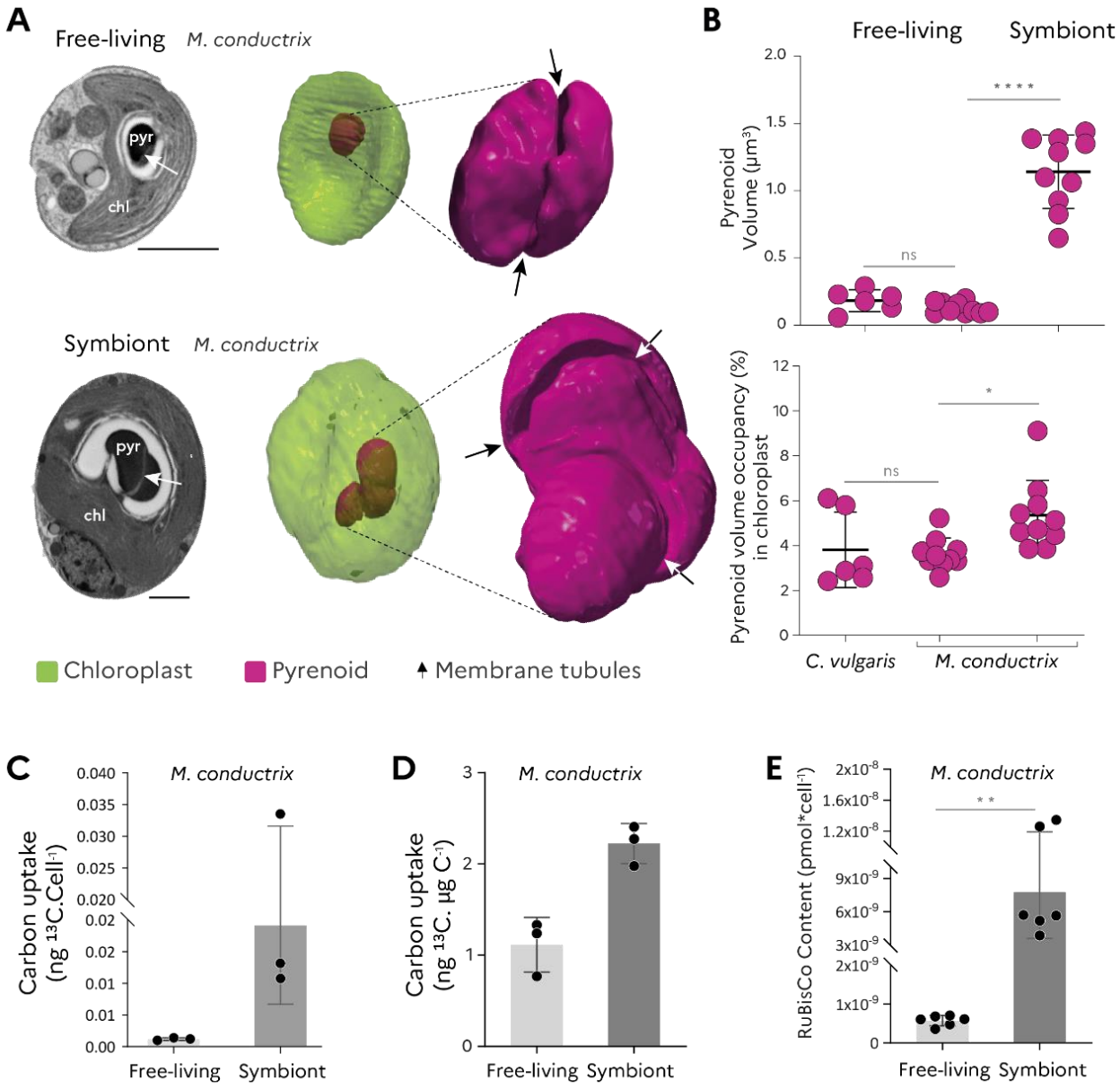

Figure 2. Expansion of the carbon fixation machinery in symbiotic microalgae. A) Representative electron micrographs and FIB-SEM-based 3D reconstruction of the chloroplast (chl, green) and its immersed pyrenoid (pyr, purple) in free-living and symbiotic microalgae (*M. conductrix*). Arrows indicate the membrane tubules crossing the pyrenoid matrix. Scale bar: 1 µm. **B)** Scatter plots represent the volume of the pyrenoid in μm^3 (mean ± SD) and pyrenoid volume occupancy (relative volume of the pyrenoid in the chloroplast) as % (mean ± SD) in free-living *C. vulgaris* (n=6) and *M. conductrix* (n=10) and the symbiotic microalgae (*M. conductrix:* n=10) in the host ciliate *Paramecium bursaria*. Non-parametric ANOVA unpaired test: ****$p < 0.0001$; *$p < 0.01$: ns, no significant difference. **C-D)** Inorganic carbon fixation rate after 1h of incubation with ^{13}C-labelled bicarbonate in free-living and symbiotic microalgae presented as carbon uptake per algal cell (C) and carbon uptake per carbon (D) in triplicates. **E)** Rubisco content (pmol) per algal cell in free-living and symbiotic state based on Rubisco immunoblot. t-test: **$p \leq 0.05$. See also Supplementary Table S6 and Fig S1.

Higher starch production in symbiotic microalgae and overnight consumption

One of the major questions in photosymbiosis is whether symbiotic microalgae store carbon energy when present inside their host (and if yes, in which quantity) or if this carbon is transferred to the host without storage. In order to investigate carbon allocation in symbiosis, we tracked the fate of the photosynthetically-fixed carbon at the subcellular scale using a correlative TEM-NanoSIMS (Transmission electron Microscopy-Nanoscale Secondary Ion Mass Spectrometry) approach. After 1h of incubation with ^{13}C-labelled bicarbonate, ^{13}C enrichment was mostly found in starch of the symbiotic microalgae (Fig. 3A), as is the case in symbiotic dinoflagellates from Foraminifera and corals (Kopp et al. 2015; LeKieffre et al. 2018). After 24h, ^{13}C enrichment was found not only in starch but also in the algal cytoplasm and algal lipid droplets (Fig. 3B). These results demonstrate that symbiotic microalgae store photosynthetically-fixed carbon during the day in the form of starch in their chloroplast, allocate part of this carbon in newly synthetized biomass for growth, and also store it in lipid droplets, possibly via an overnight reallocation from starch to lipids.

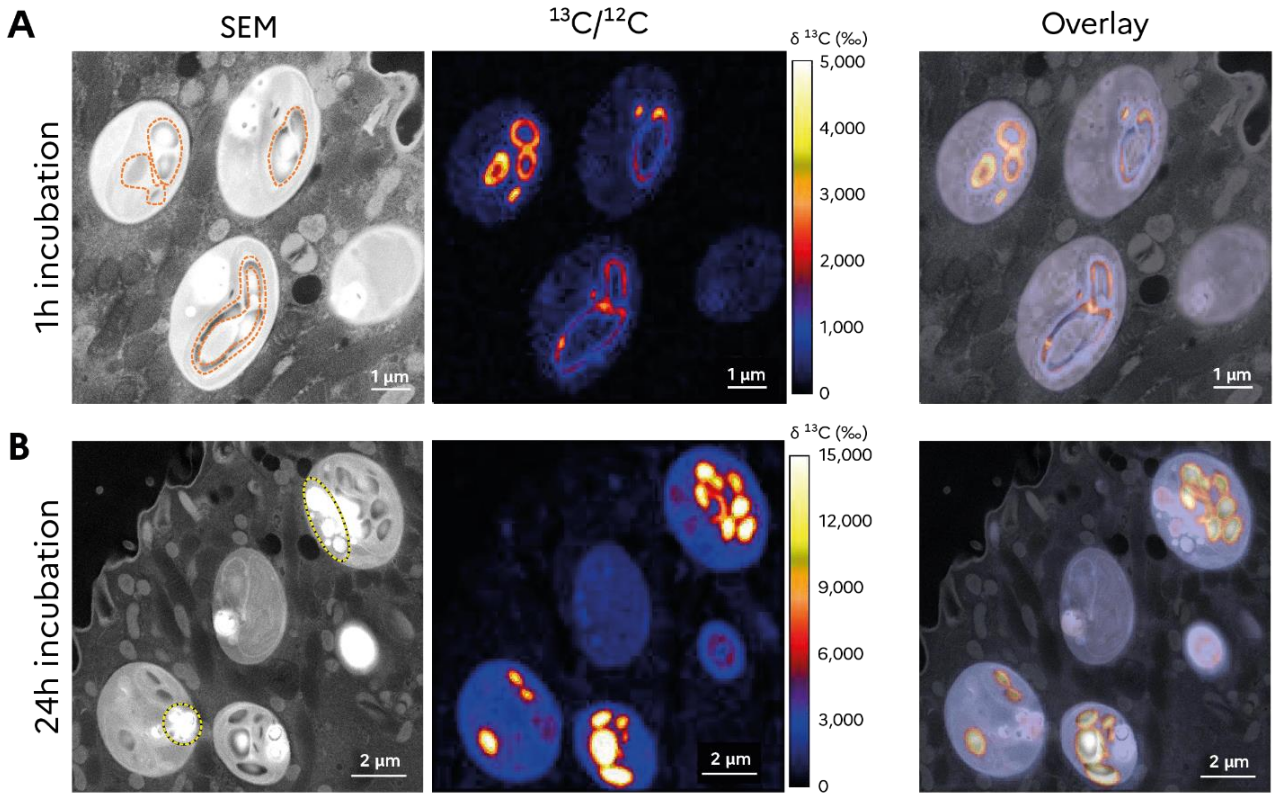

Figure 3. Subcellular tracking of fixed carbon in symbiotic microalgae using mass spectrometry imaging. A-B) SEM (Scanning Electron microscopy) and NanoSIMS (Nanoscale Secondary Ion Mass Spectrometry) images and the overlay (right) showing ^{13}C enrichment (‰, provided by the $^{13}C/^{12}C$ ion map) in symbiotic microalgae within the host *P. bursaria* after 1h (A) and 24h (B) of incubation with ^{13}C-labelled bicarbonate. At 1h, ^{13}C enrichment was mainly found in starch grains and plates of the symbiotic microalgae while at 24h, ^{13}C enrichment was also found in algal lipid droplets. Starch and lipid droplets are highlighted in SEM images by dashed circles in orange and yellow, respectively.

We then investigated whether microalgae store more or less carbon (i.e. starch and triacylglycerols - TAG - in lipid droplets) in symbiosis compared to the free-living stage, and if this storage follows the same temporal dynamics. We combined a bulk quantification of total starch and neutral lipids with FIB-SEM-based volumetrics in free-living and symbiotic microalgae over the day (morning 10 am after 2h of light *versus* afternoon 4pm after 8h of light). Starch quantification in microalgae revealed that synthesis occurs during the day outside and inside a host following the same diel dynamics (Fig. 4A). However, starch production was significantly higher in symbiosis, leading to a 4.4-fold higher starch content per cell at the end of the day (1.40 ± 0.08 pg.cell^{-1} in symbiosis in respect to 0.31 ± 0.12 pg.cell^{-1}). It is known that starch production is correlated to cell growth and energetic demands in green microalgae (Ball et al.

1990; Busi et al. 2014). In free-living microalgae, we showed that starch production mainly takes place during exponential growth phase, while at stationary phase, starch content is similar between morning and afternoon (no production at low growth rate, Fig. S2). Despite the 2-times lower growth rate of microalgae in symbiosis (Table S8), as previously reported (Takahashi 2016), microalgae produced 5.3-times more starch during the day (0.91 pg.cell^{-1} in symbiosis *vs* 0.17 pg.cell^{-1} in free-living algae) compared to free-living cells. This may indicate that symbiotic microalgae produce more starch than needed for their growth.

FIB-SEM-based 3D reconstruction allowed us to track and quantify two types of starch compartments that are produced depending on growth conditions: starch plates surrounding the pyrenoid and starch grains localized in the stroma of the chloroplast (Fig. 4B) (both labelled with ^{13}C with NanoSIMS, Fig. 3). In green microalgae (*Chlamydomonas* sp.) actively dividing cells accumulate more starch in plates, while transitory starch grains can massively increase under stress conditions (Findinier et al. 2019; He et al. 2023) Starch plates are also essential for carbon fixation and the carbon concentrating mechanism (CCM), potentially acting as an oxygen barrier for Rubisco (Toyokawa, Yamano, and Fukuzawa 2020). Compared to free-living cells, FIB-SEM-based morphometrics confirmed the higher amount of total starch per cell volume in symbiotic microalgae at the end of the day (by 2-fold: 0.057 ± 0.02% *vs* 0.030 ± 0.00% per cell volume) (Fig. S3). Specifically, FIB-SEM data revealed that starch increase mainly took place in plates surrounding the pyrenoid during the day (1.4 fold and 9-fold increase between morning and afternoon in free-living and symbiotic cells, respectively). By contrast, the relative occupancy of starch grains in the cell did not vary between morning and afternoon in free-living and symbiotic cells (Fig. 4C, Table S9-10). The fact that transitory starch grains do not accumulate in symbiotic microalgae during the day suggests that starch degradation and sugar export into the cytosol could be maintained, like in actively growing free-living cells.

In order to further understand storage dynamics in free-living and symbiotic microalgae, starch quantification was also performed on the following day (after one night in the dark). We found that overnight consumption of starch was maintained in symbiotic microalgae despite their lower growth rate (similar diel starch turnover). In free-living (exponential growth phase) and symbiotic microalgae, about 44% of starch produced during the day was consumed overnight (from 1.40 ± 0.08 pg.cell-1 in

the afternoon to 0.79 ± 0.02 pg.cell-1 the next morning in symbiotic microalgae) (Fig. 4A). Of note, this represents a 4.5-fold higher quantity of starch that is consumed in symbiosis overnight (0.61 pg.cell-1 vs 0.14 pg.cell-1 in free-living). This could indicate that nearly half of these carbohydrates/sugars have been i) tapped for algal energetic demands, ii) reallocated to other algal compartments (e.g. lipids), and/or iii) transferred to the host overnight in symbiosis.

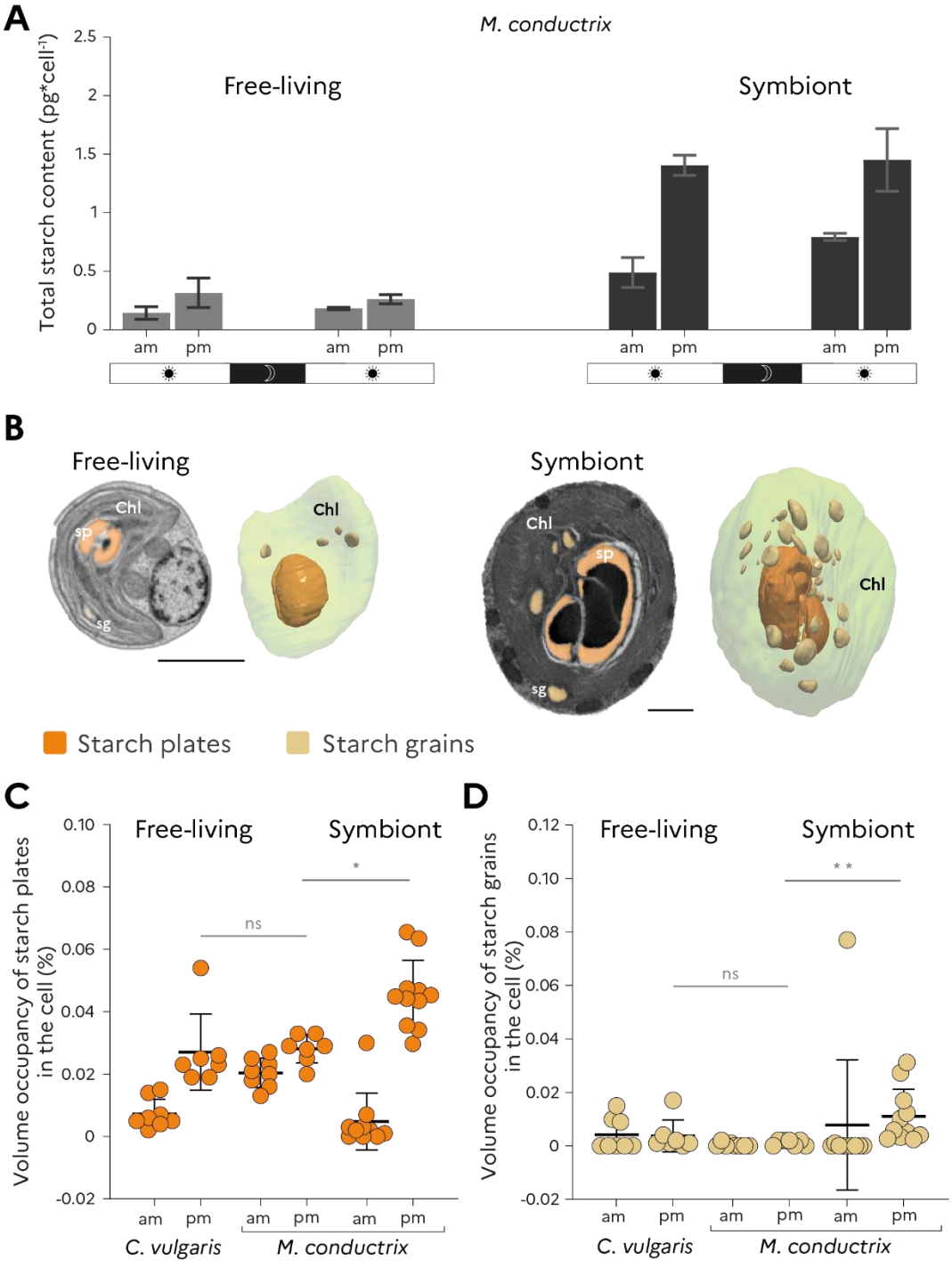

Figure 4. Quantity and diel dynamics of starch synthesis and storage in free-living *versus* symbiotic microalgae. A) Starch content per cell in free-living (*C. vulgaris* and *M. conductrix*) and symbiotic microalgae (*M. conductrix*) unveiled by enzymatic assay (n = 3) in the morning (10am) and afternoon (4pm) across two consecutive days. **B)** Electron micrographs and FIB-SEM-based 3D reconstruction of starch plates (sp, dark orange) and starch grains (sg, light orange) in the chloroplast (chl) of free-living and symbiotic microalgae. Scale bar: 1 μm. **C-D)** Scatter plots represent the relative volume of starch plates (C) and starch grains (D) in free-living and symbiotic microalgae (%) provided by FIB-SEM based volumetrics. Non-parametric ANOVA unpaired test: $^{**}p<0.01$: $^{*}p \leq 0.05$: ns, no significant difference. Size scales: 1 μm. See also Supplementary Tables S9 and S10.

Accumulation of lipid droplets overnight in symbiotic microalgae

Our 24h-incubation nanoSIMS results showed that some of the fixed carbon can be used by symbiotic microalgae for their growth (^{13}C enrichment in the algal cytoplasm), but also allocated into their cytosolic lipid droplets (Fig. 3B). It is known that lipid droplets are a major carbon storage compartment in microalgae that can fluctuate according to growth and stress conditions, such as nutrient limitation (Jouhet et al. 2022; Kong et al. 2018; Ran et al. 2019). Like starch, we tracked and quantified the neutral lipids content of free-living and symbiotic microalgae using a combination of a fluorescence-based assay (Nile Red staining quantified by spectrometry) and FIB-SEM imaging. The specificity of neutral lipid staining was verified in our microalgae using confocal fluorescence microscopy (Fig. S4). FIB-SEM-based 3D reconstruction revealed that symbiotic microalgae contained many more lipid droplets (up to 20) compared to the free-living stage (3 on average) (Fig. 5A). On average, the volume of total lipid droplets in symbiotic microalgae could be ~20 times higher (or 11.7 times higher if normalized per cell volume: 0.035± 0.007 μm^3 in symbiosis compared to 0.003 ± 0.003 μm^3 in free-living cells) (Fig. 5B, Table S10). When compared between morning and afternoon, FIB-SEM and fluorescence-based quantification showed that there was no increase in lipid droplets in both free-living and symbiotic microalgae (Fig. 5). On the following day, lipid droplets did not increase in free-living cells, whereas in symbiosis, there was an accumulation of lipid droplets (0.019 ± 0.003 to 0.034 ± 0.009 $a.u.cell^{-1}$) (Fig. 5C,Table S11). This accumulation in symbiotic microalgae seemed to be maintained the following days, up to day 7 (higher amount of lipid per cell). Overall, our results suggest that the storage of triacylglycerols (TAG) in lipids droplets increases overnight in symbiotic microalgae, likely fueled by carbon from starch, and that lipid droplets accumulate over consecutive days. This raises the question as to whether some of the photosynthetically-produced organic carbon is also transferred to the host.

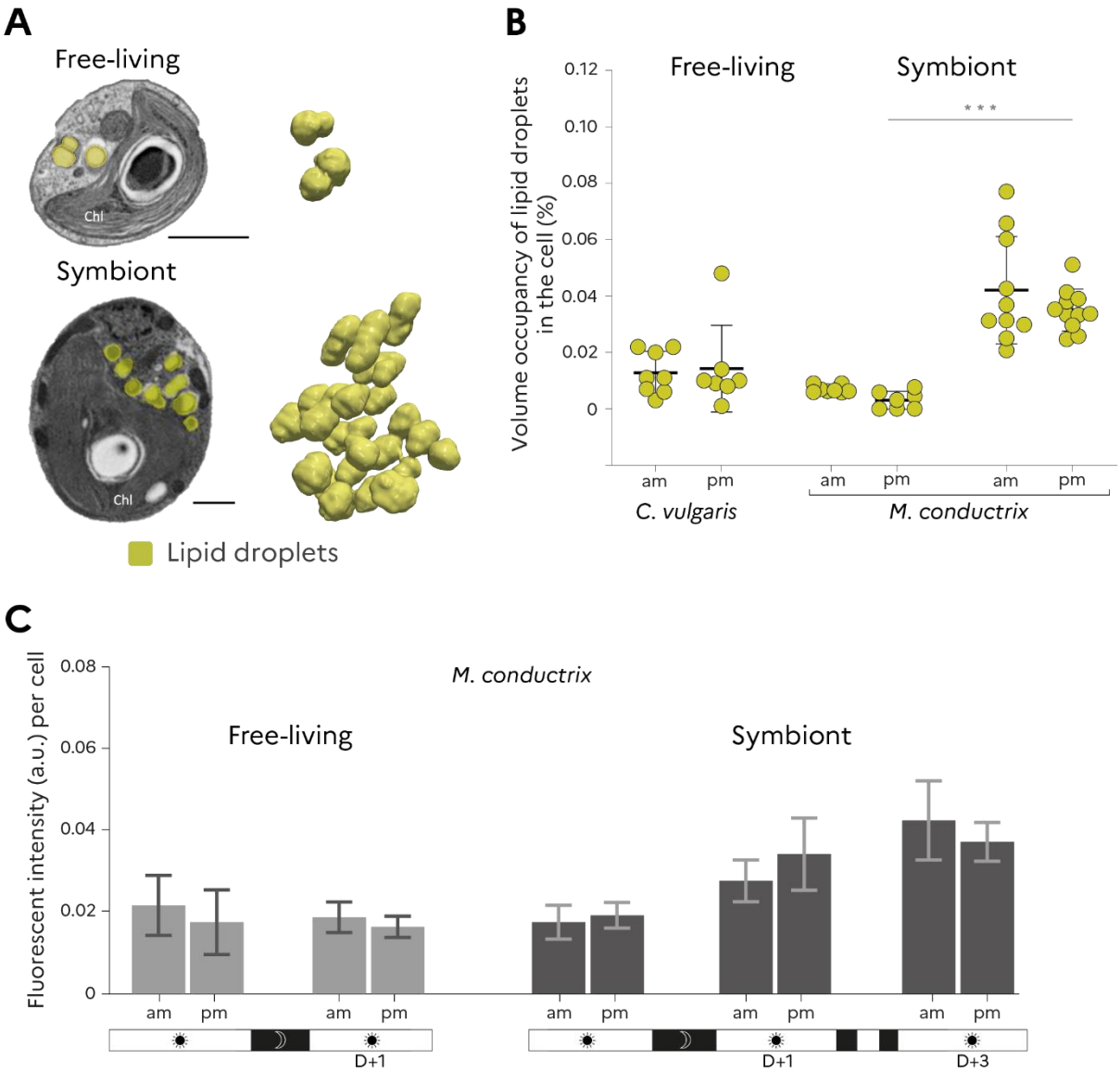

Figure 5. Accumulation of lipid droplets in symbiotic microalgae. A) Electron micrographs and FIB-SEM-based 3D reconstruction of lipid droplets (yellow) in free-living (*C. vulgaris* and *M. conductrix*) and symbiotic (*M. conductrix*) microalgae. Scale bar: 1 µm. **B)** FIB-SEM-based calculation of the volume of lipid droplets normalized by cell volume (occupancy in the algal cell as %) between free-living and symbiotic microalgae, and morning and afternoon. Statistical test: Non-parametric ANOVA unpaired test: ***p<0.0001: ns, no significant difference. **C)** Total neutral lipids per algal cell assessed using Nile Red staining in free-living and symbiotic microalgae in the morning and afternoon, over two consecutive days. In symbiotic microalgae, neutral lipids were also quantified after 7 days of culture. Fluorescence intensity (a.u.) was quantified by TECAN-based spectrometry. See also Supplementary Table S11 and Fig S4.

Photosynthetically-derived carbon is transferred to the host

Using NanoSIMS, we investigated whether photosynthetically-derived carbon is transferred and stored in host cells. After 1h, no ^{13}C enrichment was detected in the host cell (Figs. 3A and 6A). After 24h, we did not observe large structures/compartments of the host highly labelled with ^{13}C, contrary to results reported for photosymbioses involving Foraminifera and corals (Gibbin et al. 2020; Kopp et al. 2015; Krueger et al. 2018; LeKieffre et al. 2018) that store carbon in large lipid droplets highly labelled with ^{13}C. A low level of ^{13}C enrichment was, however, detected in unknown host, demonstrating transfer to the host (Fig. 6A). We hypothesize that carbon energy produced by symbionts could be rapidly used by the host upon transfer and not stored in lipid droplets or other sugar reserves. To support this, we investigated the ultrastructural microenvironment of the host in the vicinity of symbionts. 3D reconstruction revealed a high density of host mitochondria surrounding symbiotic microalgae (Figs. 6B and 6C). Tight physical interaction between host mitochondria and the symbiont-containing symbiosome was also previously observed in this model (Song et al. 2017). Proximity between symbiotic microalgae and host mitochondria were also reported in salamander embryos and cnidarian-*Symbiodiniacae* symbioses (Dunn et al. 2012; Kerney et al. 2011). Therefore, it is possible that photosynthetically-derived organic carbon of symbionts could be transferred and very rapidly respired by host mitochondria, rendering it undetectable by nanoSIMS. This mass spectrometry imaging coupled with resin embedding can only detect carbon that is incorporated into biomass or stored in large molecules such as lipids and starch (Gibbin et al. 2020). We also cannot exclude that host mitochondria can participate to the delivery of CO_2 surrounding symbiotic microalgae, so contributing to the enhanced algal carbon fixation and photosynthetic production.

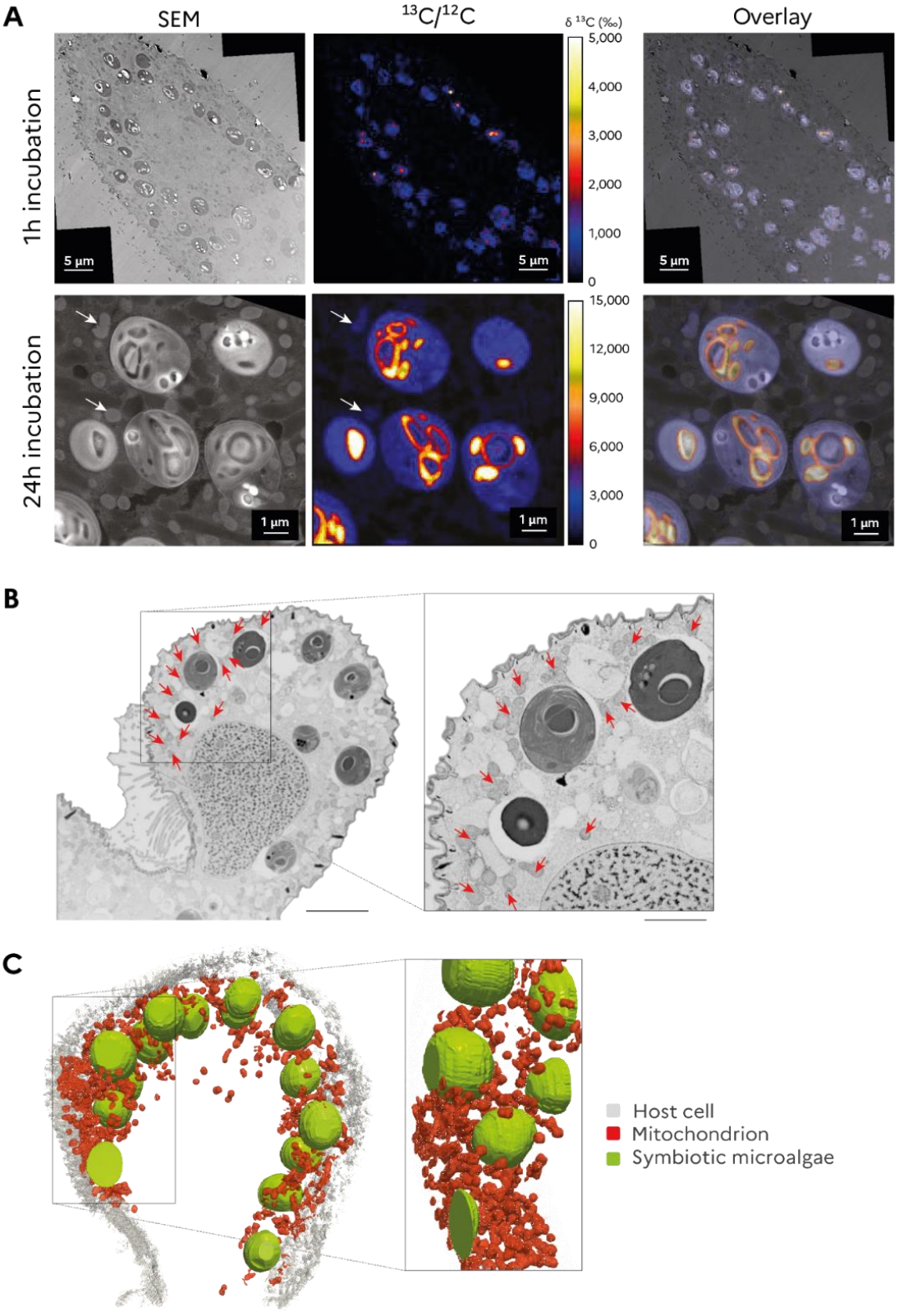
A
SEM
13C/12C
δ 13C (‰)
5,000
4,000
3,000
2,000
1,000
0
Overlay
1h incubation
5 µm
5 µm
5 µm
24h incubation
15,000
12,000
9,000
6,000
3,000
0
1 µm
1 µm
1 µm
B
C
Host cell
Mitochondrion
Symbiotic microalgae

Figure 6. Carbon transfer in the host and aggregation of host mitochondria surrounding the symbiotic microalgae. A) Correlated SEM (Scanning Electron Microscope) and NanoSIMS images of the distribution of ^{13}C enrichment in symbiotic microalgae of the host *Paramecium bursaria* after 1h and 24h-incubation with ^{13}C-labelled bicarbonate. Colors in NanoSIMS maps represent enrichment relative to an unlabeled sample. At 24h incubation, white arrows indicate carbon transfer into unknown host structures. **B)** Electron micrograph from a FIB-SEM stack obtained from the host *P. bursaria* and its symbiotic microalgae. Red arrows indicate the host mitochondria. Scale bar: 1µm. **C)** 3D reconstruction of the host mitochondria (red) surrounding the symbiotic microalgae (green).

Does the host act as a sink influencing carbon metabolism of its microalgae?

In plants and microalgae, photosynthesis and primary production are mainly driven by inputs such as light and CO_2, but also by the balance between production and consumption of energy (Demmig-Adams et al. 2017; Krapp and Stitt 1995). This is the source-sink relationship, whereby production by the source (e.g. a microalga) can be enhanced by sinks (e.g. consumption for growth and/or export out of the site of production) (Abramson et al. 2016). Here, we show that carbon uptake and starch production in symbiotic microalgae are higher than in free-living cells while cell growth is lower. In addition, NanoSIMS results demonstrate transfer of some of this carbon to the host. We therefore hypothesize that the host could act as an additional sink, whereby its energetic demands influence photosynthetic production of its intracellular microalgae (source). This source-sink concept has also been proposed to be central in other symbiotic systems, from reefs to plants (Adams et al. 2020; Andersen 2003). To further understand the source-sink relationship in photosymbiosis, we quantified starch production of symbiotic microalgae when external glucose, considered to be one of the main photosynthates transferred (Arriola et al. 2018b; Fujishima 2009; Sørensen et al. 2020), was provided to the host. An incubation experiment with ^{13}C-glucose showed that the host *Paramecium bursaria* is able to take up this sugar molecule (9565.51 ‰ enrichment) (Table S12). We then compared starch production of symbiotic microalgae in a glucose-fed host and control (host without glucose) during six hours of light (from 10 am to 4 pm). This experiment revealed that symbiotic microalgae produced 2.3 times less starch at the end of the day when the host was provided with glucose (4.27 ± 0.73 pg.cell^{-1} in control *vs* 2.52 ± 0.36 pg.cell^{-1}) (Fig. 7A). This lower starch production was not accompanied by a change in photosynthetic activity (net oxygen production) that remained similar in both conditions (Fig. S5, Table S13). Therefore, lower energetic demands of the host led to a cellular process that diminished starch production of its microalgae (but not light reactions of photosynthesis).

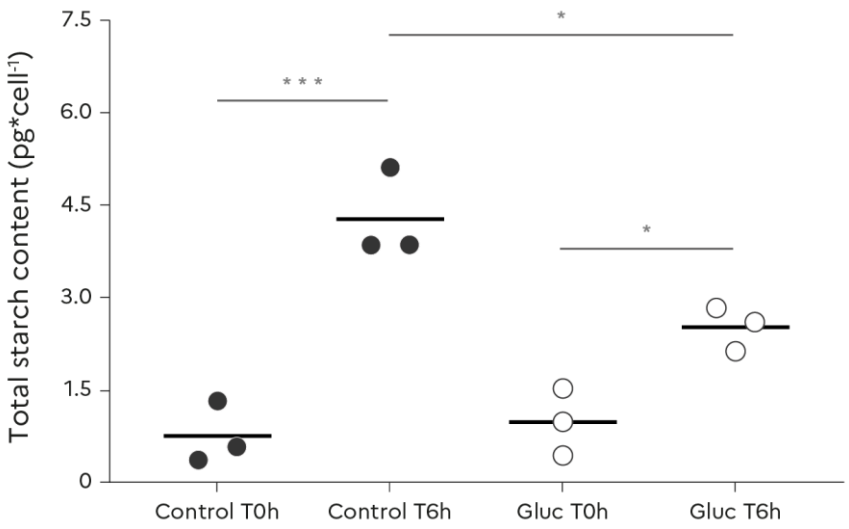

Figure 7. Starch production in symbiotic microalgae within hosts exposed to glucose. Total starch quantification of symbiont microalgae after exposure to glucose (75 mM) versus control (without glucose). Scatter plots shows the mean of biological triplicates± SD. ***p=0.0001: *p < 0.05. See also Supplementary Table S13 and Fig S5. (ANOVA, N = 12, $F_{condition}$=5.8, F_{time}=63.66; $F_{interaction}$ = 9.726).

I.3 Conclusion and Perspectives

In symbiosis versus free-living:

Larger cells	6-fold
Increase of E' related organelles	6-fold chloroplast 9-fold pyrenoid
High carbon fixation	13-fold
High **carbon storage**	5.6-fold starch 12-fold LD
✓ **Carbon dynamics**	High accumulation LD over time

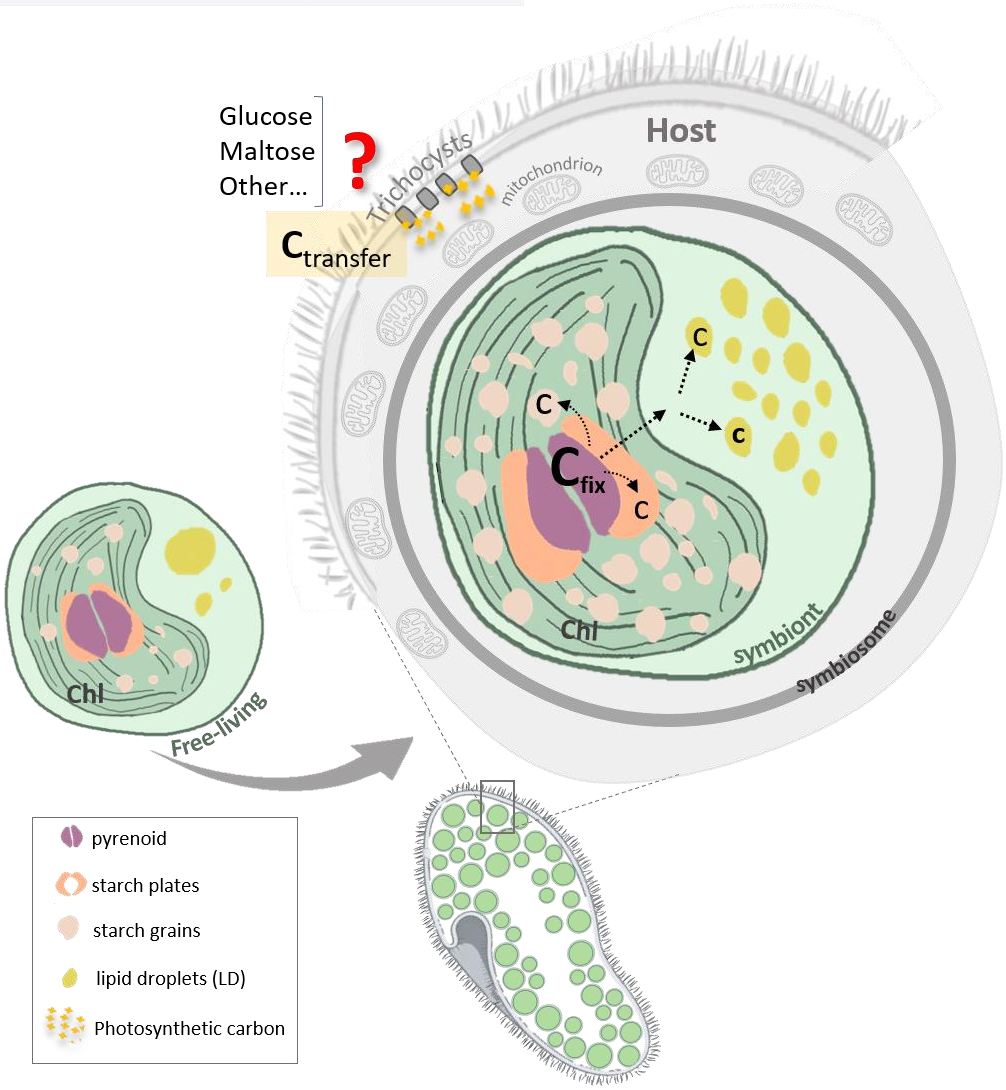

General scheme. Symbiotic microalgae have larger chloroplasts (Chl) and pyrenoid (purple), potentially linked to increased carbon fixation (C_{fix}). The dynamics of starch turnover are maintained in symbiosis, with higher production during the day and increased lipid droplets (LD) accumulation overnight. The host could benefit from the carbon exported ($C_{transfer}$) by its microalgae.

This multi-scale study provides evidence that photosynthetic production is enhanced in symbiotic microalgae compared to their free-living stage. We showed that symbiotic microalgae, the growth rate of which is repressed, have a 6-fold larger chloroplast with a 9-fold larger pyrenoid that contains 13 times more Rubisco. This is accompanied by 16-fold higher carbon fixation per microalgal cell. Enhancement of photosynthetic production in symbiotic microalgae therefore occurs in both marine (Uwizeye et al. 2021) and freshwater photosymbioses, suggesting common mechanisms within hosts. To date, the fate of this photosynthetically-derived carbon energy in photosymbiotic systems had not been fully addressed. Here, we demonstrate that the dynamics of diel starch turnover of the microalga is maintained in symbiosis, suggesting that the endogenous circadian clock known to regulate starch is maintained within a host (Graf and Smith 2011). However, symbiotic microalgae store more carbon as starch and neutral lipids compared to the free-living stage. More specifically, there is higher starch production during the day and higher consumption overnight, while neutral lipids (TAG) increase overnight and accumulate over successive days. Given the lower cell growth in symbiosis, these results indicate that symbiotic microalgae produce more organic carbon that needed for their growth. This excess of carbon energy stored in lipid droplets, which makes symbionts "fatty", could nutritionally benefit the host when algal digestion takes place, a known phenomenon when the host is under starvation (Kodama and Miyazaki 2021). On a shorter time-scale, we also showed that the host can benefit from carbon exported by its microalgae, likely for sustaining its respiration needs, consistent with high density of host mitochondria surrounding the symbionts. Therefore, the host can act as an additional sink, likely influencing photosynthetic production by its microalgal symbionts, as indicated by the observation that symbiotic microalgae produce less starch when host energetic demands are lower. Nevertheless, lipid accumulation in symbiotic microalgae within the host *Paramecium bursaria* tends to show that the host is not a strong sink, in which case a massive import of photosynthetically-produced carbon would be observed. The host may potentially regulate carbon import from its microalgae based on its energetic demands in order to avoid uncontrolled efflux of carbohydrates that could be harmful for the system. Further studies are needed to fully investigate this source-sink relationship in photosymbiosis, which may be a foundational mechanistic process underlying the metabolic integration of microalgae and host cells.

I.4 Material and Methods

Strains and culture conditions

The ciliate *Paramecium bursaria* (CCAP1660/18) in symbiosis with *Micractinium conductrix* was obtained from the Culture Collection of Algae and Protozoa (https://www.ccap.ac.uk/). The culture medium for *P. bursaria* was prepared by inoculating Volvic natural mineral water with the bacterial strain *Serratia marcescens* CIP103235TI (Pasteur institute Bacteria CIP) and 0.66 g/L protozoan pellets (Carolina Biological Supply, NC, USA) 24h before use. The microalga *Chlorella vulgaris* (CCAP 211/11B) was also obtained from the Culture Collection of Algae and Protozoa. The *Micractinium conductrix culture* was obtained in culture by isolating its symbiotic stage within the ciliate host *P. bursaria* (CCAP1660/18). Host cultured of 2 weeks-old were filtrated to recovered symbiotic microalgae of the medium. Cultures were filtrated through a 40 µm cell strainer and 10 µm filter that removed the host. The filtrate was centrifuged (2 min at 2 500 g) and plated on modified solid High Salt Medium (HSM) (Gorman and Levine 1965; Sueoka 1960). Microalgae were maintained at 20°C with a 12:12 h light/dark cycle - light intensity of 40 µE m^{-2} s^{-1} - and re-streaked on plates every week. After a period of growth, an individual colony of *M. conductrix* was re-streaked onto a fresh plate to establish a pure strain. All cultures (host and free-living microalgae) were maintained at 20°C under with a 12:12 h light/dark cycle with a light intensity of 40 µE m^{-2} s^{-1}. Prior to carrying out experiments, free-living microalgal strains were transferred to liquid medium and maintained in the same conditions under constant agitation (80 rpm). The concentration of free-living and symbiotic microalgal cells was assessed with a LUNA-FLTM automated fluorescence cell counter (Logos Biosystems Inc., Anyang-si, Gyeonggi-do, South Korea).

Physiological measurements: starch and neutral lipid quantification and photosynthetic oxygen measurements

Starch extraction was carried out by physicochemical disruption of cells following previous protocols (Wong et al. 2019). Briefly, cell cultures (triplicate samples for each experimental condition) were suspended in 1.2 ml of NaOH (1 M) in a centrifuge tube. The suspension was placed in a water bath at 90 °C for 10 min and then cooled to room temperature. Total starch content was then quantified with

a commercial starch kit (Amylase/Amyloglucosidase Method - Product Code STA-20, SIGMA) and a spectrometer following the manufacturer's instructions. The effect of external glucose on the total starch content of symbiotic microalgae was addressed by adding 75mM of glucose to the culture medium and incubating host cells containing symbiotic microalgae for 6 hours (from 10 am to 4 pm). Starch extraction and total starch quantification was carried out as described above. The control condition (without glucose) followed the same procedure. Total starch quantification is summarized in Tables S7 and S13.

Neutral lipids was quantified by Nile Red (Sigma Aldrich) fluorescent staining (excitation wavelength at 532 nm and emission at 565 nm), as previously described (Abida et al. 2015; Cooksey et al. 1987). Cultures were first adjusted to a density of 1 million cells per ml. Nile Red solution (40 µl of a 2.5 µg.ml-1 stock solution in DMSO) was added to replicate 160 µl sub-samples of cell suspension in a black 96-well plate. Fluorescence was then measured using a TECAN infinite M1000 PRO (λ_{ex} = 530 nm). Nile Red staining was verified on our cells using confocal fluorescence microscope (Fig. S4). Micrographs showing the lipid droplets in microalgae were obtained using a Zeiss LSM 900 microscope using a 450–490-nm excitation filter. The results of neutral lipid quantification are summarized in Table S11.

Oxygen measurements was conducted following (Yee et al. 2023). Briefly, 500 µL of sample was used to measure oxygen in a WALZ KS-2500 water-jacketed chamber (Heinz Walz GmbH) paired with a FSO2-1 oxygen meter and optical microsensor (PyroScience GmbH). Samples were illuminated at 300 µmol photons m^{-2} sec^{-1} with stirring at 20° C in a MINI-PAM-II controlled by WinControl-3 software (Heinz Walz GmbH). Gross maximum oxygen production was calculated by the equation: $O_{2gross} = O_{2net}$ – respiration. The results of O_2 production rate analyses are summarized in Table S14.

Sample preparation for electron microscopy

High-pressure freezing (HPM100, Leica) followed by freeze substitution (EM ASF2, Leica) was conducted to prepare samples for electron microscopy following the protocols of (Decelle et al., 2019, 2021, Uwizeye et al 2021). Both free-living and symbiotic microalgae were harvested at exponential growth phase and concentrated by 2 min centrifugation at 2 500 g prior to cryo-fixation.

Focused Ion Beam-Scanning Electron Microscope (FIB-SEM)

Focused Ion Beam (FIB) tomography was performed with either a Zeiss NVision 40 or a Zeiss CrossBeam 550 microscope (Zeiss, Germany). The resin block containing the cells was fixed on a stub with carbon paste and surface-abraded with a diamond knife in a microtome to obtain a flat and clean surface. Samples were then metallized with 4 nm of platinum to avoid charging during observations. Inside the FIB-SEM, a second platinum layer (1–2 μm) was deposited locally on the analyzed area to mitigate possible curtaining artefacts. The sample was then abraded slice by slice with the Ga+ ion beam (generally with a current of 700 pA at 30 kV). Each exposed surface was imaged by scanning electron microscopy (SEM) at 1.5 kV and with a current of ~1 nA using the in-lens EsB backscatter detector. In general, similar milling and imaging mode were used for all samples. Automatic correction of focus and astigmatism was performed during image acquisition, usually at approximately hourly intervals. For each slice, a thickness of 6 to 8 nm was removed, and SEM images were generally recorded with a pixel size between 6 to 8 nm, providing an isotropic voxel size. Whole volumes were imaged with 800–2000 frames, depending on the cell type and volume. Raw electron microscopy data are deposited in the Electron Microscopy Public Image Archive (EMPIAR), accession code EMPIAR-XXX.

FIB-SEM analysis, segmentation and morphometrics

Image processing was initiated using software Fiji (https://imagej.net/Fiji) to crop selected cells and perform registration. Segmentation was based on pixel classification by a semi-automatic method adopted from (Uwizeye et al. 2020) using 3D slicer software (https://www.slicer.org/) and a supervised semi-automatic pixel classification mode (3 to 15 slices automatically segmented for each region of interest- ROI). Along with the cell, the main organelles and structures of the algal cells (nucleus, chloroplast, mitochondria, pyrenoid, starch and lipid droplets) were segmented. Morphometric analyses were calculated using the Statistics Module in 3D slicer. Results are provided in supplementary Tables S1-S4, S9-10.

^{13}C bulk enrichment (Elemental Analyzer–Isotope Ratio Mass Spectrometry) and isotope analysis

Elemental analyzer isotope ratio mass spectrometry (EA-IRMS) and isotope analysis was conducted on free-living (*Chlorella vulgaris* and *Micractinium conductrix*) and symbiotic microalgae (*M. conductrix* from *P. bursaria* CCAP1660/18) to detect ^{13}C-bicarbonate assimilation after 1 hour of treatment. An equivalent of 0.4 mg fresh weight (corresponding to 10^7 cells) was used for the bulk analysis (Kimball et al. 1959). Cells were harvested at exponential growth phase (e.g. after 4 days of culture). For ^{13}C enrichment, 10% of $H^{13}CO_3$ as a final concentration was used as the isotopic solution and added to modified HSM medium and bacterized Volvic-Pellet medium for free-living and symbiotic microalgae, respectively. After incubation, free-living algae were counted before centrifugation (15,000 rcf for 1 min at 20°C). Supernatant was discarded and the pellet was rinsed by three serial centrifugations, once with modified HSM and twice with MiliQ water. After the final centrifugation (15,000 rcf for 1 min at 20°C), cells were transferred into tin capsules for EA-IRMS analysis. For isolating symbiotic microalgae, host cells were mechanically disrupted by sonication (amplitude 40% * 2min, E 1J/s, 20ms - On/80ms - Off, Branson sonifier250) followed by a centrifugation (5 000 g for 2 min at 20°C) and two sequential filtration steps (40 µm cell strainer and 10 µm filter). The supernatant was discarded and symbiotic cells transferred into tin capsules for EA-IRMS analysis. All tin capsules were dried at room-temperature for one week before EA-IRMS analysis (LIENSs platform, La Rochelle). Control samples (unlabeled) were not incubated with ^{13}C-labelled bicarbonate isotopes but otherwise followed the same steps. Carbon assimilation was calculated as described in (Uwizeye 2021). In brief, ^{13}C-uptake per cell in free-living and symbiotic microalgae was estimated from the calculated ^{13}C-excess and averaged total carbon. Data was expressed as carbon uptake per cell and carbon uptake normalized per carbon (Table S5). In the same experimental conditions, we also incubated cells with ^{13}C-labelled glucose for 24h to see whether host cells can uptake this molecule. 2.5 mL of ^{13}C-glucose was added in the culture flask to reach a final concentration of 1mM. Results are provided in Table S12.

Rubisco quantification

Total protein extracts were obtained from microalgal cells in exponential phase of growth (e.g. 4 days) in 50 mM Tris buffer pH 8.0 supplemented with protein inhibitor cocktail (539131, Calbiochem). Free-living and symbiotic microalgae were disrupted by bead beating with a Precellys device (Bertin Technologies) using micro glass beads (500 µm) with two 30 seconds cycles at 5000 rpm. After centrifugation, proteins in the supernatant were precipitated overnight at -20°C in 100% acetone. After a second centrifugation, the pellet was solubilized for 5 min (RT) in 50 mM Tris (pH 6.8), 2% sodium dodecyl sulphate, 10 mM EDTA, and protein inhibitor cocktail. After a second centrifugation, supernatant was retained and protein quantified with the DC Protein assay kit II (Biorad). Proteins samples (1.5µg and 3µg of proteins) of free living (*C. vulgaris and M. conductrix*) and symbiotic microalgae (*M. conductrix* from *P. bursaria* CCAP1660/18) were loaded on 10% SDS-PAGE gels (Mini-PROTEAN TGX Precast Protein Gels, Biorad) and blotted onto nitrocellulose membranes. A Rubisco positive control (AS01017S, Agrisera) was used to generate a standard curve. Membranes were blocked for 1h with 5% low fat milk powder in TBS-T Tween 0.1% and probed with anti-RBCL antibody (AS03037, Agrisera, 1:10000, ON) and secondary HRP conjugated anti rabbit antibody (111-035-003) (Interchim, 1:10000, 1h) in TBS-T containing 5% low fat milk powder. Antibody incubations were followed by washing in TBS-T. All steps were performed at room temperature with agitation. Blots were developed for 1min with ECL Prime detection kit (RPN2232, Amersham) according the manufacturer's instructions (GE Heathcare). Images of the blot were obtained using a CCD imager (Chemidoc MP system, Biorad) and ImageJ software. Data was expressed as rubisco per cell (Table S6).

Data analysis

Morphometric data was analyzed with Graphpad Prism 6 software and R studio. Statistical comparisons were performed with non-parametric unpaired ANOVA for a multiple comparison with Dunn's test correction.

Data Availability

Raw 3D electron microscopy images data have been deposited on EMPIAR: DOI:. All other study data are included in the article and/or supporting information.

Acknowledgments

This project received funding from the LabEx GRAL (ANR-10-LABX-49-01), financed within the University Grenoble Alpes graduate school (Ecoles Universitaires de Recherche) CBHEUR- GS (ANR-17-EURE-0003). JD was supported by CNRS and ATIP-Avenir program funding. We thank Anders Meibom and Stephane Escrig for help with NanoSIMS analysis. We also thank the EA-IRMS platform (Gael Guillou and Benoit Lebreton) - a FEDER funding. We thank Guy Schoehn and Christine Moriscot, and the electron microscope facility at IBS, which is supported by the Rhône-Alpes Region, the Fondation Recherche Medicale (FRM), the fonds FEDER, the Center National de la Recherche Scientifique (CNRS), the CEA, the University of Grenoble, EMBL, and the GIS Infrastructures en Biologie Sante et Agronomie (IBISA). We thank Ian Probert for critically reading the manuscript and suggesting improvements.

Competing interests

The authors declare no competing interest.

Author contributions

A.C.G. and J.D. designed research, interpreted results, and drafted the manuscript with the support of G.C. J.D. supervised the work. A.C.G., B.G. and J.D. jointly performed the sample preparation for microscopy. P.H.J., N.L.S. and Y.S. conducted FIB-SEM imaging, and A.C.G. analyzed the data. C.L. conducted nanoSIMS analyses and analyzed the data. F.C. and D.Y. performed and assisted with experiments. A.C.G. and J.D. wrote the manuscript with G.C.

Supplementary data

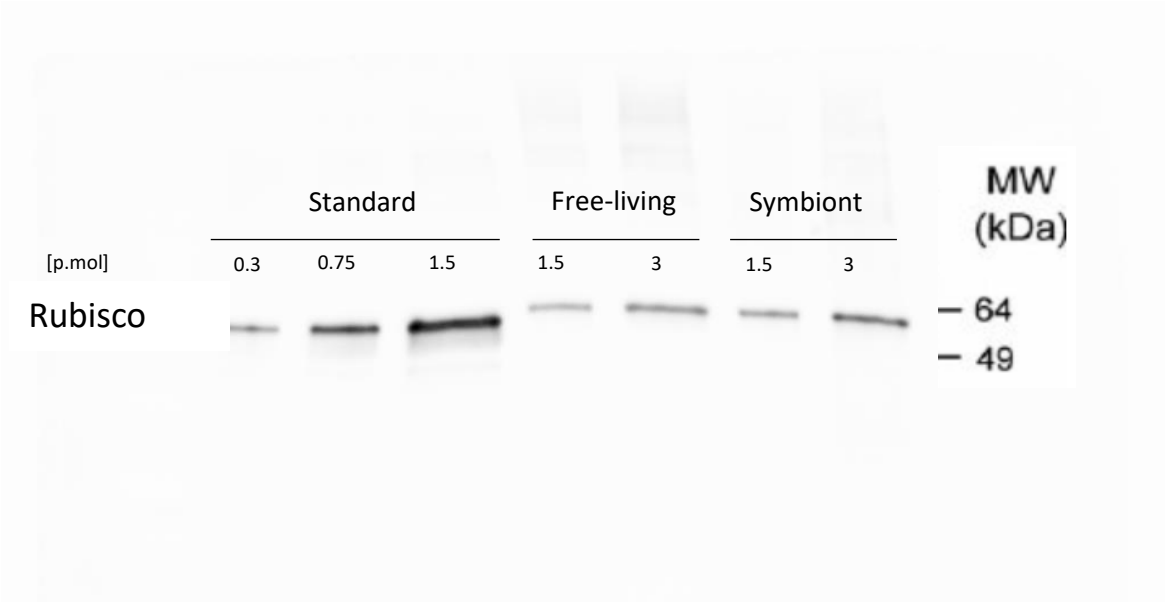

Fig. S1 Western blot analysis of ribulose-1,5-bisphosphate carboxylase (RuBisCo). First 3 lines to the left represent Rubisco standard at different concentrations expressed in pico mol. The remaining lanes correspond to Rubisco protein extracted from free-living (*M. conductrix;* $2.3*10^8$ total cells) and symbiotic microalgae (*M. conductrix* in symbiosis with *P. bursaria* CCAP1660/18; $2*10^7$ total cells) in two different quantities. Last line corresponds to molecular marker protein.

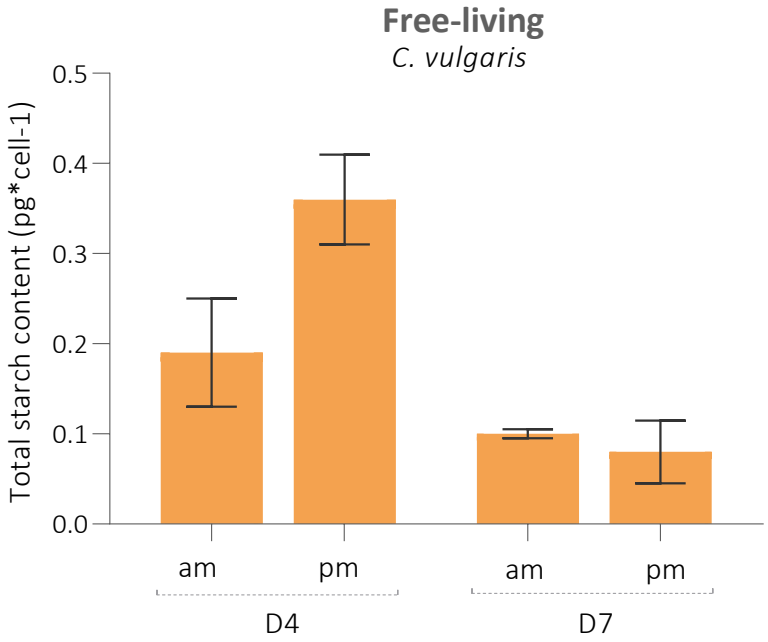

Fig. S2 Total starch quantification over the cell growth of free-living *Chlorella vulgaris*. Starch quantification was assessed by enzymatic assay (Amylase/Amyloglucosidase Method - Product Code STA-20, SIGMA). Cells were harvested at day 4=D4 and day 7=D7 of culture, corresponding to the mid and late exponential growth phase. Bar plots represent the mean of total starch content per cell of biological triplicates ± SE.

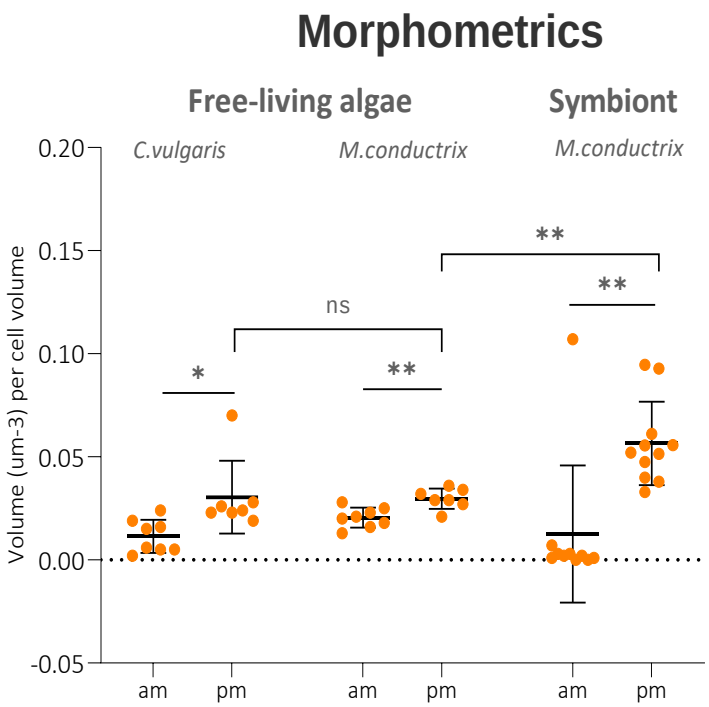

Fig. S3 Volume of total starch per algal cell volume (% occupancy) calculated from FIB-SEM volumetrics between both free-living microalgae (*C. vulgaris* and *M. conductrix*) and symbiotic microalgae (*M. conductrix* of *P. bursaria* CCAP1660/18) harvested in the morning and afternoon.

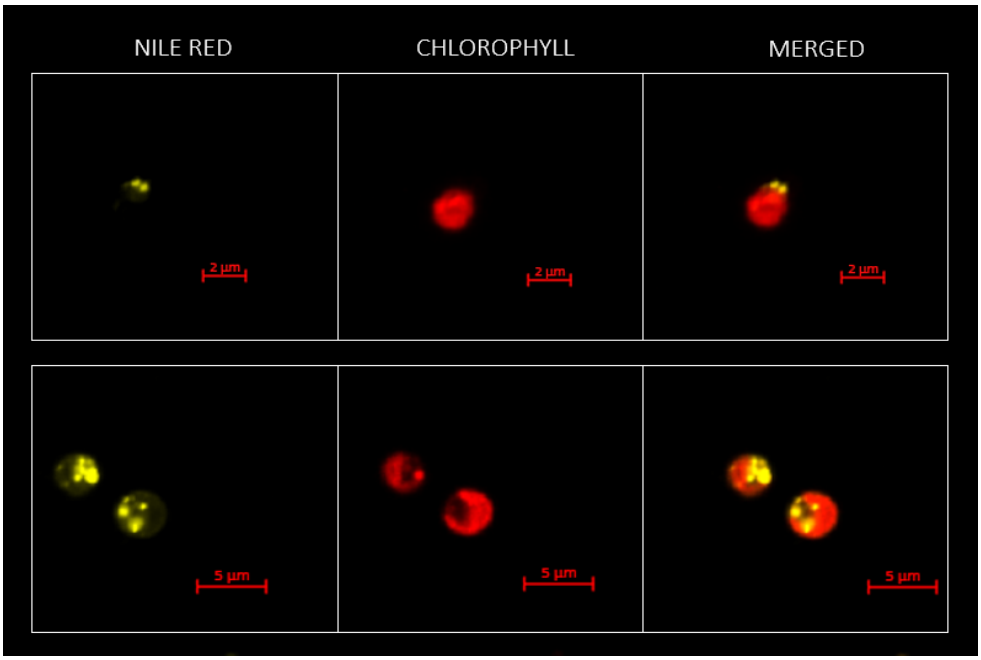

Fig. S4 Nile Red staining coupled with confocal fluorescence microscopy to observe neutral lipids in free-living (*M. conductrix*) and symbiotic microalgae (*M. conductrix* of *P. bursaria* CCAP1660/18). Nile red staining shows that neutral lipids are mainly localized in lipid droplets (yellow) in the algal cytoplasm, outside the chloroplast (visible in red by chlorophyll autofluorescence).

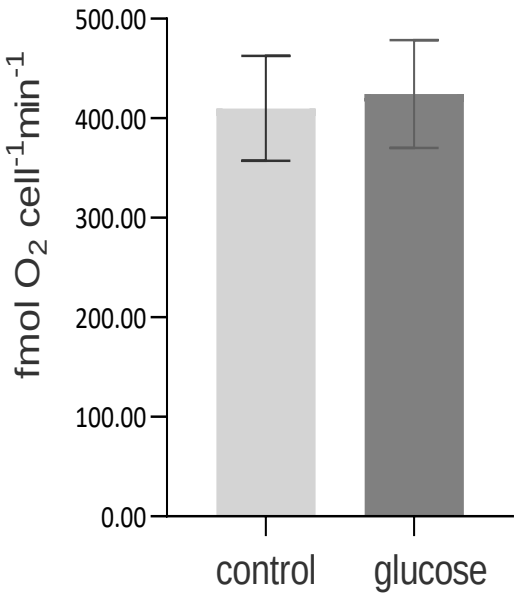

Fig. S5 Measurements of gross maximum photosynthetic oxygen production of *Paramecium bursaria* in symbiosis with *Micractinium conductrix* exposed glucose (75 mM) compared to the control for 6 hours in light). Bar plots show the mean values of triplicate measurements and ± SEM.

Table S1. FIB-SEM based morphometrics of free-living (*Chlorella vulgaris* and *Micractinium conductrix*) and symbiotic (*M. conductrix* of *P. bursaria* CCAP1660/18) microalgae revealing the volume of the cell, total starch, lipid droplets, pyrenoid, nucleus, mitochondrion and chloroplast (μm^3).

Chlorella vulgaris	$Cell_1$ (μm^3)	$Cell_2$ (μm^3)	$Cell_4$ (μm^3)	$Cell_5$ (μm^3)	$Cell_8$ (μm^3)	$Cell_9$ (μm^3)	**Average (μm^3)**	**STD (μm^3)**
total starch	0.14	0.36	0.01	0.07	0.39	2.12	0.51	0.80
starch plates	0.14	0.36	0.01	0.07	0.37	0.42	0.23	0.18
starch grains	0.00	0.00	0.00	0.00	0.02	1.70	0.29	0.69
lipid droplets	0.36	0.43	0.06	0.21	0.22	0.13	0.24	0.14
cell	10.27	13.82	5.49	10.26	15.89	17.49	12.20	4.40
pyrenoid	0.23	0.29	0.06	0.13	0.22	0.18	0.18	0.08
nucleus	0.65	0.93	0.70	1.07	1.53	0.75	0.94	0.33
mitochondrion	0.40	0.66	0.18	0.37	0.47	0.59	0.45	0.17
chloroplast	3.70	5.00	2.40	4.27	7.55	6.93	4.98	1.96

Micractinium conductrix	$Cell_1$ (μm^3)	$Cell_2$ (μm^3)	$Cell_3$ (μm^3)	$Cell_4$ (μm^3)	$Cell_5$ (μm^3)	$Cell_6$ (μm^3)	$Cell_7$ (μm^3)	$Cell_8$ (μm^3)	$Cell_9$ (μm^3)	$Cell_{10}$ (μm^3)	**Average (μm^3)**	**STD (μm^3)**
total starch	0.20	0.08	0.31	0.14	0.11	0.11	0.26	0.27	0.19	0.28	0.20	0.08
starch plates	0.20	0.08	0.30	0.11	0.24	0.26	0.14	0.11	0.18	0.27	0.19	0.08
starch grains	0.00	0.00	0.02	0.00	0.02	0.00	0.00	0.00	0.01	0.01	0.01	0.01
lipid droplets	0.07	0.06	0.07	0.04	0.07	0.07	0.04	0.06	0.05	0.04	0.06	0.02
cell	10.41	6.10	11.07	5.54	8.22	9.26	6.06	6.58	6.56	8.08	7.79	1.94
pyrenoid	0.17	0.09	0.20	0.09	0.16	0.11	0.09	0.10	0.11	0.18	0.13	0.04
nucleus	0.97	0.79	1.04	0.76	0.86	0.95	0.76	0.78	0.74	0.83	0.85	0.11
mitochondrion	0.29	0.16	0.31	0.18	0.22	0.22	0.17	0.23	0.17	0.19	0.21	0.05
chloroplast	5.12	2.79	5.20	2.32	3.83	4.41	2.69	3.09	2.97	3.49	3.59	1.02

***Micractinium conductrix* (isolated from *P. bursaria* CCAP 1660/18)**	$Cell_1$ (μm^3)	$Cell_2$ (μm^3)	$Cell_3$ (μm^3)	$Cell_4$ (μm^3)	$Cell_5$ (μm^3)	$Cell_6$ (μm^3)	$Cell_7$ (μm^3)	$Cell_8$ (μm^3)	$Cell_9$ (μm^3)	$Cell_{10}$ (μm^3)	**Average (μm^3)**	**STD (μm^3)**
total starch	2.90	3.17	2.37	2.12	1.72	2.11	2.24	0.34	0.40	0.28	1.77	1.07
starch plates	2.56	2.29	1.99	1.99	1.60	2.09	1.75	0.34	0.40	0.28	1.53	0.86
starch grains	0.35	0.89	0.38	0.13	0.13	0.02	0.49	0.00	0.00	0.00	0.24	0.29
lipid droplets	0.91	1.33	0.80	0.92	0.64	0.68	1.00	0.63	0.45	0.76	0.81	0.25
cell	51.61	59.18	55.69	47.93	42.39	45.84	54.39	28.06	26.22	24.23	43.55	12.97
pyrenoid	1.06	1.44	1.39	1.35	1.29	0.93	1.39	1.10	0.83	0.65	1.14	0.27
nucleus	2.53	2.60	3.35	2.40	2.05	1.83	2.46	1.81	1.67	1.84	2.25	0.52
mitochondrion	1.76	1.94	2.31	1.67	1.45	1.88	1.86	1.01	0.82	0.78	1.55	0.52
chloroplast	27.60	32.14	30.07	26.28	23.72	24.04	29.38	12.07	12.76	11.18	22.92	7.97

Table S2. Volume occupancy (organelle-volume/cell-volume ratio) based on FIB-SEM morphometrics in free-living (*Chlorella vulgaris* and *Micractinium conductrix*) and symbiotic (*M. conductrix* of *P. bursaria* CCAP1660/18) microalgae of starch, lipid droplets, pyrenoid, nucleus, mitochondrion and chloroplast (%).

Chlorella vulgaris	$Cell_1$ (%)	$Cell_2$ (%)	$Cell_4$ (%)	$Cell_5$ (%)	$Cell_8$ (%)	$Cell_9$ (%)	**Average (%)**	**STD (%)**
starch plates	1.32	2.59	0.17	0.65	2.33	2.40	1.58	1.02
starch grains	0.00	0.00	0.00	0.00	0.12	9.73	1.64	3.96
lipid droplets	3.54	3.11	1.12	2.06	1.39	0.75	2.00	1.12
cell	46.70	44.53	37.86	40.30	34.74	38.82	40.49	4.42
pyrenoid	2.20	2.10	1.06	1.29	1.36	1.02	1.51	0.52
nucleus	6.29	6.74	12.67	10.43	9.61	4.27	8.34	3.10
mitochondrion	3.90	4.77	3.34	3.61	2.93	3.38	3.66	0.63
chloroplast	36.05	36.16	43.78	41.66	47.51	39.63	40.80	4.47

Micractinium conductrix	$Cell_1$ (%)	$Cell_2$ (%)	$Cell_3$ (%)	$Cell_4$ (%)	$Cell_5$ (%)	$Cell_6$ (%)	$Cell_7$ (%)	$Cell_8$ (%)	$Cell_9$ (%)	$Cell_{10}$ (%)	**Average (%)**	**STD (%)**
starch plates	1.97	1.32	2.67	2.26	1.65	2.05	2.94	2.84	2.72	3.29	2.37	0.62
starch grains	0.00	0.00	0.17	0.06	0.00	0.02	0.22	0.04	0.17	0.16	0.08	0.08
lipid droplets	0.70	0.90	0.59	0.58	0.90	0.68	0.91	0.77	0.69	0.49	0.72	0.15
cell	34.47	35.03	35.68	36.09	33.62	36.91	34.17	34.83	35.67	37.94	35.44	1.31
pyrenoid	1.63	1.53	1.78	1.49	1.50	1.56	1.97	1.23	1.61	2.25	1.66	0.29
nucleus	9.31	12.88	9.41	12.47	11.80	13.73	10.49	10.25	11.23	10.24	11.18	1.50
mitochondrion	2.77	2.59	2.76	2.76	3.51	3.17	2.72	2.37	2.61	2.41	2.77	0.34
chloroplast	49.16	45.76	46.94	44.28	47.02	41.86	46.58	47.67	45.31	43.22	45.78	2.18

Micractinium conductrix (isolated from P. bursaria CCAP 1660/18)	$Cell_1$ (%)	$Cell_2$ (%)	$Cell_3$ (%)	$Cell_4$ (%)	$Cell_5$ (%)	$Cell_6$ (%)	$Cell_7$ (%)	$Cell_8$ (%)	$Cell_9$ (%)	$Cell_{10}$ (%)	**Average (%)**	**STD (%)**
starch plates	4.95	3.87	3.57	4.15	3.77	4.56	3.21	1.21	1.54	1.14	3.20	1.40
starch grains	0.67	1.50	0.68	0.27	0.30	0.04	0.90	0.00	0.00	0.00	0.44	0.50
lipid droplets	1.77	2.24	1.44	1.92	1.50	1.49	1.84	2.25	1.70	3.12	1.93	0.51
cell	28.75	27.99	27.66	27.53	27.18	31.37	29.54	39.55	35.43	36.11	31.11	4.38
pyrenoid	2.06	2.43	2.49	2.81	3.03	2.02	2.55	3.92	3.15	2.68	2.71	0.56
nucleus	4.91	4.39	6.01	5.01	4.84	3.99	4.52	6.45	6.39	7.59	5.41	1.14
mitochondrion	3.41	3.28	4.16	3.48	3.43	4.10	3.42	3.61	3.12	3.21	3.52	0.35
chloroplast	53.48	54.30	53.99	54.83	55.95	52.44	54.01	43.01	48.68	46.15	51.68	4.27

Table S3. FIB-SEM based morphometrics of free-living (*Chlorella vulgaris* and *Micractinium conductrix*) and symbiotic (*M. conductrix* of *P. bursaria* CCAP1660/18) microalgae revealing the volume of the pyrenoid and chloroplast (μm^3).

Chlorella vulgaris	$Cell_1$ (μm^3)	$Cell_2$ (μm^3)	$Cell_3$ (μm^3)	$Cell_4$ (μm^3)	$Cell_5$ (μm^3)	$Cell_8$ (μm^3)	$Cell_9$ (μm^3)	**Average (μm^3)**	**STD (μm^3)**
cell	10.27	13.82	5.49	10.26	15.89	17.49	12.20	4.40	
pyrenoid	0.23	0.29	0.06	0.13	0.22	0.18	0.18	0.08	
chloroplast	3.70	5.00	2.40	4.27	7.55	6.93	4.98	1.96	

Micractinium conductrix	$Cell_1$ (μm^3)	$Cell_2$ (μm^3)	$Cell_3$ (μm^3)	$Cell_4$ (μm^3)	$Cell_5$ (μm^3)	$Cell_6$ (μm^3)	$Cell_7$ (μm^3)	$Cell_8$ (μm^3)	$Cell_9$ (μm^3)	$Cell_{10}$ (μm^3)	**Average (μm^3)**	**STD (μm^3)**
cell	10.41	6.10	11.07	6.06	6.58	5.54	8.22	9.26	6.56	8.08	7.79	1.94
pyrenoid	0.17	0.09	0.20	0.09	0.10	0.09	0.16	0.11	0.11	0.18	0.13	0.04
chloroplast	5.12	2.79	5.20	2.69	3.09	2.32	3.83	4.41	2.97	3.49	3.59	1.02

***Micractinium conductrix* (isolated from *P. bursaria* CCAP 1660/18)**	$Cell_1$ (μm^3)	$Cell_2$ (μm^3)	$Cell_3$ (μm^3)	$Cell_4$ (μm^3)	$Cell_5$ (μm^3)	$Cell_6$ (μm^3)	$Cell_7$ (μm^3)	$Cell_8$ (μm^3)	$Cell_9$ (μm^3)	$Cell_{10}$ (μm^3)	**Average (μm^3)**	**STD (μm^3)**
cell	51.61	59.18	55.69	47.93	42.39	45.84	54.39	28.06	26.22	24.23	43.55	12.97
pyrenoid	1.06	1.44	1.39	1.35	1.29	0.93	1.39	1.10	0.83	0.65	1.14	0.27
chloroplast	27.60	32.14	30.07	26.28	23.72	24.04	29.38	12.07	12.76	11.18	22.92	7.97

Table S4. Volume occupancy (organelle-volume/cell-volume ratio, %) of the pyrenoid within the chloroplast based on FIB-SEM morphometrics in free-living (*Chlorella vulgaris* and *Micractinium conductrix*) and symbiotic (*M. conductrix* of *P. bursaria* CCAP1660/18) microalgae.

Chlorella vulgaris	$Cell_1$ (%)	$Cell_2$ (%)	$Cell_4$ (%)	$Cell_5$ (%)	$Cell_8$ (%)	$Cell_9$ (%)	**Average (%)**	**STD (%)**
pyrenoid	6.11	5.80	2.42	3.10	2.87	2.57	3.81	1.68
chloroplast	93.89	94.20	97.58	96.90	97.13	97.43	96.19	1.68

Micractinium conductrix	$Cell_1$ (%)	$Cell_2$ (%)	$Cell_3$ (%)	$Cell_4$ (%)	$Cell_5$ (%)	$Cell_6$ (%)	$Cell_7$ (%)	$Cell_8$ (%)	$Cell_9$ (%)	$Cell_{10}$ (%)	**Average (%)**	**STD (%)**
pyrenoid	3.31	3.34	3.80	3.37	3.19	3.74	4.23	2.59	3.55	5.22	3.63	0.70
chloroplast	96.69	96.66	96.20	96.63	96.81	96.26	95.77	97.41	96.45	94.78	96.37	0.70

Micractinium conductrix* (isolated from *P. bursaria* *CCAP 1660/18)	$Cell_1$ (%)	$Cell_2$ (%)	$Cell_3$ (%)	$Cell_4$ (%)	$Cell_5$ (%)	$Cell_6$ (%)	$Cell_7$ (%)	$Cell_8$ (%)	$Cell_9$ (%)	$Cell_{10}$ (%)	**Average (%)**	**STD (%)**
pyrenoid	3.85	4.48	4.61	5.13	5.42	3.86	4.72	9.11	6.47	5.81	5.35	1.56
chloroplast	96.15	95.52	95.39	94.87	94.58	96.14	95.28	90.89	93.53	94.19	94.65	1.56

Table S5. Carbon uptake rate calculated based on 1h incubation with ^{13}C-bicarbonate in free-living (*Micractinium conductrix*) and symbiotic (*M. conductrix* of *P. bursaria* CCAP1660/18) microalgae.

Sample	Isotope	condition / time	Replicate	Number of cells	liso (ng ^{13}C/sample)	liso (pg ^{13}C.cell-1)	liso (pg ^{13}C. pg C-1)
Free-living *M. conductrix*	^{13}C	1h	1	4.20E+07	42.03	**0.0010**	**0.0008**
Free-living *M. conductrix*	^{13}C	1h	2	1.63E+08	203.51	**0.0012**	**0.0013**
Free-living *M. conductrix*	^{13}C	1h	3	6.30E+07	88.47	**0.0014**	**0.0012**
	^{13}C						
Symbiotic *M. conductrix* (1660/18)	^{13}C	1h	1	1.17E+07	391.84	**0.0335**	**0.0024**
Symbiotic *M. conductrix* (1660/18)	^{13}C	1h	2	1.90E+07	204.96	**0.0108**	**0.0023**
Symbiotic *M. conductrix* (1660/18)	^{13}C	1h	3	1.70E+07	224.15	**0.0132**	**0.0020**

Sample	Isotope	condition / time	liso (ng ^{13}C/sample)	liso (pg ^{13}C.cell-1)	SD	liso (pg ^{13}C. pg C-1)	SD
Free-living *M. conductrix*	^{13}C	1h	111.34	**0.0012**	0.0002	**0.0011**	0.0003
Symbiotic *M. conductrix* (1660/18)	^{13}C	1h	273.65	**0.0192**	0.0125	**0.0022**	0.0002

Table S6. Rubisco quantification in free-living (*Micractinium conductrix*) and symbiotic (*M. conductrix* of *P. bursaria* CCAP1660/18) microalgae (pmol / cell) based on western blot. (See also Figure S1).

Sample/replicate	Rubisco* pmol						Rubisco (pmol/cell)						Rubisco (pmol / µg prot / cell)					
	1	2	3	4	5	6	1	2	3	4	5	6	1	2	3	4	5	6
Free-living *M. conductrix*	0.30	0.17	0.28	0.32	0.42	0.48	1.03E-09	7.19E-10	1.06E-09	1.09E-09	1.83E-09	1.85E-09	6.85E-10	4.79E-10	7.08E-10	3.62E-10	6.10E-10	6.15E-10
Symbiotic *M. conductrix* (1660/18)	0.25	0.38	0.32	0.33	0.81	0.59	8.58E-09	1.89E-08	8.47E-09	1.16E-08	4.05E-08	1.56E-08	5.72E-09	1.26E-08	5.64E-09	3.85E-09	1.35E-08	5.21E-09

Sample/replicate	cell number						Rubisco* pmol	Rubisco pmol/cell	Rubisco (pmol/ µg prot)	Rubisco (pmol / cell)
	1	2	3	4	5	6				
Free-living *M. conductrix*	2.95E+08	2.95E+08	2.30E+08	2.30E+08	2.63E+08	2.63E+08	0.329	1.262E-09	0.151	5.77E-10
Symbiotic *M. conductrix* (1660/18)	2.88E+07	2.88E+07	2.00E+07	2.00E+07	3.75E+07	3.75E+07	0.445	1.727E-08	0.201	7.75E-09

Average	SD
Free-living *M. conductrix*	1.32E-10
Symbiotic *M. conductrix* (1660/18)	4.16E-09

Table S7. Total starch quantification based on enzymatic assay (pg.cell^{-1}) over the day (morning and afternoon) in free-living (*Micractinium conductrix*) and symbiotic (*M. conductrix* of *P. bursaria* CCAP1660/18) microalgae (three replicates).

	M.conductrix **free-living am**	***M.conductrix*** **free-living pm**	***M.conductrix*** **free-living D+1 am**	***M.conductrix*** **free-living D+1 pm**
	0.095	0.206	0.171	0.256
	0.200	0.454	0.192	0.303
	0.138	0.288	0.183	0.226
Average	1.143	0.316	0.182	0.261
Std.Dev.	0.052	0.126	0.010	0.038

	M.conductrix **symbiont am**	***M.conductrix*** **symbiont pm**	***M.conductrix*** **symbiont D+1 am**	***M.conductrix*** **symbiont D+1 pm**
	0.629	1.328	0.788	1.660
	0.462	1.389	0.826	1.544
	0.378	1.498	0.767	1.150
Average	0.489	1.405	0.793	1.451
Std.Dev.	0.127	0.086	0.029	0.267

Table S8. Cell counting of free-living and symbiotic *M. conductrix* and the host *Paramecium bursaria*. Growth rate was calculated based on the following equation: ln (N of cells final)-ln(N of cells initial)/time2-time1 (h).

	Free-living ***M. conductrix***	**Symbiont** ***M. conductrix***	**Host** ***P. bursaria***
DOC	n° of cells	n° of cells	n° of cells
0	1.44E+05	193000	441
4	8.19E+06	558500	793
5	9.66E+06	1090000	1913
11	2.81E+07	1180000	1677

	Growth rate		
	Free-living ***M. conductrix***	**Symbiont** ***M. conductrix***	**Host** ***P. bursaria***
Days			
0-4	0.042092	0.011068	0.006117
4-5	0.006878	0.027862	0.036682
5-11	0.007415	0.000551	-0.00092
0-11	**0.01998**	**0.00686**	**0.00506**

Table S9. Volume (μm^3) of carbon reserves (starch plates, starch grains and lipid droplets) based on FIB-SEM volumetrics in free-living (*Chlorella vulgaris* and *Micractinium conductrix*) and symbiotic (*M. conductrix* of *P. bursaria* CCAP1660/18) microalgae. Table shows the compartments and structures that were segmented from different datasets (in the morning=AM and in the afternoon=PM) to assess the diel carbon dynamics.

***Chlorella vulgaris* AM time point**	$Cell_1$ (%)	$Cell_2$ (%)	$Cell_3$ (%)	$Cell_4$ (%)	$Cell_5$ (%)	$Cell_6$ (%)	$Cell_7$ (%)	$Cell_8$ (%)	**Average (%)**	**STD (%)**
starch plates	0.002	0.005	0.014	0.007	0.006	0.004	0.005	0.015	0.007	0.005
starch grains	0.000	0.000	0.010	0.009	0.000	0.015	0.000	0.000	0.004	0.006
total starch	0.002	0.005	0.024	0.016	0.006	0.019	0.005	0.015	0.011	0.008
lipid droplets	0.011	0.020	0.003	0.007	0.006	0.011	0.022	0.022	0.013	0.007
pyrenoid	0.009	0.012	0.014	0.015	0.012	0.010	0.008	0.014	0.012	0.003

***Chlorella vulgaris* PM time point**	$Cell_1$ (%)	$Cell_2$ (%)	$Cell_3$ (%)	$Cell_4$ (%)	$Cell_5$ (%)	$Cell_6$ (%)	$Cell_7$ (%)	**Average (μm^3)**	**STD (μm^3)**
starch plates	0.023	0.023	0.025	0.019	0.054	0.019	0.026	0.027	0.012
starch grains	0.000	0.001	0.001	0.004	0.017	0.001	0.002	0.004	0.006
total starch	0.023	0.024	0.026	0.023	0.070	0.019	0.028	0.031	0.018
lipid droplets	0.009	0.014	0.010	0.010	0.048	0.001	0.008	0.014	0.015
pyrenoid	0.013	0.012	0.015	0.018	0.012	0.012	0.013	0.014	0.002

***Micractinium conductrix* AM time point**	$Cell_1$ (%)	$Cell_2$ (%)	$Cell_3$ (%)	$Cell_4$ (%)	$Cell_5$ (%)	$Cell_6$ (%)	$Cell_7$ (%)	$Cell_8$ (%)	**Average (μm^3)**	**STD (μm^3)**
starch plates	0.023	0.018	0.020	0.016	0.021	0.013	0.025	0.027	0.020	0.004
starch grains	0.001	0.000	0.000	0.000	0.000	0.000	0.000	0.002	0.0003	0.001
total starch	0.023	0.018	0.020	0.016	0.021	0.013	0.025	0.028	0.021	0.005
lipid droplets	0.006	0.006	0.007	0.009	0.006	0.009	0.007	0.006	0.007	0.001
pyrenoid	0.015	0.015	0.016	0.015	0.016	0.015	0.014	0.018	0.015	0.001

***Micractinium conductrix* PM time point**	$Cell_1$ (%)	$Cell_2$ (%)	$Cell_3$ (%)	$Cell_4$ (%)	$Cell_5$ (%)	$Cell_6$ (%)	$Cell_7$ (%)	**Average (μm^3)**	**STD (μm^3)**
starch plates	0.020	0.025	0.029	0.029	0.033	0.033	0.028	0.028	0.004
starch grains	0.000	0.002	0.000	0.002	0.002	0.002	0.000	0.001	0.001
total starch	0.021	0.027	0.029	0.032	0.036	0.034	0.029	0.030	0.005
lipid droplets	0.000	0.000	0.005	0.000	0.006	0.003	0.008	0.003	0.003
pyrenoid	0.016	0.016	0.018	0.020	0.018	0.022	0.012	0.017	0.003

***Micractinium conductrix* (isolated from *P. bursaria CCAP 1660/18)* AM**	$Cell_1$ (%)	$Cell_2$ (%)	$Cell_3$ (%)	$Cell_4$ (%)	$Cell_5$ (%)	$Cell_6$ (%)	$Cell_7$ (%)	$Cell_8$ (%)	$Cell_9$ (%)	$Cell_{10}$ (%)	**Average (%)**	**STD (%)**
starch plates	0.001	0.002	0.000	0.030	0.000	0.003	0.000	0.003	0.002	0.007	0.005	0.009
starch grains	0.000	0.000	0.000	0.077	0.000	0.000	0.001	0.000	0.000	0.000	0.008	0.024
total starch	0.001	0.002	0.000	0.107	0.000	0.003	0.001	0.003	0.002	0.007	0.013	0.033
lipid droplets	0.030	0.031	0.037	0.021	0.066	0.077	0.060	0.043	0.031	0.025	0.042	0.019
pyrenoid	0.031	0.031	0.023	0.007	0.031	0.025	0.026	0.024	0.027	0.032	0.026	0.007

***Micractinium conductrix* (isolated from *P. bursaria CCAP 1660/18)* PM**	$Cell_1$ (%)	$Cell_2$ (%)	$Cell_3$ (%)	$Cell_4$ (%)	$Cell_5$ (%)	$Cell_6$ (%)	$Cell_7$ (%)	$Cell_8$ (%)	$Cell_9$ (%)	$Cell_{10}$ (%)	$Cell_{11}$ (%)	**Average (%)**	**STD (%)**
starch plates	0.066	0.047	0.030	0.063	0.047	0.045	0.034	0.043	0.044	0.036	0.045	0.045	0.011
starch grains	0.027	0.005	0.003	0.031	0.004	0.010	0.006	0.012	0.017	0.002	0.003	0.011	0.010
total starch	0.093	0.052	0.033	0.095	0.052	0.056	0.040	0.056	0.061	0.038	0.048	0.057	0.020
lipid droplets	0.033	0.038	0.041	0.025	0.026	0.039	0.035	0.051	0.033	0.034	0.030	0.035	0.007
pyrenoid	0.032	0.031	0.027	0.030	0.029	0.033	0.031	0.033	0.034	0.035	0.035	0.032	0.003
cell													

Table S10. Volume occupancy (%) of carbon storage (starch and lipid droplets) in free-living (*Chlorella vulgaris* and *Micractinium conductrix*) and symbiotic (*M. conductrix* of *P. bursaria* CCAP1660/18) microalgae. Table shows the volume occupancy (%) that each structure/compartment occupies in the cell in the morning (AM) and in the afternoon (PM).

***Chlorella vulgaris* AM time point**	$Cell_1$ (%)	$Cell_2$ (%)	$Cell_3$ (%)	$Cell_4$ (%)	$Cell_5$ (%)	$Cell_6$ (%)	$Cell_7$ (%)	$Cell_8$ (%)	**Average (%)**	**STD (%)**
starch plates	0.002	0.005	0.014	0.007	0.006	0.004	0.005	0.015	0.007	0.005
starch grains	0.000	0.000	0.010	0.009	0.000	0.015	0.000	0.000	0.004	0.006
total starch	0.002	0.005	0.024	0.016	0.006	0.019	0.005	0.015	0.011	0.008
lipid droplets	0.011	0.020	0.003	0.007	0.006	0.011	0.022	0.022	0.013	0.007
pyrenoid	0.009	0.012	0.014	0.015	0.012	0.010	0.008	0.014	0.012	0.003

***Chlorella vulgaris* PM time point**	$Cell_1$ (%)	$Cell_2$ (%)	$Cell_3$ (%)	$Cell_4$ (%)	$Cell_5$ (%)	$Cell_6$ (%)	$Cell_7$ (%)	**Average (μm^3)**	**STD (μm^3)**
starch plates	0.023	0.023	0.025	0.019	0.054	0.019	0.026	0.027	0.012
starch grains	0.000	0.001	0.001	0.004	0.017	0.001	0.002	0.004	0.006
total starch	0.023	0.024	0.026	0.023	0.070	0.019	0.028	0.031	0.018
lipid droplets	0.009	0.014	0.010	0.010	0.048	0.001	0.008	0.014	0.015
pyrenoid	0.013	0.012	0.015	0.018	0.012	0.012	0.013	0.014	0.002

***Micractinium conductrix* AM time point**	$Cell_1$ (%)	$Cell_2$ (%)	$Cell_3$ (%)	$Cell_4$ (%)	$Cell_5$ (%)	$Cell_6$ (%)	$Cell_7$ (%)	$Cell_8$ (%)	**Average (μm^3)**	**STD (μm^3)**
starch plates	0.023	0.018	0.020	0.016	0.021	0.013	0.025	0.027	0.020	0.004
starch grains	0.001	0.000	0.000	0.000	0.000	0.000	0.000	0.002	0.0003	0.001
total starch	0.023	0.018	0.020	0.016	0.021	0.013	0.025	0.028	0.021	0.005
lipid droplets	0.006	0.006	0.007	0.009	0.006	0.009	0.007	0.006	0.007	0.001
pyrenoid	0.015	0.015	0.016	0.015	0.016	0.015	0.014	0.018	0.015	0.001

***Micractinium conductrix* PM time point**	$Cell_1$ (%)	$Cell_2$ (%)	$Cell_3$ (%)	$Cell_4$ (%)	$Cell_5$ (%)	$Cell_6$ (%)	$Cell_7$ (%)	**Average (μm^3)**	**STD (μm^3)**
starch plates	0.020	0.025	0.029	0.029	0.033	0.033	0.028	0.028	0.004
starch grains	0.000	0.002	0.000	0.002	0.002	0.002	0.000	0.001	0.001
total starch	0.021	0.027	0.029	0.032	0.036	0.034	0.029	0.030	0.005
lipid droplets	0.000	0.000	0.005	0.000	0.006	0.003	0.008	0.003	0.003
pyrenoid	0.016	0.016	0.018	0.020	0.018	0.022	0.012	0.017	0.003

***Micractinium conductrix* (isolated from *P. bursaria CCAP 1660/18)* AM**	$Cell_1$ (%)	$Cell_2$ (%)	$Cell_3$ (%)	$Cell_4$ (%)	$Cell_5$ (%)	$Cell_6$ (%)	$Cell_7$ (%)	$Cell_8$ (%)	$Cell_9$ (%)	$Cell_{10}$ (%)	**Average (%)**	**STD (%)**
starch plates	0.001	0.002	0.000	0.030	0.000	0.003	0.000	0.003	0.002	0.007	0.005	0.009
starch grains	0.000	0.000	0.000	0.077	0.000	0.000	0.001	0.000	0.000	0.000	0.008	0.024
total starch	0.001	0.002	0.000	0.107	0.000	0.003	0.001	0.003	0.002	0.007	0.013	0.033
lipid droplets	0.030	0.031	0.037	0.021	0.066	0.077	0.060	0.043	0.031	0.025	0.042	0.019
pyrenoid	0.031	0.031	0.023	0.007	0.031	0.025	0.026	0.024	0.027	0.032	0.026	0.007

***Micractinium conductrix* (isolated from *P. bursaria CCAP 1660/18)* PM**	$Cell_1$ (%)	$Cell_2$ (%)	$Cell_3$ (%)	$Cell_4$ (%)	$Cell_5$ (%)	$Cell_6$ (%)	$Cell_7$ (%)	$Cell_8$ (%)	$Cell_9$ (%)	$Cell_{10}$ (%)	$Cell_{11}$ (%)	**Average (%)**	**STD (%)**
starch plates	0.066	0.047	0.030	0.063	0.047	0.045	0.034	0.043	0.044	0.036	0.045	0.045	0.011
starch grains	0.027	0.005	0.003	0.031	0.004	0.010	0.006	0.012	0.017	0.002	0.003	0.011	0.010
total starch	0.093	0.052	0.033	0.095	0.052	0.056	0.040	0.056	0.061	0.038	0.048	0.057	0.020
lipid droplets	0.033	0.038	0.041	0.025	0.026	0.039	0.035	0.051	0.033	0.034	0.030	0.035	0.007
pyrenoid	0.032	0.031	0.027	0.030	0.029	0.033	0.031	0.033	0.034	0.035	0.035	0.032	0.003
Cell													

Chapter II

3D reconstruction: assessing heterogeneity of algal carbon storage in a multicellular photosymbiosis

Authors: Andrea Catacora-Grundy[1], Daniel Wangpraseurt[2] and Johan Decelle[1]

1. Cell and Plant Physiology Laboratory, CNRS, CEA, INRAE, IRIG, University Grenoble Alpes, 38054 Grenoble, France
2. Scripps Institution of Oceanography, UC San Diego

Light is a major factor affecting photosynthesis. Symbiotic microalgae in a large benthic (fixed) multicellular host organism could be exposed to different light intensities, and photosynthesis may be heterogeneous among the symbiont population. Recent coral optics studies have revealed the presence of steep light gradients and optical microniche in tissues of symbiont-bearing corals. The impact of light stratification on the metabolism and physiology of symbiotic microalgae needs to be considered and evaluated using subcellular approaches. In Chapter II, we will assess morphological differences in symbiotic microalgae experiencing different light exposure (*in hospite*) in the coral *Favites abdita* using 3D electron microscopy (FIB-SEM). This work was conducted in collaboration with D. Wangpraseurt from Scripps Institution of Oceanography (USA).

II.1 Introduction

Tropical coral reefs are highly diverse and productive ecosystems, providing a range of services that benefit communities of invertebrates and fishes but is also of high economic value for our society (tourism, fishery) (Roberty et al. 2024). Cnidarian (corals, anemones) host a microbial community of symbionts (photosynthetic dinoflagellates - Symbiodinicaeae, bacteria, archaea, viruses, etc.), forming a microbiome. The symbiotic dinoflagellates Symbiodinicaeae (commonly referred to as zooxanthellae) supply the host with photosynthetically produced carbohydrates (i.e., glucose and glycerol, lipids including sterols and fatty acids and amino acids) (Jacobovitz, Hambleton, and Guse 2023) that support host coral metabolism, growth, reproduction, and survival (Davy et al. 2012; Muscatine 1990). In return, the host provides shelter, inorganic nutrients (e.g. nitrogen compounds), and protection from predators (Yellowlees et al. 2008). Within the host, dinoflagellates typically reside within gastrodermis cells (Fig. 1).

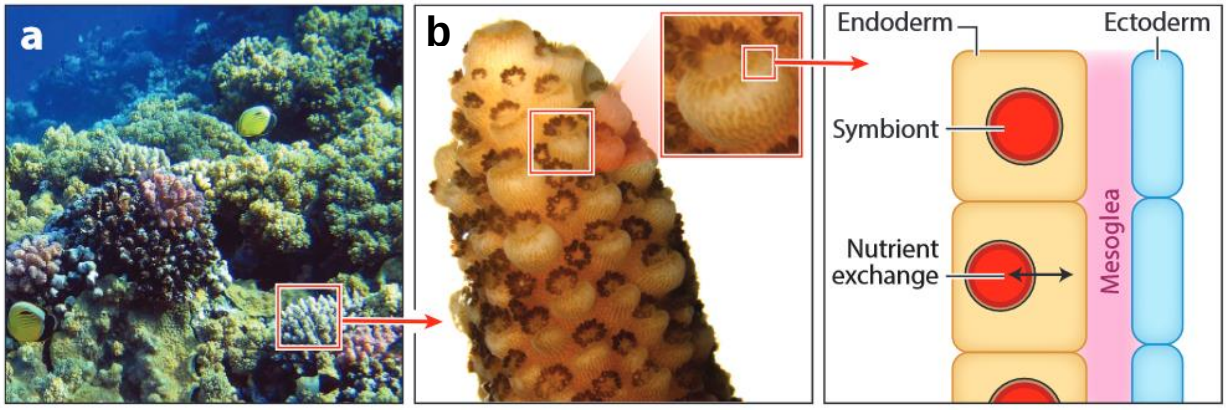

Figure 1. Corals **a)** are composed of many identical polyps. **b)** All polyps are connected by a continuous tissue layer, all stretched over the aragonitic calcium carbonate skeleton. The scheme shows the endoderm (or gastrodermis) and the ectoderm (or epidermis) connected by gelatinous mesoglea. Photosynthetic dinoflagellates symbionts (family Symbiodiniaceae) reside inside the coral's endodermal cells in the symbiosome (Jacobovitz et al. 2023).

Since decades, the translocation of photosynthetically fixed carbon in reef symbioses has been a major subject of study since it is the main energetic source powering this symbiotic association. Dinoflagellate carbon metabolism is primarily driven by photosynthesis. Although carbon translocation to the host has never been fully quantified, previous studies estimated that most of the fixed carbon (~90%) of the

dinoflagellate is transferred to the host (Davy et al. 2012; Falkowski et al. 1984). So, this raises the question of whether symbiotic microalgae store their fixed carbon in starch granules and how carbon homeostasis is affected in a host. It is also possible that carbon metabolism is heterogeneous among the symbiont algal population. Benthic large multicellular hosts have different micro-niches where symbionts can experience different light intensities so impacting their carbon metabolism and overall physiology in a host.

In their natural environment, cnidarian-dinoflagellates experience different irradiance in both space and time, ultimately varying the availability and quality of light for photosynthesis (Anthony and Hoegh-Guldberg 2003). With depth, light accessibility can trigger adaptation strategies in corals (Falkowski, Jokiel, and Kinzie 1990). For example, excessive sunlight in shallow waters can be a stress factor, causing symbiont expulsion or degradation, leading to bleaching of the coral colony (Glynn 1996; Hoegh-Guldberg 1999). In addition, (Wangpraseurt et al. 2014) have reported differential light exposure and spectral quality in corals suggesting *in situ* photo-acclimation of symbiotic microalgae. Thus, symbiotic dinoflagellates experience significant spatio-temporal fluctuations of light. It is argue that light-limited photosynthesis was shown to affect carbon production of symbiotic dinoflagellates (Dubinsky and Falkowski 2011). Nevertheless, the impact of this light distribution on the photobiology of symbiotic microalgae within a benthic multicellular host requires further exploration at the nanoscale. Symbiotic dinoflagellates store fixed carbon in the form of starch (outside the chloroplast) and neutral lipids (as lipid droplets) (Hillyer et al. 2017; Matthews et al. 2017). In addition to light intensity, carbon metabolism of symbiotic dinoflagellates can also be influenced by host nutrition. For instance, symbiotic dinoflagellates of the anemone *Aiptasia pallida Verrill* showed different carbon partitioning and differences in the chloroplast volume under low light and host-starved conditions (Davy and B. Cook 2001). In starved hosts, low light resulted in diminished starch and lipid production in the symbiotic dinoflagellates, whereas high light resulted in increased synthesis of both carbon storage. In addition, low light induced an increase in the chloroplast volume of the symbiotic dinoflagellates, as assessed by 2D electron microscopy (Muller-Parker, Lee, and Cook 1996). While the carbon metabolism and partitioning in green algae are extensively documented, our knowledge of the carbon metabolism dynamics in symbiotic algae is still limited. While considerable efforts have been deployed to gain a better

understanding of the carbon translocation between symbiotic algae and cnidarian hosts, the physiological state of the symbiont, in particular, its central carbon metabolism, is not fully understood.

Chapter II is a study in collaboration with Ph.D. Daniel Wangpraseurt (Principal Investigator at UC San Diego Jacobs School of Engineering). In combination with contextual measurements (light intensity), I analyzed FIB-SEM data for morphometrics analyses of symbiotic dinoflagellates in the coral *Favites abdita* collected from the shallow reef flat next to Heron Island Research Station (152°69′ E, 20°299′ S) (Southern Great Barrier Reef, Australia). Photophysiological measurements and sample collection and preparation were carried out in Sidney, Australia. We applied FIB-SEM-based 3D reconstruction to understand the impact of light variations on the subcellular architecture and morphometrics of symbiotic dinoflagellates within coral host tissues. Primary emphasis will be given to photosynthetic-related organelles (e.g. chloroplast), cell volume, and carbon storage (e.g. starch). Samples were collected at two different regions of the host – top and bottom - as shown in Fig. 1.

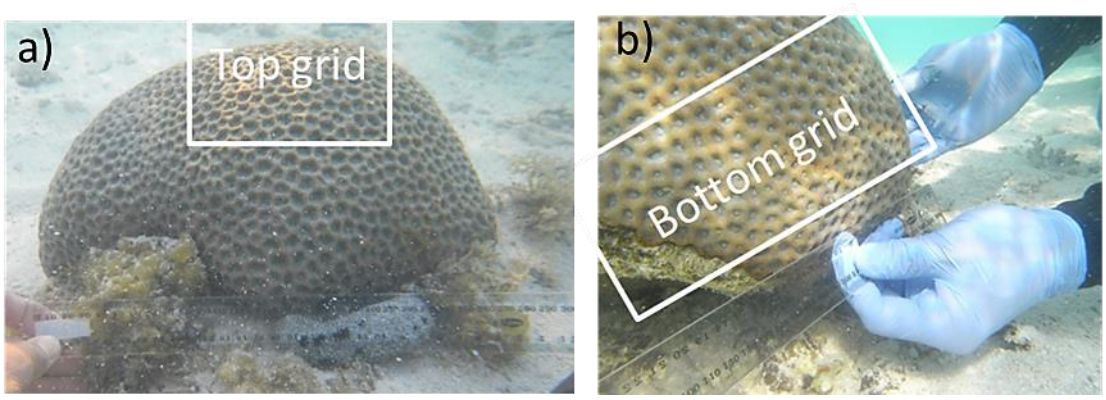

Figure 1. Sampling of top and bottom symbiont dinoflagellates colonies of *Favites abdita* coral host. The bottom grid is facing (southwest).

II.2 Results and Discussions

Focused Ion Beam Scanning Electron Microscope (FIB-SEM) was used to evaluate the morphometrics of symbiotic microalgae (belonging to the *Symbiodinium* clade C and D) (Coral Traits Database) inhabiting both the upper and lower regions of *Favites abdita* coral specimen ('top' and 'bottom' part). The coral colony was situated near the shoreline, characterized by a medium-sized colony exhibiting apparent visual vitality, albeit with minimal superficial abrasions. Segmentation and 3D reconstruction,

which strongly rely on image contrast, allowed us to evaluate the volume of the cell, chloroplast, and starch (e.g., starch granules) of symbiotic microalgae localized at the top and the bottom region of the coral tissue. From the stack registration we observed more dispersed distribution of symbiotic microalgae at the top region of the coral, while in the bottom region, symbiotic cells where clearly more packed (Fig. 2). Some characterizations about microalgae pattern distribution within a coral date from the 80's. It was observed that in coral tips of stony corals (e.g. *Favites abdita*), where light exposure is high, symbiotic microalgae density is less. The opposite was observed in lower parts of the coral (Falkowski et al. 1984). Similarly, (Titlyanov et al. 2001) observed higher cell density and reduction in cell volume of symbiotic microalgae localized on low light areas of the coral *Stylophora pistillata.* These observations are in accordance with our observation *F. abdita.*

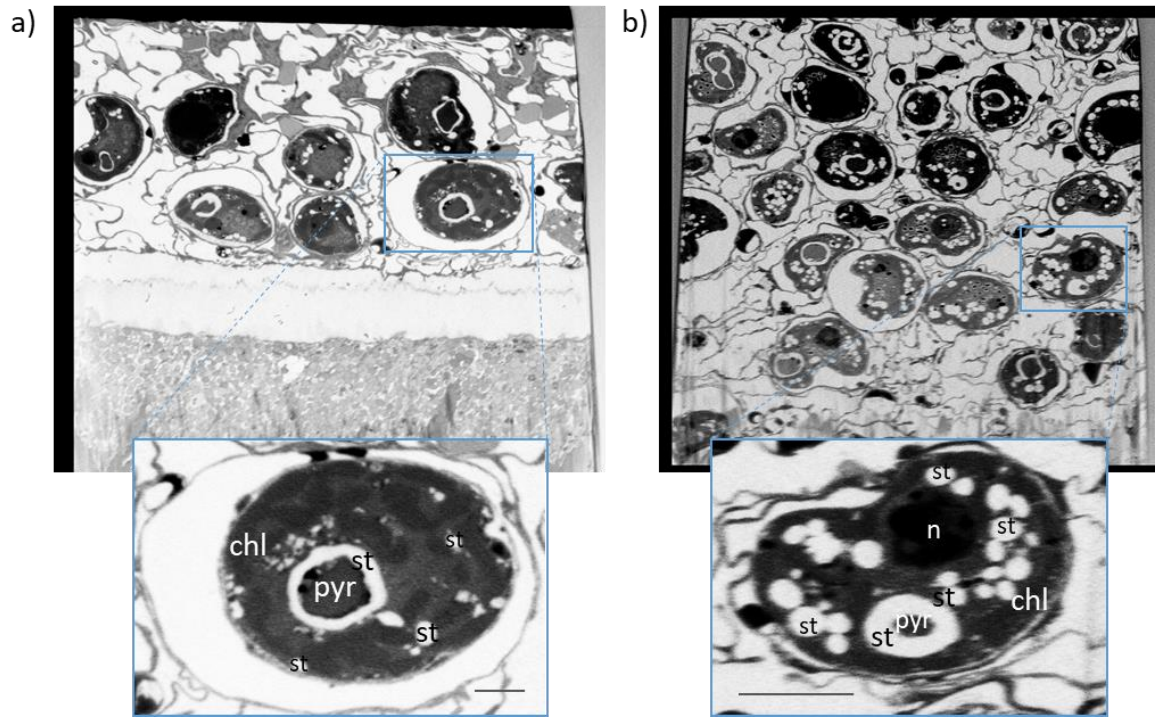

Figure 2. Single FIB-SEM micrographs of top **a)** and bottom. **b)** sampling of symbiotic cells in the host *Favites abdita.* Zoom box in blue show some cellular structures of the cell: chl=chloroplast, pyr=pyrenoid, st=starch, n=nucleus. Scale bar: 2 μm.

Microalgae in different host regions exhibited notable variations in size. Specifically, microalgae localized at the top of the coral were 8.2 times larger than those found at the bottom ($2.43*10^{7} \pm 5.86*10^{6}$;

pixels n=9 *versus* $2.96*10^6 \pm 6.99*10^6$ pixels ; n=22) (Fig. 3). This first indicate the heterogeneous nature of the symbiotic algal population within a single host. We then evaluated the subcellular morphometrics of the chloroplast. Because of limitations on image analysis due to poor contrast (Fig. 1), only three cells per region were exploited. Our findings revealed that chloroplasts of microalgae in the upper region of the coral were 1.7 times larger compared to those situated at the lower region ($4.65*10^6 \pm 1.28*10^{6;}$ pixels n=3 versus $2.69*10^6 \pm 7.34*10^6$ pixels ; n=3) (Fig. 3b). In terms of volume occupancy in the algal cell, the chloroplast of symbiotic microalgae represented 20.84 ± 6.25% of the cell volume in the top region of the coral compared with 23.63 ± 2.6% of the cell volume in the bottom part (Fig. 3c). So, even if more replicates are needed to conclude, we do not see major differences in terms of chloroplast volume of microalgae in the top and bottom regions of the host. As for starch, this glucose polymer was arranged as cytoplasmic granules surrounding the chloroplast. Morphometric analysis reveals that microalgae in the top region exhibited a 2.4-fold greater quantity of starch granules compared to those in the "bottom" region ($8.49*10^5 \pm 3.60*10^5$ pixels; n=6, versus $3.60*10^5 \pm 1.20*10^5$ pixels; n=15). Yet, if we normalize by cell volume (volume occupancy), starch granules were 3.2-fold higher in microalgae in the bottom region of the coral host (3.8 ± 0.9%; n=6 *versus* 12.0 ± 4.2%; n=15). 3D reconstruction and morphometric analysis therefore revealed morphological differences (cell, chloroplast and starch volume) in symbiotic dinoflagellates residing in different regions of the coral host. Such investigation sheds light on previously unknown morphological characteristics among colonies in the same host at high-resolution, advancing our understanding of these symbiotic associations. It was observed that the diversion of photosynthetic carbon (e.g. glycerol) from the microalgae leads to a partial reduction in algal synthesis of triacylglycerol (TG) and starch (Dubinsky and Falkowski 2011). Thus, we could argue that lower starch storage in top region of the coral may indicate a higher translocation of photosynthetic carbon than bottom region. While we cannot conclude the physiological status of the symbiotic

microalgae, we need to further investigate if the higher starch observed in 'bottom' microalgae is linked to a lower translocation of photosynthetic carbon to the host.

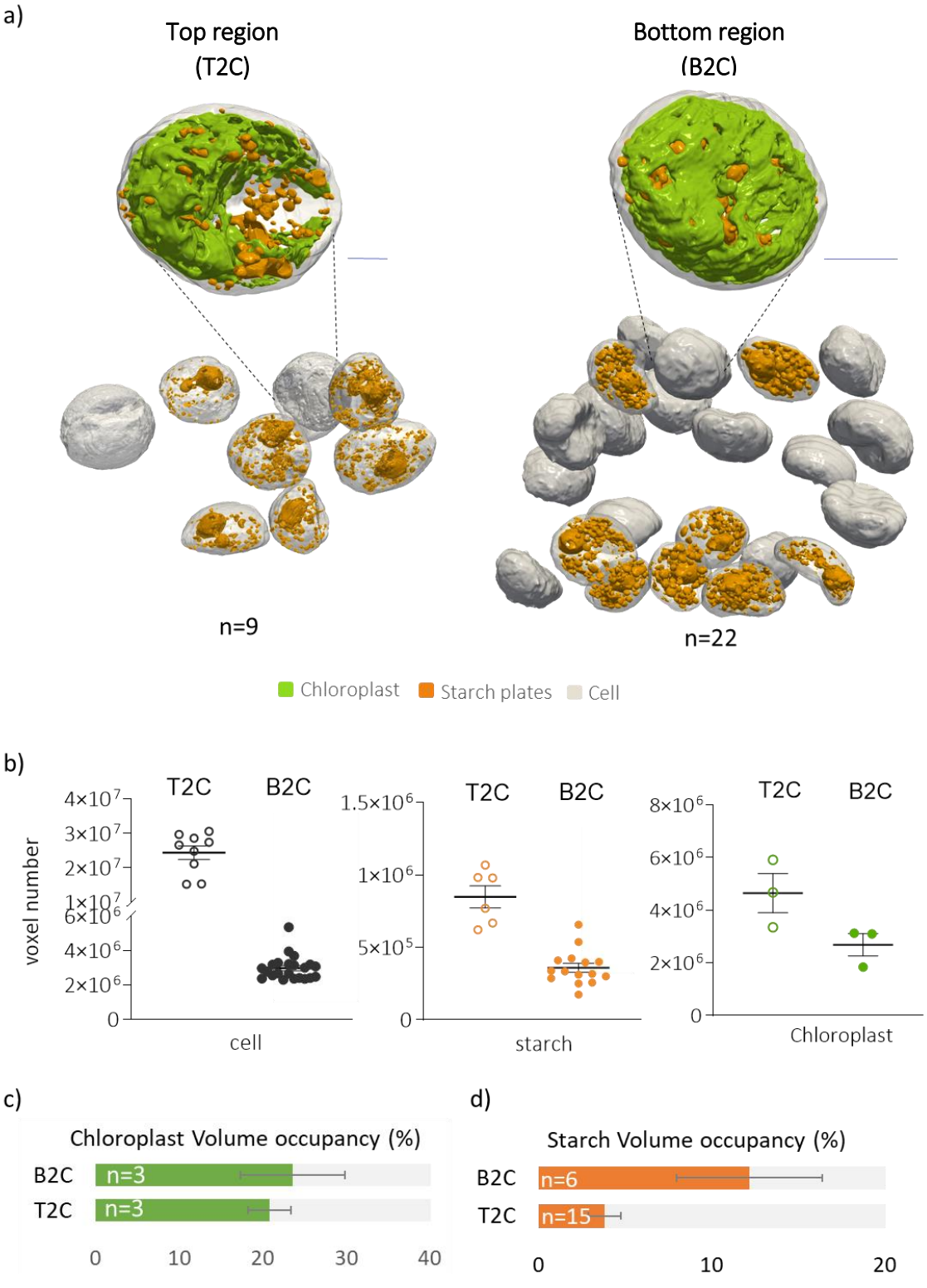

Figure 2. FIB-SEM reconstruction and morphometrics of symbiotic dinoflagellates within the coral host tissue (*F. abdita*). a) We show a single dinoflagellate cell from the top (T2C) (left) and bottom (B2C) (right) part of the coral tissue in *F. abdita*. All segmented cells imaged from the sampling are shown below. Only cells with high contrast were used to assess the morphometrics of starch compounds (showed in orange) in both conditions. **b)** Morphometrics of cell, starch, and chloroplast expressed as the number of voxels are shown. The plot shows the average of voxel number ± SD. Scale = 2μm. **c)** Percentage of the chloroplast and starch volume d) occupied in the cell in both conditions.

Paramecium-Chlorella single-celled symbiosis also showed heterogeneity across symbiotic cells in terms of cell size and carbon storage dynamics. These findings suggest the presence of heterogeneous microenvironments within the host, whereby symbiotic microalgae, despite occupying a common spatial niche (a single-celled swimming host). These differences may impact the physiological and metabolic activities of symbiotic cells and potential services to the host. In corals, the quantity of light is a key environmental parameter regulating the nature of this photosymbiosis (Falkowski et al. 1990). Irradiance, which refers to the intensity of light energy that is absorbed by pigment molecules (e.g. chlorophyll) in photosynthetic organisms will stimulate symbiont photosynthesis and thus, sustain carbon transfer to the host (Davy and B. Cook 2001). It has been reported that the optical environment within the host tissue is likely to vary substantially from the ambient macro-environment (Wangpraseurt, Larkum, et al. 2012). Photons scatter beneath the coral skeleton, and only a portion of them are used in photochemical reactions by symbionts (Enríquez, Méndez, and -Prieto 2005). In addition, lower cell layers in coral tissue are subject to more light-limiting conditions (Wangpraseurt, Weber, et al. 2012). In this work, we compared the morphometrics of cells localized at the top and bottom regions of the coral tissue, exposed to opposite light environments within the same host. Of note, more but smaller cells were observed at the bottom region of the corals. Samples were all collected near the end of the afternoon. We consider that starch content quantified by FIB-SEM may reflect starch synthesis of symbiotic microalgae throughout the day in the coral tissue. Starch volume (in terms of voxel number) was higher in 'bottom' symbiotic microalgae (exposed to more light-limiting conditions). (Muller-Parker et al. 1996), reported that in food-deprived anemones *Aiptasia,* low light led to decreased starch and lipid synthesis in the symbiotic dinoflagellates, while light intensity increases production of both carbon reserves. Furthermore, low light conditions prompted an increase in the chloroplast volume of the symbiotic dinoflagellates, as calculated by 2D microscopy (Muller-Parker et al., 1996). Additionally,

they did not observe differences in the area of symbiotic microalgae from anemones maintained under low light. Our results were different in the coral *Favites abdita:* chloroplast volume did not significantly vary between bottom and top regions of the host and starch grains. It is necessary to further investigate the physiological context of cells to better understand the dynamics of the different spatial distributions of symbiotic dinoflagellates in the coral tissue. Finally, segmentation of chloroplasts and starch granules was contingent upon the contrast quality of the cells within the image stack. Improvements in contrast and resolution can be achieved in FIB-SEM imaging, by using high-pressure freezing (HPF) during sample preparation to better preserve samples. Yet, this remains challenging because of the limited accessibility of these technologies near marine stations or coral ecosystems.

II.3 Conclusion and perspectives

Our results based on 3D electron microscopy revealed morphological differences of symbiotic microalgae localized in the bottom and top region of a single multicellular host. This heterogeneity within the symbiont population highlights the different microenvironments that experience microalgae. While more contextual measurements are needed, our morphometric quantification showed that the cell volume and carbon storage of microalgae can vary within the same host individual. This was also observed in Chapter I, in the freshwater model *Paramecium-Chlorella*. A complementary study is ongoing in collaboration with D. Wangpraseurt, for a contextual analysis of light conditions respect to different spatial distribution of symbiotic microalgae within the host tissue.

II.4 Material and Methods

Corals sampling

In situ measurements were conducted on the shallow reef flat adjacent to Heron Island Research Station (152°69′ E, 20°299′ S) in the Southern Great Barrier Reef, Australia. Samples were acquired at 16:30 hours at depths ranging from 0.3 to 2 meters, measured from the sediment benthos to the water surface. Measurements were specifically undertaken on days characterized by clear skies and abundant sunlight. Environmental parameters at the research site were continuously monitored throughout the study duration. A single colony of *Favites abdita*, situated near the shoreline, was selected for investigation. This coral colony was found to be growing on sediment benthos with minimal algae present near its

base. Sampling involved obtaining small fragments from both the top and bottom regions of the colony, each containing approximately 6-7 structurally intact polyps. Subsequently, the specimens were transported in seawater. Upon completion of sampling, 5 hours were allotted for tissue recovery, after which the samples were fixed in a relaxed state at around 22:00 hours. Each sample exhibited dimensions of approximately 1 centimeter in thickness and 5 centimeters in diameter.

Microscopy sample preparation

The following conditions were used for embedding the block for FIB-SEM acquisition postfix 2% OsO4 buffer (1, 5 H), Wash MQ. (3x 10-15 min), 1,2% uranyl acetate in water overnight, wash MQ. 3x 10-15 min. Dehydration:70% EtOH. 2x 15 min, 96% EtOH. (2x 15 min), 100% EtOH (3x 15 min), 100% Acetone (2x 10-15 min). Epoxy: Epon/acetone 1:3 (45 min), 1:1 (45 min), 3:1 (45 min), Epon, 2 H or overnight and Embedded at 60 °C for 24 H. Samples were cut on an Ultramicrotome Leica EM UC7, at marine biological section, University of Copenhagen (Core Facility for Integrated Microscopy-Panum- University of Copenhagen).

Stack alignment

Image sequences were stacked, registered, and cropped using Fiji software and its plugin Multistackreg. The transformation matrix was extracted from the plugin. The shearing caused by the 54° angle of the electron beam was corrected using the transformation matrix that was previously extracted, with an in-house Python code (collab. P. Perrenot, CEA Liten).

Segmentation and 3D reconstruction

Image processing was initiated using the Fiji software (https://imagej.net/Fiji). This involved cropping selected cells and performing registration. Segmentation was performed using a semi-automatic method adopted from (Uwizeye et al. 2020) based on pixel classification, with 3D Slicer software (https://www.slicer.org/) and a supervised semi-automatic pixel classification mode used to automatically segment 3 to 15 slices for each region of interest (ROI). The main organelles and structures of the algal cells, including the nucleus, chloroplast, mitochondria, pyrenoid, starch, and lipid droplets, were segmented. Morphometric analyses were calculated using the Statistics Module in 3D

Slicer. Three components of the symbiotic microalgae were segmented: the chloroplast, the starch granules in the cell, and the complete cell.

Chapter III

Potential sugar transporters involved in the photosymbiosis between *Paramecium bursaria* and its microalgae

Authors: Andrea Catacora Grundy[1], Caroline Juery[1], Fabien Chevalier[1], and Johan Decelle[1]

1. Cell and Plant Physiology Laboratory, CNRS, CEA, INRAE, IRIG, University Grenoble Alpes, 38054 Grenoble, France

Carbohydrates are central in photosymbiotic associations, and are considered the main metabolites translocated from the symbiotic algae to the host. Yet, there are still molecular mechanisms awaiting further elucidation, particularly regarding the cellular mechanisms enabling translocation of photosynthetically-derived carbon. In Chapter III, we conducted a transcriptomic analysis to study the sugar expression of the transportome of the microalga (*Micractinium conductrix*) and the host (the ciliate *Paramecium bursaria*) potentially involved in carbon transfer.

III.1 Introduction

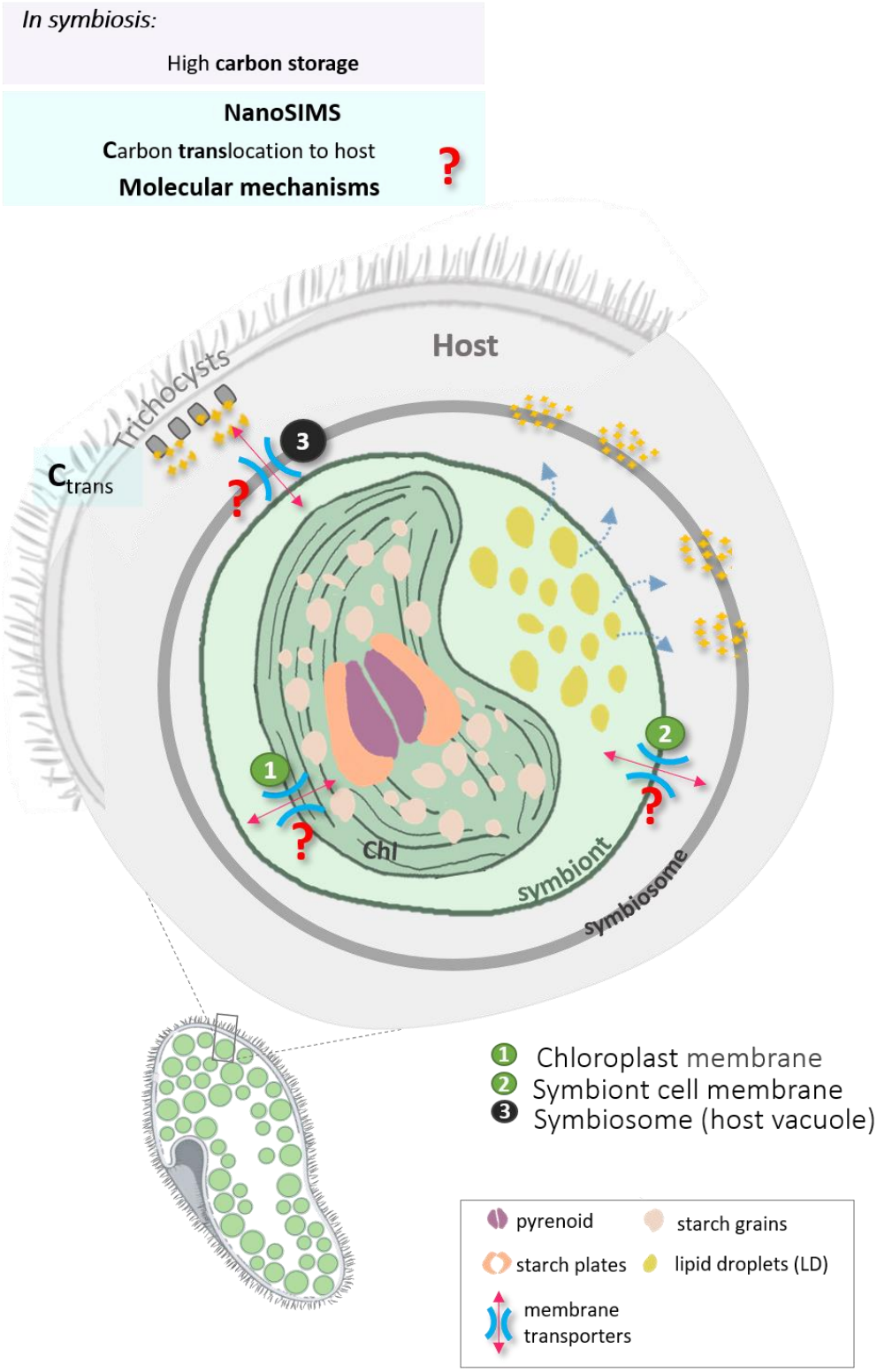

General scheme 1. Chapter I showed the potential impact of the host on the carbon metabolism of the symbiotic microalgae. In symbiosis, the photosynthetic machinery is more developed, and carbon storage (e.g. total starch and lipid droplets) is higher. In addition, our NanoSIMS showed that carbon transfer might take place in this

photosymbiotic model, as ^{13}C signal was observed in the host tissue (Chapter I. Fig 6-pag.45). Although the nature of the metabolite transfer to the host was not determined, it is likely that they involve sugars (e.g. glucose, maltose) from photosynthetic carbon. We hypothesize that excess of carbon stored in the symbiotic microalgae is eventually transferred to the host as sugars (Fig 1. blue arrows). The host may also act as a sink to remove excess carbon from microalga via its transporters at the symbiosome membrane.

While it is generally accepted that photosynthates of the symbiotic microalgae fulfill host energy demands, the mechanisms underlying carbon translocation are to be elucidated. The translocation and exchange of organic carbon supporting photosymbiosis have been investigated in numerous studies (Burriesci et al. 2012; Davy et al. 2012; Hofmann and Kremer 1981; Kopp et al. 2015). The transport of sugars across the plasma membrane, whether through active or passive diffusion, necessitates the involvement of a transporter or channel protein (Sproles et al. 2018; Vander Heiden, Cantley, and Thompson 2009). Like in other photosymbiotic organisms, in *Paramecium-Chlorella*, the symbiotic microalgae are generally enclosed in a host-derived cell membrane referred to as the symbiosome (General scheme Chapter I). This structure serves as a barrier through which any exchange of organic molecules must pass (Wakefield and Kempf, 2001). Consequently, the transfer of compounds between symbiotic partners requires the participation of transporters embedded within the cell membrane (Fig. 2) of the symbiotic microalgae and eventually the symbiosome.

Sugar transporters are recognized as essential components in the overall metabolism of organisms. They coordinate the movement of sugars across cell membranes to support crucial processes, like nutrient uptake, energy production, and cellular signaling (Lizák et al. 2019). Our knowledge of the diversity and function of sugar transporters has improved in the last decade, especially in plants (Eom et al. 2015, 2015; Hennion et al. 2019). For instance, the main sugar transporters involved in sugar efflux in plants are members of the SWEET family (Sugar Will Eventually be Exported Transporter: hexose and sucrose transporters) (Bezrutczyk et al. 2018; Chen et al. 2010). Other important sugar transporters are SUTs (or SUC; Sucrose Transporters), and MSTs (or STP; Mono-Saccharide Transporters) typically involved in sugar influx–-uptake into plant cells (Chen 2014).

Glucose membrane transporters (GLUT-type) within the Solute Carrier family (SLCA2) are of particular interest in symbiotic interactions due to their high affinity for glucose and their localization

in internal membranes (Joost, Wandel, and Schürmann 2009; Sproles et al. 2018). GLUT proteins, with approximately 12 transmembrane alpha helices, also play a crucial role in glucose sensing (Thorens and Mueckler 2010). They serve a dual function by facilitating glucose entry into the cell and initiating glucose metabolism through glucokinase phosphorylation (Díaz Hernández and Burgos Herrera 2002). For instance, in the cnidarian-dinoflagellate symbiosis, phylogenetic investigation revealed potential GLUT sugar transporters (Sproles et al. 2018). In addition to GLUT and SWEET, other sugar transporters could be candidates in photosymbiosis, and therefore requiring a specific attention in the photosymbiosis between the host *Paramecium bursaria* and the microalga *Micractinium*.

In this chapter, we performed a transcriptomic analysis focusing on the sugar transportome in the single-cell photosymbiotic model *Paramecium bursaria*. We compared the sugar transportome of symbiotic microalgae (*M. conductrix*) *versus* its free-living form (data from (Arriola et al. 2018a). We also analyzed the expression of the sugar transportome of the host (*P. bursaria*) in symbiosis *versus* the aposymbiotic stage. We aimed to highlight potential sugar transporters involved in the translocation of sugars from this photosymbiotic unicellular model.

III.2 Results

We analyzed and compared the expression of the transportome (all transporters) of the microalgae and host in symbiosis, in comparison with their free-living forms (not in symbiosis). Clustering analyses of the algal transportome expression in symbiosis *versus* free-living revealed distinct gene expression patterns (i.e. there is a significant separate cluster for the free-living microalgae), with notable variability observed in symbiosis (Fig. 1a). Similar analyses were performed on the host transportome (Fig. 1b), revealing two distinct clusters corresponding to symbiotic and aposymbiotic host stages. These results demonstrate a distinct expression profile of the transportome during symbiosis, characterized by both up-and-down-regulation of specific transporter genes.

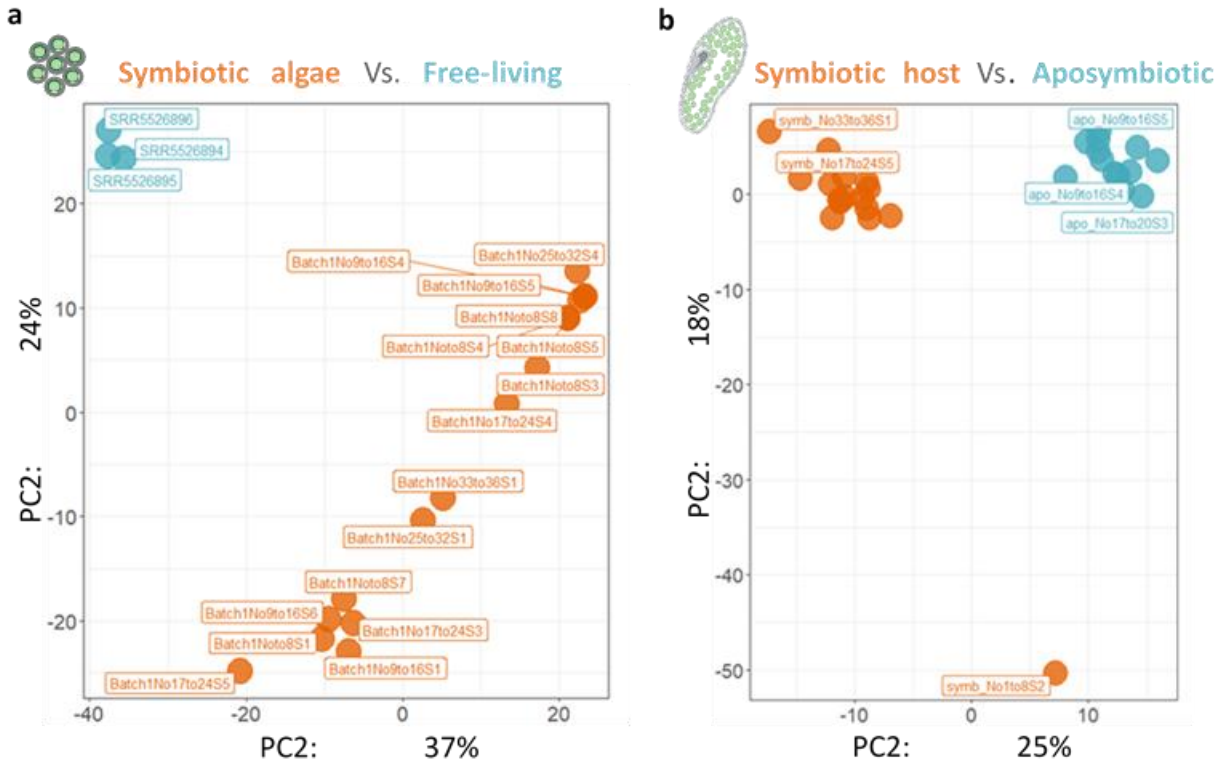

Figure 1. Clustering analysis of expressed transportome (all transporters) in the symbiotic microalgae *Micractinium conductrix* versus its free-living form (a), and in the host *Paramecium bursaria* in symbiosis *versus* aposymbiotic (algae-less) (b).

During symbiosis, 48.1% of the transporters of the microalgae were remodeled (35.7% up– and 12.4% down- regulated) while for the host, 9.8% of the transporters were remodeled (7.5% up– and 2.3% down-regulated) (Fig. 2).

Since sugar transporters are considered to be essential in symbiotic associations, we specifically identified and compared the expression of the sugar transportome of microalgae and host in symbiosis compared to their free-living stages. For the microalgae, our analysis revealed that 55% of the sugar transportome was remodeled in symbiosis. More particularly, 45% of sugar transporters were up-regulated and 10% down-regulated (Fig. 2a, Table 1). Several sugar transporters were also still expressed but not differentially expressed. Concerning the host, transcriptomic results indicate that 9.1% of the sugar transportome was remodeled, with 6.8% up-regulated genes and 2.3% down-regulated genes (Fig. 2b, Table 1). Overall, this study shows that both host and microalgae exhibit specific sugar transporter genes that are upregulated in symbiosis, which provide new insights into their potential role in symbiosis.

Figure 2. Differential gene expression (expressed in percentage) of sugar transporters, all transporters,

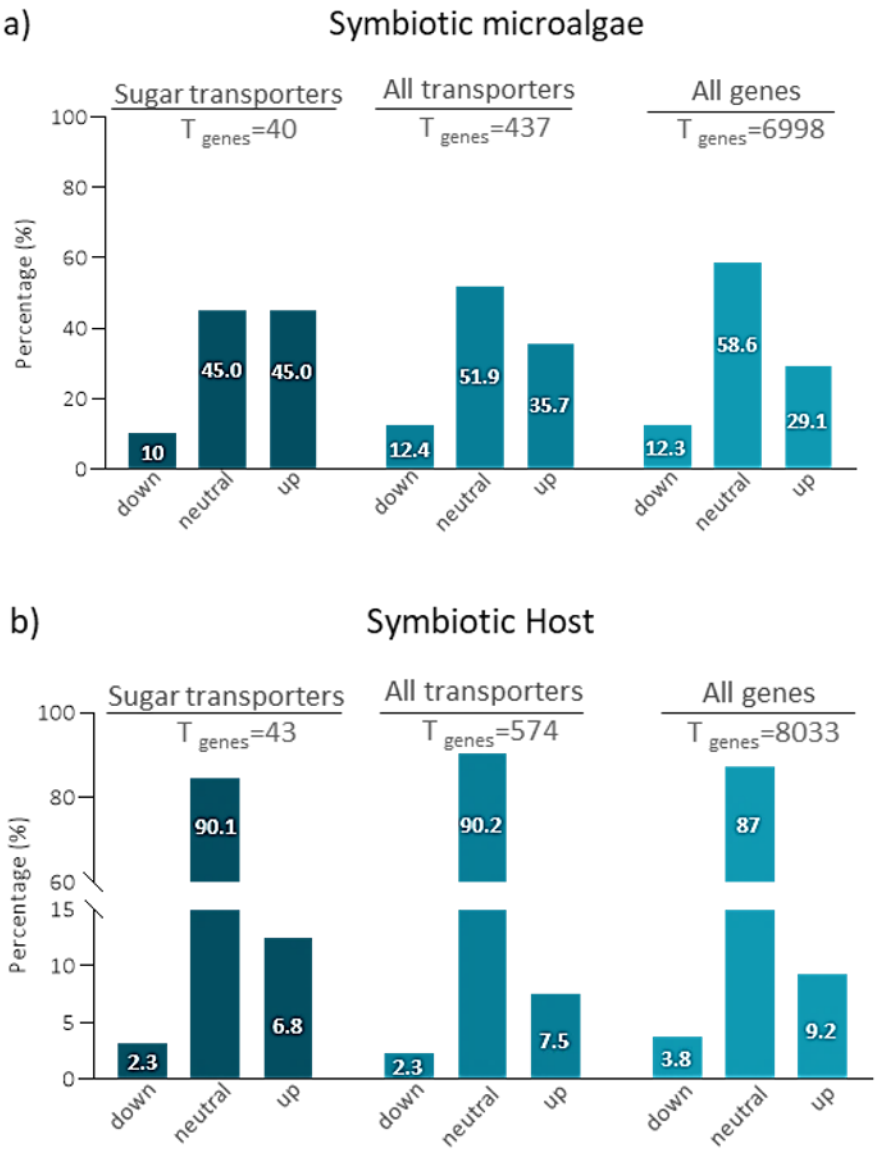

and all genes in the symbiotic microalgae *M. conductrix and* symbiotic host *P. bursaria.*

Table 1. Number of sugar transporters, all transporters, and all genes expressed in symbiotic microalgae and symbiotic host

Symbiotic algae				
Micractinium conductrix	**down**	**neutral**	**up**	**Sum**

Sugar transporters	4	18	18	40
All transporters	54	227	156	437
All genres	863	4101	2051	6998

Symbiotic Host *Paramecium bursaria*	**down**	**neutral**	**up**	**Sum**
Sugar transporters	1	39	3	43
All transporters	13	518	43	574
All genres	302	6991	740	8033

In microalgae, among the sugar transporter genes that were upregulated in symbiosis, we identified genes corresponding to seven *Triose-phosphate Transporter* (TPT) genes (PF03151), four *Sugar (and other) transporter* genes (PF00083) and one *Nucleotide-sugar transporter* gene (PF04142) (Fig. 3, Table 2). These results highlight that some *Triose-phosphate Transporter* (TPT) genes are important for symbiosis, likely to export sugars from the plastid to the cytosol. *In silico* sub-cellular localization analyses predicted that the up-regulated genes of TPT could be localized in the chloroplast and/or vacuole and/or plasma membrane of symbiotic microalgae. The four upregulated *Sugar (and other) transporter* (PF00083) genes were predicted to be localized in the plasma membrane and/or cell membrane and/or lysosome, and/or vacuole (Table 3). As for TPTs, localization prediction needs further experimental validation. In addition to TPTs, two genes of PF00083 were annotated by the TCDB database as *putative Inositol Transporter 2*, described in the plant *Arabidopsis thaliana*. Another up-regulated gene from the PF00083 family corresponds to a *Hexose H^+ symporter*, homologous to *Chlorella kessleri* (Table 4). As for down-regulated genes, we have identified four sugar transporter genes: one gene from the *Sugar (and other) transporter* (PF00083), two genes from the *Triose-phosphate Transporter (TPT)* (PF03151), and one gene from the *Nucleotide-sugar transporter* (PF04142) (Fig. 3, Table 2). It is noteworthy that during symbiosis, 18 sugar transporter genes of the microalgae remain neutral, which accounts for 45% of the sugar transportome, and can still play a role in the metabolic exchange between partners (Fig. 2, Supp. Table 2). Finally, we observed 2 upregulated genes annotated as Aquaporin (AQPs) in the symbiotic microalgae (Supp Table 4.). This membrane transporter can facilitate the movement of different substrates including glycerol, a carbon source likely to be translocated from the microalgae to the host.

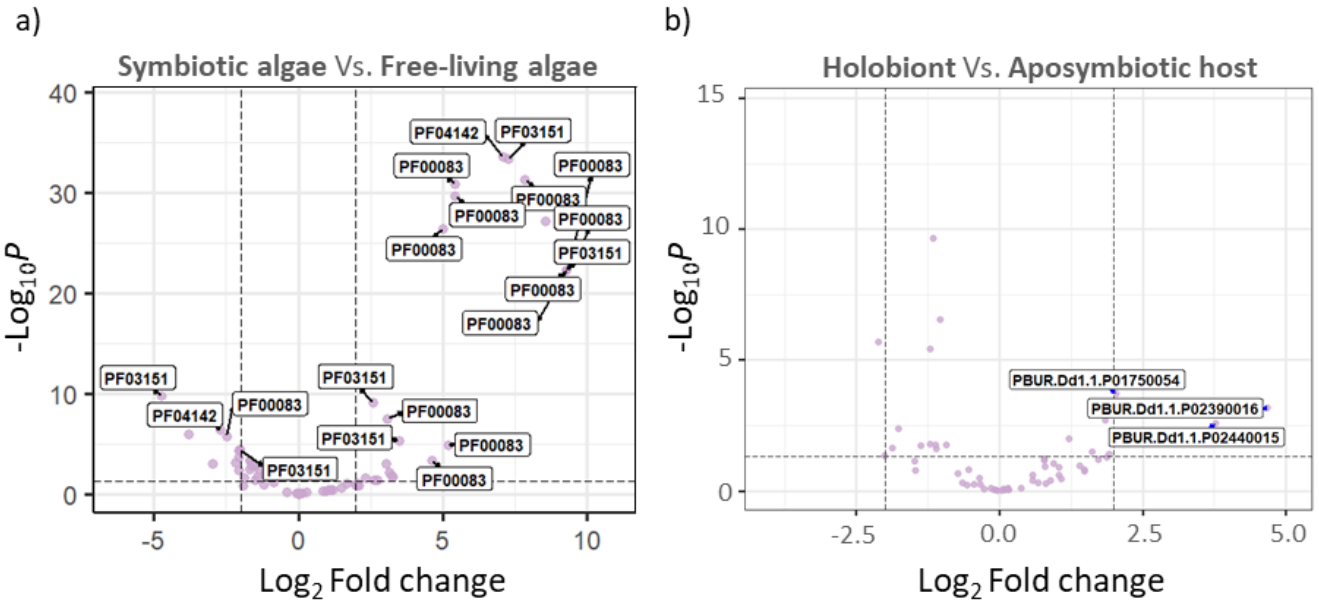

Figure 3. Volcano plots showing the differentially expressed sugar transporters in a) symbiotic microalgae *Micractinium conductrix* compared to the free-living stage and b) symbiotic host *Paramecium bursaria* compared to the aposymbiotic stage. The right top part of the Volcano plots shows the significant up-regulated genes (depicted by individual purple dots) while the left part contains the significant down-regulated genes.

Table 2. List of up- and down-regulated sugar transporters in symbiotic microalgae *Micractinium conductrix versus* free-living from different Pfam families.

Symbiotic microalgae *M. conductrix*	**Pfam**	**Description**	**N of genes**	**Localization prediction (Wolf_Psort)**
up	PF03151	Triose-phosphate Transporter family (TPT)	11	Chloroplast/vacuole/plasma membrane
	PF00083	Sugar (and other) transporter	4	Plasma membrane
	PF04142	Nucleotide-sugar transporter	1	vacuole
down	PF03151	Triose-phosphate Transporter (TPT) family	2	Plasma membrane
	PF00083	Sugar (and other) transporter	1	Plasma membrane
	PF04142	Nucleotide-sugar transporter	1	Plasma membrane

Table 3. Annotated up- and down-regulated sugar transporters and predicted localization in the symbiotic microalgae *Micractinium conductrix* compared to the free-living stage.

	Pfam	Seq ID	Localization prediction	TCDB annotation	Species homolog
Symbiotic microalgae *M. conductrix*	PF00083	gene_2994	Lysosome/vacuole	putative inositol transporter 2	*A.thaliana*
	PF00083	gene_2995	Cell membrane	putative inositol transporter 2	*A.thaliana*
	PF00083	gene_5578	Lysosome/vacuole	Hexose H+ symporter/antiporter	*Chlorella kessleri*
	PF03151	gene_4635	Chloroplast	Triose_phosphate/ phosphate_translocator	*Brassica_oleracea*
	PF00083	gene_8223	plasma membrane	NA	
	PF03151	gene_1644	Chloroplasts	NA	
	PF03151	gene_3348	vacuole	NA	
	PF03151	gene_359	vacuole	NA	
	PF03151	gene_4554	vacuole	NA	
	PF03151	gene_4634	plasma membrane	NA	
	pf03151	gene_8965	Chloroplasts	NA	
	PF04142	gene_6175	vacuole	NA	

In the host *P. bursaria,* three sugar transporter genes were found to be up-regulated in symbiosis and only one down-regulated. TCDB database showed that one of the up-regulated genes (PBUR.Dd1.1.P01750054) corresponds to the *GLUT3 or SLC2a3a* gene (Table 5). Glucose membrane transporter (GLUT-type) is one of the most known sugar transporters from the MFS family. Our in-silico analyses predicted that this GLUT sugar transporter of the host could be in the plasma membrane (Table 5). The other two up-regulated genes of the symbiotic host were both annotated as *Phosphate transporter and receptor.* Of note, 39 sugar transporter genes (87.1%) were shown to be neutral during symbiosis, so still expressed and potentially important (Fig. 2, Supp. Table 3)

Table 4. List of up- and down-regulated sugar transporters in symbiotic host *Paramecium bursaria* compared to its apo-symbiotic stage.

Symbiotic host	Pfam	Description	N of genes	Localization prediction
up	PF00083	Sugar (and other) transporter	3	Plasma membrane
down	PF00083	Sugar (and other) transporter	1	Plasma membrane

Table 5. List of specific upregulated genes in the symbiotic host *Paramecium bursaria*

	Pfam	Seq ID	Prediction localization (Wolf_PSORT)	TCDB annotation	Localization prediction
Symbiotic host *P.bursaria*	PF00083	PBUR.Dd1.1. P02440015	Lysosome/Vacuole	Phosphate transporter and receptor (transceptor)	Plasma membrane
	PF00083	PBUR.Dd1.1. P01750054	Cell membrane	GLUT 3 or SLC2a3a	Plasma membrane
	PF00083	PBUR.Dd1.1. P02390016	ER	Phosphate transporter and receptor (transceptor)	Plasma membrane

III.3 Conclusion and discussion

These results showed that the microalgae *M. conductrix* and the host *P. bursaria* exhibit a specific expression of their transporters and in particular their sugar transporters in symbiosis with specific up- and down-regulated genes.

Algal sugar transporters expressed in symbiosis

In microalgae, 55.5% of the sugar transportome is remodeled, whereby 45% up-regulated genes and 10% down-regulated genes were found. Up-regulated genes encoding sugar transporters belong to 3 main Pfams: *Triose-phosphate Transporter family* (TPT) (PF03151), *Sugar (and other) transporter* (PF00083), and *Nucleotide-sugar transporter* (PF04142). The seven up-regulated genes of the *Triose-phosphate Transporter family* (TPT) (PF03151) need to be further analyzed to understand their

localization and function in sugar transport. However, it is known that genes belonging to the TPT family transporters are involved in the export of phosphorylated sugars (e.g. Triose Phosphate - TPs) synthesized in the plastid of microalgae (Weber and Linka 2011). Their main function is to allocate a portion of the fixed carbon in the form of triose phosphate to sucrose synthesis whereas the rest of the trioses are retained in the chloroplast are used to drive transitory starch synthesis (Kaschuk et al. 2009; Moog et al. 2015). In plants-mycorrhizal symbiosis, high levels of triose phosphate export from the chloroplast enhance its utilization for sucrose synthesis and carbon export, satisfying the carbon demand of the mycorrhizal symbiont (Bukhov 2004; Kaschuk et al. 2009). Whether this is the case in the symbiotic model *Paramecium-Chlorella*, needs to be further addressed. In addition to TPTs, TCDB annotation revealed the identity of the two up-regulated sugar transporter genes as *Putative Inositol transporter 2*, predicted to be localized in the Lysosome/vacuole and cell membrane. Inositol transporters are part of the MST-like superfamily (Major Sugar Transport-like) characterized in the plants *A. thaliana* and *Oryza sativa* (Lemonnier et al. 2014; Wang et al. 2008). They mediate the active uptake of hexoses (e.g. glucose, fructose, xylose, etc.) by sugar/hydrogen symport (Schneider et al. 2007). This type of transporter was already described in the parasitic ciliate *Tetrahymena vorax*, involved in the transport of different inositol isomers (e.g. myo-, scyllo-, and D-chiroinositol) across the plasma membrane (Kersting and Ryals 2004). To our knowledge, no identification of *Inositol transporter 2* has been reported on other photosymbiotic organisms. Thus, the involvement of this sugar transporter, which may indicate specific sugar metabolites exported by the microalgae, needs to be further studied. Additionally, a *Hexose H+ symporter/antiporter* predicted to be localized in the algal cell membrane was found to be up-regulated in the symbiosis. *Hexose H+ symporter* has already been largely studied and reported in the non-symbiotic green algae *Chlorella kessleri* (Tanner 2000). This algae is known to be a heterotroph, being able to uptake glucose as a carbon source, very likely through this *Hexose H+ symporter /antiporter* (Caspari et al. 1994). It has been observed that symbiotic *Chlorella* in *Hydra* can be heterotrophic under dark conditions (McAuley 1986). Further functional studies are required to determine the exact role of this sugar transporter in the photosymbiotic microalgae. In the symbiotic microalgae we also observed 2 upregulated genes annotated as Aquaporin (AQPs) (Supp Table 4.). These molecules are involved in the transport of various molecules (e.g. H_2O, glycerol, urea, NH_3, CO_2, etc.) and have been characterized in different plants (*Arabidopsis thaliana, Oryza sativa, Zea mays,*

Citrus sinensis, etc). NIPs, a specific subfamily of AQPs, are less active in water transport but permeable to organic molecules (Deshmukh, Sonah, and Bélanger 2016). NIP1 transports glycerol and silicon in cellular membranes (Giovannetti et al. 2012; Hara-Chikuma and Verkman 2006). In cnidarians, 16 AQPs are internal and predicted to function as glycerol channels through structural analysis (Sproles et al. 2018). Thus, it could be possible that glycerol, a type of sugar, is transfer to the ciliate host through AQPs.

In addition, in our work we identified one gene annotated as SWEET (Sugars Will Eventually Be Exported Transporters) but not differentially expressed in symbiosis. First discovered in plants, these transporters are involved in sugar efflux from glucose producing cells (Eom et al. 2015). We cannot exclude the involvement of this sugar transporter in the system giving the dynamics of carbon metabolism and carbon storage of the symbiotic microalgae. Overall, gene annotation of up-regulated sugar transporters in the symbiotic microalgae *M. conductrix* was challenging. This was because these microalgae are not a model organism and their gene-to-protein identity is not available in current public databases. Consequently, our study would require additional phylogenetic analyses to further characterize these potential sugar transporters. Yet, some of the reported upregulated sugar transporters were also observed in other symbiotic organisms (terrestrial and marine), indicating a shared molecular mechanism. Deeper characterization of the candidate's sugar transporters genes likely involved in the translocation of carbon in this model is necessary via molecular and biochemical approaches.

HOST sugar transporters expressed in symbiosis

Regarding the host, 9.1% of its sugar transportome was remodeled, whereby 6.8% up-regulated genes and 2.3% down-regulated genes were found. It is interesting to note that this 9% remodeling is very low compared to the nearly 50% remodeling of the sugar transportome of the microalga. Overall, three up-regulated genes of the same Pfam include GLUT *3 or SLC2a3a* and *Phosphate transporter and receptor (transceptor)*.

GLUT gene has been reported in other photosymbiotic host, such as cnidarians (*Aiptasia* and *Cassiopea andromeda*) and *Hydra* in symbiosis with Symbiodiniaceae and *Chlorella*-like microalgae, respectively. In the sea anemone *Aiptasia*, GLUT protein (GLUT8) was shown to exhibit higher levels of mRNA expression in symbiosis *versus* non-symbiotic stage (Lehnert et al. 2014). Later, a phylogenetic analysis

identified two classes of putative GLUT transporters in cnidarians, highlighting the involvement of GLUT proteins in the transport of algal photosynthates (Sproles et al., 2020). In addition, *in silico* localization prediction suggests that these conserved sugar transporters are likely situated within the internal membrane of the symbiotic anemone. In the freshwater animal *Hydra viridissima*, it was reported that one up-regulated gene showed sequence with similarities with GLUT8 of *Aiptasia* (Lehnert et al. 2014; Sproles et al. 2018) was up-regulated in the host. It is possible that maltose produced by symbiont microalgae is transformed into glucose and transported to the host cytoplasm through glucose transporters (Hamada et al. 2018). Of note, *Hydra* and *P. bursaria* are hosts of *Chlorella*-like microalgae of the Trebouxiophyceae class. Thus, the common identification of this up-regulated gene coding for GLUT could indicate a conserved mechanism for transporting photosynthate across the symbiosome membrane, in both unicellular and multicellular photosymbiosis. Additionally, (Sproles et al. 2018) identified that the predicted ligand of GLUT in cnidarians is maltose, a disaccharide known to be excreted by the symbiotic microalgae *M. conductrix*. A more detailed analysis is required to confirm the sugar substrate of GLUT identified in *P. bursaria* and identify if the GLUT gene encodes for a protein containing a dileucine motif near the N-terminus, required to be localized in the endosome membrane (e.g. potentially the symbiosome in the host) (Augustin, Riley, and Moley 2005) . In a recent investigation, increased transcription levels of glucose transporters GLUT3 and GLUT8 were also observed in the medusa *Cassiopea andromeda* in comparison to bleached medusae (Carabantes et al., 2024). GLUT is likely involved in symbiosis, more particularly, in the host part of *P. bursaria*, probably involving the symbiosome membrane.

Two genes identified as Phosphate *transporter and receptor (transceptor)* were also upregulated in the symbiotic host. This gene was previously described in *Saccharomyces cerevisiae* as a phosphate transporter rather than a glucose transporter (Wykoff and O'Shea 2001). It could be that in *Paramecium-Chlorella* system, this transporter mediates the phosphate translocation from the host to the symbiotic microalgae. Yet, further investigation on the protein structure and functional experiments are required.

Overall, several sugar transporters undergoing remodeling in both symbiotic microalgae and the host were also identified in other multicellular organisms photosymbiotic organisms, which highlights their involvement in the translocation of photosynthetic carbon as a shared mechanism. Further

investigations of the identified proteins in this work in both the microalgae and host are needed. Samples were harvested in the afternoon for the symbiotic host and aposymbiotic state of the host and the symbiotic microalgae. Given the dynamic of carbon storage observed in Chapter I, it is important to address the sugar transportome with a temporal resolution. This will help us better understand the involvement of membrane transporters in the translocation of sugar compounds in photosymbiosis. Finally, to validate the candidate genes observed and their substrate, an experimental approach is required as this in silico analysis cannot alone provide conclusive results.

III.4 Material and Methods

Strains and cultural conditions

The ciliate *Paramecium bursaria* (CCAP1660/18) in symbiosis with *Micractinium conductrix* was obtained from the Culture Collection of Algae and Protozoa (https://www.ccap.ac.uk/*)*. The culture medium for *P. bursaria* was prepared by inoculating Volvic natural mineral water with the bacterial strain *Serratia marcescens* CIP103235TI (Pasteur Institute Bacteria CIP) and 0.66 g/L protozoan pellets (Carolina Biological Supply, NC, USA*)* 24h before use. An aposymbiotic host was obtained from a *Paramecium bursaria* (CCAP1660/18) culture. Cell cultures were exposed to 1µM of paraquat (herbicide, Wynca Brand) in volvic water at 20°C under constant high light (light intensity 75 µE m^{-2} s^{-1}) for 7 days. Single symbiotic and aposymbiotic ciliates of *P. bursaria* were collected for transcriptomic analysis.

RNAseq samples preparation

Sequencing was handled using the SMARTseq2kit (https://scientifix.com.au/smart-seq-single-cell-kit.html) (Picelli et al. 2014). 36 samples of symbiotic *Paramecium bursaria* (CCAP1660/18) and 20 samples of aposymbiotic *Paramecium bursaria* were used for this analysis independently. To harvest the cells, individual Paramecium was carefully separated using a binocular microscope and a sterile filtered tip. Subsequently, each sorted cell was placed into a 0.2 PCR tube containing lysis buffer and promptly subjected to rapid freezing in liquid nitrogen. The samples were forwarded to the Genomics Core Facility at EMBL (https://www.embl.org/groups/genomics/) for further nucleic acid processing. In summary, libraries were constructed following the tagmentation protocol outlined by Hennig et al.

in 2018 (G3, 8:79). A total of eighteen pre-amplification cycles were employed to prepare cDNA, which was subsequently sequenced on the NextSeq500 platform using 150-base paired-end reads.

Illumina sequencing and transcriptome analysis

Each sample underwent single-end mode sequencing, generating an average of 10 and 13 million reads per cDNA library for symbiotic and aposymbiotic datasets, respectively. Initial processing entailed trimming raw reads via trimmomatic 0.39, resulting in an average loss of 800,000 reads per sample in both symbiotic and aposymbiotic datasets. Before quantifying read abundance on the Paramecium genome, reads associated with Micractinium conductrix were excluded, particularly in symbiotic samples, utilizing STAR_2.5.2b. Symbiotic samples exhibited 500,000 reads aligned to Micractinium conductrix, while aposymbiotic samples showed an average of less than 300 reads.

Differential gene expression analysis of the symbiotic microalgae concerning its free-living form was made by using the symbiotic ciliate (microalgae reads) compared to (Arriola et al. 2018a) study. To be precise, samples corresponding to the control condition in this study (*M. conductrix* microalgae grown at pH 7.6) were used as references (NCBI: SRR5526896, SRR5526895, SRR5526894). Samples were aligned with those obtained from symbiotic microalgae on the reference genome of *Micractinium conductrix* (strain SAG.241.80)(Assembly: ASM224581v2) (Arriola et al. 2018a). Alignments, read counts, and DEG (differential expression genes) were processed with the same workflow as *P. bursaria* reads. For differential gene expression analysis of symbiotic host, *Paramecium bursaria* (Dd1 strain genome) (Cheng et al. 2020) served as the reference (https://paramecium.i2bc.paris-saclay.fr/download/Paramecium/bursaria/). For all samples, reads were aligned with STAR_2.5.2b. Counts were obtained with feature Counts v2.0.1. To ensure data quality, samples with read counts surpassing the average across libraries were selected to construct the counts matrix. Subsequently, the counts matrix was imported into R, and differential gene expression analysis was conducted using the DESeq2 R package.

Sugar transporters annotation

To unveil sugar transporters in the genome of both *Micractinium conductrix* and *Paramecium bursaria*, annotated proteins were predicted from the sequenced genomes using Interproscan script

vinterproscan-5.60-92.0 and TCDB gblast.pl script. All putative transporters were selected using the following items: egrep -i carrier|Carrier|transport|Transport|channel|Channel|permease|symporter|exchanger|antiporter|periplasmic|facilitator"; for sugar transporters specifically, we used egrep -i "ose|saccharides|carbohydrates|sugar|sugars". We then parsed each annotation manually to curate the annotations.

Supplementary data

Table S1. List of downregulated genes in symbiotic microalgae and symbiotic host.

	Pfam	Protein_ID	Prediction localization (Wolf_PSORT)	FC_status
Symbiotic microalgae *M. conductrix*	PF00083	gene_238	plasma membrane	down
	PF03151	gene_4081	plasma membrane	down
	PF03151	gene_4741	plasma membrane	down
	PF04142	gene_6184	plasma membrane	down

	Pfam	Protein_ID	Prediction localization (Wolf_PSORT)	FC_status
Symbiotic host *P. bursaria*	PF00083	PBUR.Dd1.1.P07340006	plasma membrane	down

Table S2. List of neutral expressed sugar transporter in the symbiotic microalgae *Micractinium conductrix*

	Pfam	Protein_ID	Prediction localization (Wolf_PSORT)	FC_status
Symbiotic microalgae *M. conductrix*	PF00083	gene_1063	plasma membrane	neutral
	PF00083	gene_1088	plasma membrane	neutral
	PF00083	gene_2313	plasma membrane	neutral
	PF00083	gene_3943	plasma membrane	neutral
	PF00083	gene_4015	Nucleus	neutral
	PF00083	gene_6004	plasma membrane	neutral
	PF00083	gene_6450	plasma membrane	neutral
	PF00083	gene_6451	plasma membrane	neutral
	PF00083	gene_6495	plasma membrane	neutral
	PF00083	gene_6580	plasma membrane	neutral
	PF00083	gene_7316	plasma membrane	neutral
	PF00083	gene_7779	plasma membrane	neutral
	PF00083	gene_7897	plasma membrane	neutral
	PF00083	gene_7898	plasma membrane	neutral
	PF00083	gene_7899	plasma membrane	neutral
	PF00083	gene_8522	plasma membrane	neutral
	PF00083	gene_946	plasma membrane	neutral
	PF03151	gene_1057	plasma membrane	neutral
	PF03151	gene_3330	Chloroplasts	neutral
	PF03151	gene_5447	plasma membrane	neutral
	PF03151	gene_5877	plasma membrane	neutral
	PF03151	gene_5878	plasma membrane	neutral
	PF03151	gene_7554	Chloroplasts	neutral
	PF03151	gene_8088	plasma membrane	neutral
	PF03151	gene_8713	vacuole	neutral
	PF03151	gene_8759	plasma membrane	neutral
	PF03151	gene_9189	plasma membrane	neutral
	PF03151	gene_9252	plasma membrane	neutral
	PF03151	gene_9428	plasma membrane	neutral
	PF03151	gene_9849	plasma membrane	neutral
	PF04142	gene_234	vacuole	neutral
	PF04142	gene_3366	plasma membrane	neutral
	PF04142	gene_377	plasma membrane	neutral

Table S3. List of neutral expressed sugar transporter in the symbiotic host *Paramecium bursaria*

	Pfam	Protein_ID	Prediction localization (Wolf_PSORT)	FC_status
Symbiotic host *P. bursaria*	PF00083	PBUR.Dd1.1.P09580026	plasma membrane	neutral
	PF00083	PBUR.Dd1.1.P09580028	plasma membrane	neutral
	PF00083	PBUR.Dd1.1.P05350062	plasma membrane	neutral
	PF00083	PBUR.Dd1.1.P04980028	plasma membrane	neutral
	PF00083	PBUR.Dd1.1.P05730084	plasma membrane	neutral
	PF00083	PBUR.Dd1.1.P06690088	plasma membrane	neutral
	PF00083	PBUR.Dd1.1.P05790011	plasma membrane	neutral
	PF00083	PBUR.Dd1.1.P09970011	plasma membrane	neutral
	PF00083	PBUR.Dd1.1.P03200089	plasma membrane	neutral
	PF00083	PBUR.Dd1.1.P03840066	plasma membrane	neutral
	PF00083	PBUR.Dd1.1.P05350115	plasma membrane	neutral
	PF00083	PBUR.Dd1.1.P08620122	plasma membrane	neutral
	PF00083	PBUR.Dd1.1.P07340005	plasma membrane	neutral
	PF00083	PBUR.Dd1.1.P00220081	plasma membrane	neutral
	PF00083	PBUR.Dd1.1.P00750076	plasma membrane	neutral
	PF00083	PBUR.Dd1.1.P08070005	plasma membrane	neutral
	PF00083	PBUR.Dd1.1.P01750042	plasma membrane	neutral
	PF00083	PBUR.Dd1.1.P01300080	plasma membrane	neutral
	PF00083	PBUR.Dd1.1.P04890080	plasma membrane	neutral
	PF00083	PBUR.Dd1.1.P01220069	plasma membrane	neutral
	PF00083	PBUR.Dd1.1.P08070004	plasma membrane	neutral
	PF00083	PBUR.Dd1.1.P00310009	plasma membrane	neutral
	PF00083	PBUR.Dd1.1.P07340004	plasma membrane	neutral
	PF00083	PBUR.Dd1.1.P09450010	plasma membrane	neutral
	PF00083	PBUR.Dd1.1.P07810054	plasma membrane	neutral
	PF00083	PBUR.Dd1.1.P03070018	plasma membrane	neutral
	PF00083	PBUR.Dd1.1.P08450018	plasma membrane	neutral
	PF00083	PBUR.Dd1.1.P02390034	plasma membrane	neutral
	PF00083	PBUR.Dd1.1.P05900025	plasma membrane	neutral
	PF00083	PBUR.Dd1.1.P08070006	plasma membrane	neutral
	PF00083	PBUR.Dd1.1.P01560050	plasma membrane	neutral
	PF00083	PBUR.Dd1.1.P01430056	plasma membrane	neutral
	PF00083	PBUR.Dd1.1.P05790012	plasma membrane	neutral

Table S4. List of up-regulated genes ID as Aquaporin transporters in *Micractinium. conductrix*

Gene ID	Pfam	Pfam ID	Log2FC	FC2 status	TCDB query	Localization prediction
gene_7368	PF00230	Major intrinsic protein	2.559	UP	Aquaporin_SIP1-1_-_Arabidopsis_thaliana_(Mouse-ear_cress).	Plasma membrane
gene_838	PF00230	Major intrinsic protein	8.571	UP	Aquaporin_1_-_Nicotiana_tabacum_(Common_tobacco).	Plasma membrane

General Conclusions

Symbiosis was at the origin of the plastids and mitochondria in eukaryotes and continues to play an important role in our ecosystems. Symbiotic associations involving a photosynthetic partner (photosymbioses) are particularly interesting because they represent a natural example of the potential process leading to plastid acquisition. A central aspect of photosymbiosis is the photosynthetically-fixed carbon because it is considered as the main energy that is used to fuel and meet the energetic demands of the host. While we now possess a more extensive comprehension of some of the cellular and molecular mechanisms occurring in aquatic photosymbioses, it is necessary to gain more understanding at the subcellular level, in particular on the morphology and metabolism of the symbiotic microalgae within the host. Previous studies have revealed that subcellular imaging is relevant for studying the cellular and subcellular bases of algal physiology (Decelle et al. 2019; Engel et al. 2015; Flori et al. 2017; Uwizeye 2021; Uwizeye et al. 2020). Linking morphological changes with physiological measurements is a powerful and required approach to shed the light on the symbiotic life of an algal cell inside a host. By exploring the subcellular organization of a microalgal cell, we can visualize the ultrastructural organization of symbiotic organisms and assess morphometrics with important physiological aspects of symbiosis. In addition, by comparing the non-symbiotic state of the microalga (if possible) in terms of physiology and morphology, we can gain a highlight potential key mechanism that take place inside a host. Morphological remodeling of photosynthetic-related organelles can reveal the importance of photosynthesis supporting the association. the effect of the host in the microalgae morphology and physiology remains poorly understood. In addition, while the role of translocated carbon in photosymbiosis is known to be central, the characterization of the molecular players ensuring the metabolic connectivity between partners, particularly enabling sugar flux, need further attention. To tackle the current knowledge gaps in photosymbiosis, we conducted a study in the single-celled photosymbiotic model *Paramecium bursaria* (Chapter I) and in the multicellular photosymbiotic host *Favites abdita* (Chapter II). We unveiled morphological and physiological differences in the cellular organization (chloroplast morphometrics) and carbon storage of the symbiotic microalgae with temporal resolution (chapter I) and versus different spatial distribution within a multicellular host (chapter II). In Chapter III, we conducted a transcriptomic analysis to unveil the potential sugar

transporters (sugar transportome) involved in the carbon translocation by comparing symbiotic and non-symbiotic microalgae and host.

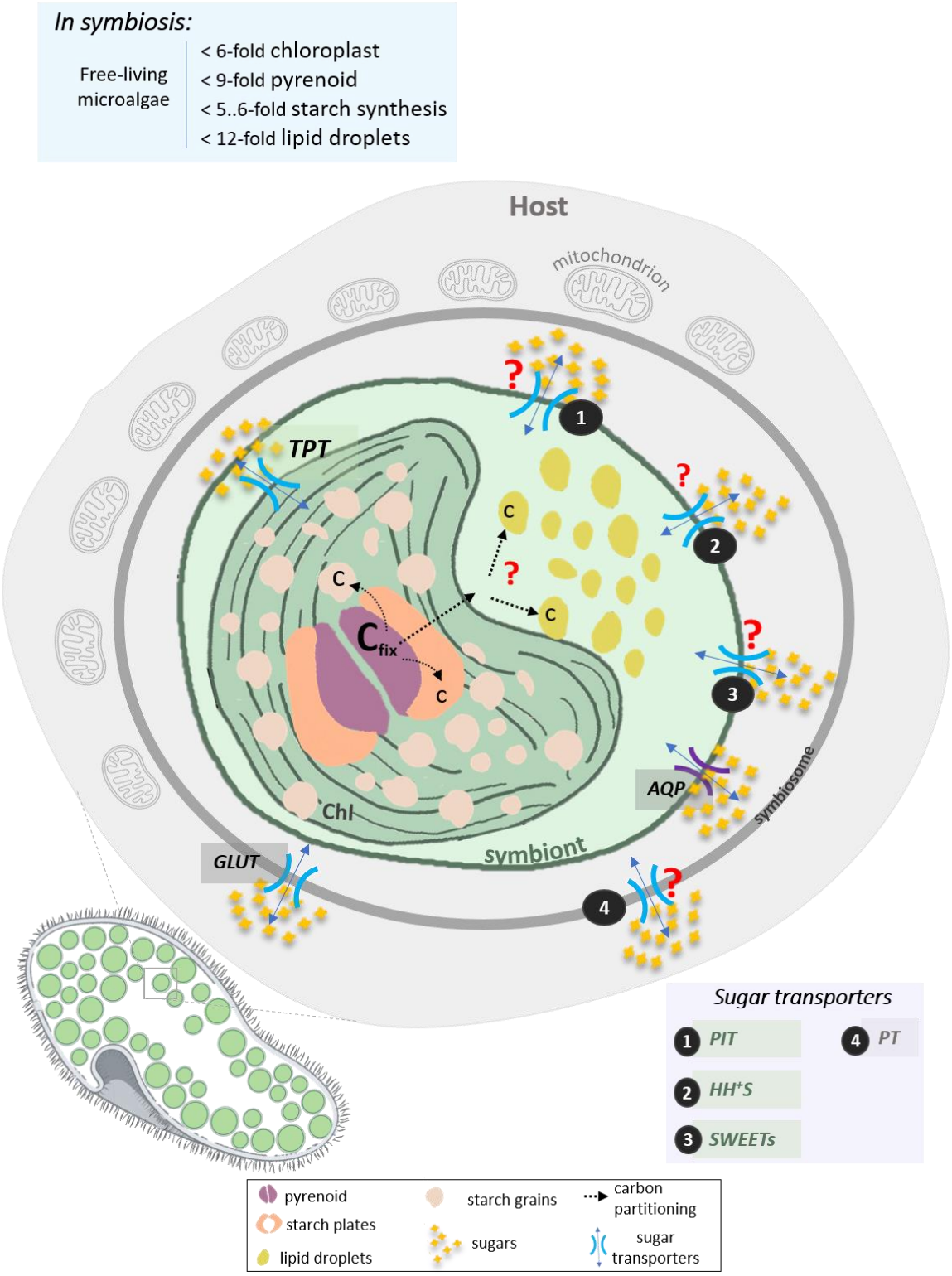

Hypothetical scenario in the photosymbiosis between Paramecium bursaria and its microalgae that summarize the results obtained in the PhD thesis. Symbiotic microalgae *Micractinium conductrix* of *Paramecium bursaria* undergoes an overall remodeling of its photosynthetic capacities. In symbiosis, the microalgae exhibited larger cell size, accompanied by enlarged chloroplasts (chl) and pyrenoid (purple). The volume increase of photosynthetic-related organelles was accompanied by a higher Rubisco (Ribulose bisphosphate carboxylase/oxygenase) content and carbon fixation (represented as 'c') per cell compared to their free-living forms. Temporal dynamics of fixed carbon reveal starch synthesis during daylight hours in starch plates and starch grains (orange), followed by consumption during the night. Moreover, lipid droplets (yellow) accumulate over successive days within the symbiotic microalgae, possibly by receiving carbon for starch overnight. The symbiotic microalgae are maintained inside the host symbiosome (gray) and closely enveloped by host mitochondria. Transcriptomic analysis on the sugar transportome of the microalgae and the host in symbiosis revealed sugar transporter genes likely involved in carbon translocation (including TPT, Inositol, Hexose H^+ in the microalgae, and GLUT, and Aquaporins=AQP in the host). In our proposed model, we hypothesize that the increase of carbon fixation and storage observed in symbiotic microalgae (Chapter I) is linked by the host's role as an external sink (removing photosynthetic products thanks to transporters).

In Chapter I, we aimed to assess the impact of symbiosis on the central carbon metabolism of the algae. We revealed significant morphological and physiological differences in symbiotic microalgae compared to their free-living form (the microalga *Micractinium conductrix*). Most significant differences were observed in the photosynthesis-related organelles: the chloroplast and the pyrenoid are larger in symbiotic microalgae. These transformations were previously reported in other photosymbiotic unicellular organisms (Decelle et al. 2019; Uwizeye 2021), suggesting shared mechanisms among microalgae in symbiosis. Our analysis also revealed that the morphological transformation observed in symbiosis is linked to the physiology of the microalgae: not only do symbiotic microalgae have larger pyrenoids but have increased Rubisco content. Consequently, carbon fixation capability per microalgal cell is significantly enhanced. Furthermore, our investigation sheds light on the fate of photosynthetically-derived carbon energy within photosymbiotic systems. It was not clear whether symbiotic microalgae could store carbon in symbiosis as it is largely considered that most of this carbon is transferred to the host for covering its energetic demands. In this study, we found that microalgae do store carbon as starch, and even in higher proportion during the day compared to the

free-living stage. In addition, diel starch turnover in microalgae follows the same dynamic as in non-symbiotic microalgae, so there is consumption of this starch overnight (decrease of starch). To our knowledge, this carbon storage dynamic was not fully addressed in symbiotic microalgae. Furthermore, we observed that microalgae store more carbon not only as starch but also as neutral lipids compared to their free-living stage. Specifically, our temporal resolution analysis revealed a gradual accumulation of lipids over successive days, possibly due to starch consumption overnight. Despite this higher storage of starch and lipids, and starch consumption overnight, we noticed that symbiotic microalgae exhibit a slower rate of cell division. Therefore, this dynamic of carbon storage may be modulated by the host energetic demands.

Why do symbiotic microalgae show an enhancement in carbon storage and carbon turnover?

Previous investigations have indicated that the host serves as an external factor that modulate and even boost the photosynthetic capacity of the symbiont through the uptake of photosynthetically-generated carbohydrates (Adams et al. 2020). Essentially, in non-symbiotic cells, photosynthesis yields carbohydrates proportional to the organism's consumption or storage capacity (Körner, 2013). Consequently, the host's consumption (external sink) of carbohydrates may increase the photosynthetic productivity of symbiotic algae. Thus, it is likely that the host has an influence to favor and sustain the high carbon production of its symbiont, as less starch production is observed when the system is fueled by an external source of carbon (Chapter I). Further investigations are warranted to fully elucidate the dynamics of this source-sink relationship in photosymbiosis. Of note, a higher accumulation of lipids was observed in the system over the days in the symbiotic microalgae (Chapter I). This indicates that the microalgae can store carbon energy and suggests that the host's ability to absorb carbon is relatively weak or highly regulated in the system. More studies need to address in the future this carbon homeostasis in symbiotic cells to better describe the nature of this association.

Starch plates, starch grains, and pyrenoid temporal dynamic

Our microscopic approach assessed in Chapter I revealed the dynamics of starch plates and pyrenoid volume in symbiotic microalgae throughout the day (Fig. 1). The increase in starch plates and the

formation of a pyrenoid are closely linked physiologically in certain algae. Starch plates encircle the pyrenoid, creating a distinct starch sheath in the cell. In has been observed that starch sheath (e.g. plates) can are formed rapidly under low CO_2 levels (Kuchitsu, Tsuzuki, and Miyachi 1988). In *Chlamydomonas reinhardtii*, a model organism of green microalgae, it was suggested that this starch sheath serves as a barrier, preventing CO_2 diffusion from the pyrenoid (Toyokawa et al. 2020). In this work, they identified the induction of the Carbon Concentrating Mechanism (CCM) with the formation of starch sheets indicating a functional relationship. Furthermore, Mutations in SAGA, a protein called starch granules abnormal 1 (SAGA1) known to interact with Rubisco in these starch plates, lead to abnormal starch plates and the presence of multiple pyrenoids without the typical pyrenoid tubule network (Itakura et al. 2019). To our knowledge, there are no reports about pyrenoid tending to expand throughout the day. Consequently, there is a lack of evidence concerning any physiological link associated with this phenomenon. The pronounced augmentation of starch plates encircling the pyrenoid in symbiotic microalgae underscores a potential Carbon Concentrating Mechanism (CCM) in symbiosis that has yet to be fully elucidated.

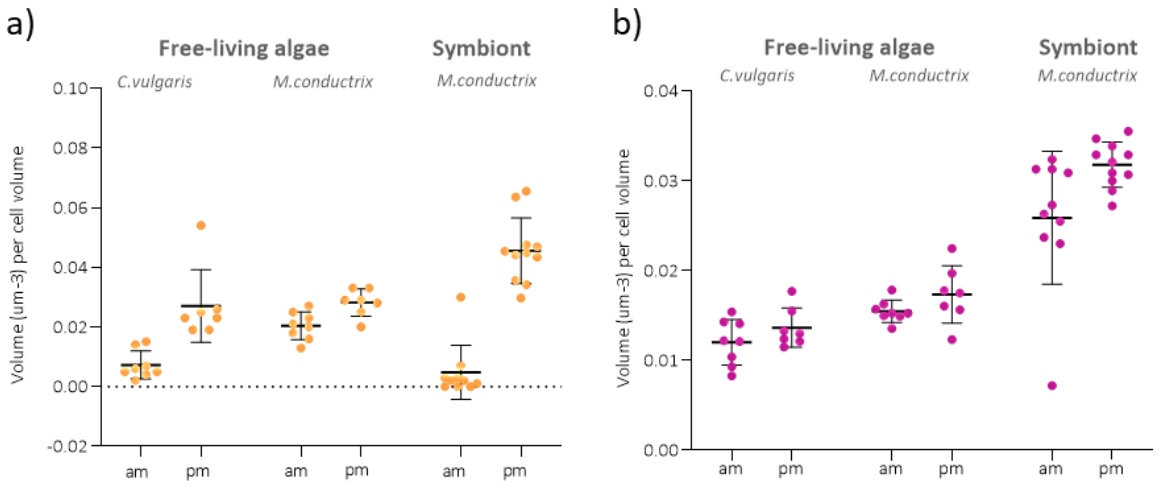

Figure 1. Volume of starch plates and pyrenoid of symbiotic microalgae *M. conductrix* during morning *versus* afternoon.

What is the nature and mechanisms of carbon translocation in photosymbiosis?

NanoSIMS experiment of chapter I showed ^{13}C-labeled structures in trichocysts (defense structures localized below the cilia) of the host. Yet, we could not track high labeling in other host structures/organelles contrary to what is observed in other photosymbiotic organisms, such as lipid reserves (Kopp et al. 2015; Krueger et al. 2018; Sproles et al. 2020). Because of the dynamics of carbon storage observed and quantified in this system, we could hypothesize that carbon translocation is dynamic, and thus, a pulse-chase experiment could be complementary to this work. We also need to consider the possibility that carbon transferred is rapidly respired by the host, so "invisible" by NanoSIMS. The density of host mitochondria may reflect this rapid use of the translocated carbohydrates.

Symbiotic microalgae's carbon release in the system was mostly described indirectly, through isolating them from the host and re-culturing (Muscatine 1967; Reisser t981, 1986; Kessler et al. t991). How much of the physiology changes when cells are no longer *in hospite* is unknown. This is an open question that needs to be further addressed. In our work, we assessed a carbon storage quantification of symbiotic microalgae in the host microenvironment, in which, symbiotic microalgae were removed from host tissue only to assess measurements. Additionally, it has been suggested that 57% of the completely fixed carbon is transferred to the *Paramecium* host (Reisser, 1976). Shibata et al. (2016, 2021) have extensively studied the dynamics of maltose release in the symbiotic microalgae *Chlorella variabilis* (also symbiont of the *Paramecium bursaria*). Their research has elucidated the impact of maltose on symbiotic microalgae upon cultivation, establishing a correlation between maltose release and starch synthesis. However, a complementary study is needed *in hospite*, to gain a comprehensive understanding of the physiological dynamics of these microalgae. From our observations, it appears that fixed-carbon may undergo distinct paths: i) part of fixed carbon remains within the symbiotic microalgae, ii) is directed towards long-term storage (e.g. lipid droplets), like what is observed in our nanoSIMS data and, iii) some of the fixed carbon is transported to the host. Additionally, it should be noted that *P. bursaria*, being a motile cell, may expend energy at a rate beyond our current measurement capabilities. For example, studies on *Paramecium caudatum* have indicated that a substantial portion of metabolic

energy (approximately 70% of the total) is devoted solely to propulsive activity (Katsu-Kimura et al. 2009).

Fueling the host with external sugar: what is the long-term effect on the system?

In Chapter I, we aimed to further understand the source-sink relationship in photosymbiosis. Thus, we assessed starch production in symbiotic microalgae when the host organism received external glucose, a central photosynthate product exchanged between partners. Our experiment revealed that symbiotic microalgae produced less starch at the end of the day when the host was provided with glucose (Chapter I). Therefore, it is probable that decreased energy demand in the host triggered a cellular process leading to reduced starch production in its microalgae.

Within the same frame of experiment, we follow the impact of external glucose in the long-term and observe the impact on the symbiotic association. At 48 hours post-exposure, we observed host cells containing numerous vacuoles housing brown symbiotic microalgae (Fig. 2a), with some microalgae found outside host cells. By the seventh day, certain host cells had shed most or all symbiotic microalgae while remaining viable. Host cells, at the end of the experiment (7 days), exhibited a similar appearance to aposymbiotic cells generated through chemical methods in laboratory conditions. (Fig.2b, c). These observations warrant further exploration into the ultimate impact of glucose on the symbiotic association. Notably, in terms of the physiological and morphological state of both, microalgae and host after the breakdown of the symbiotic association.

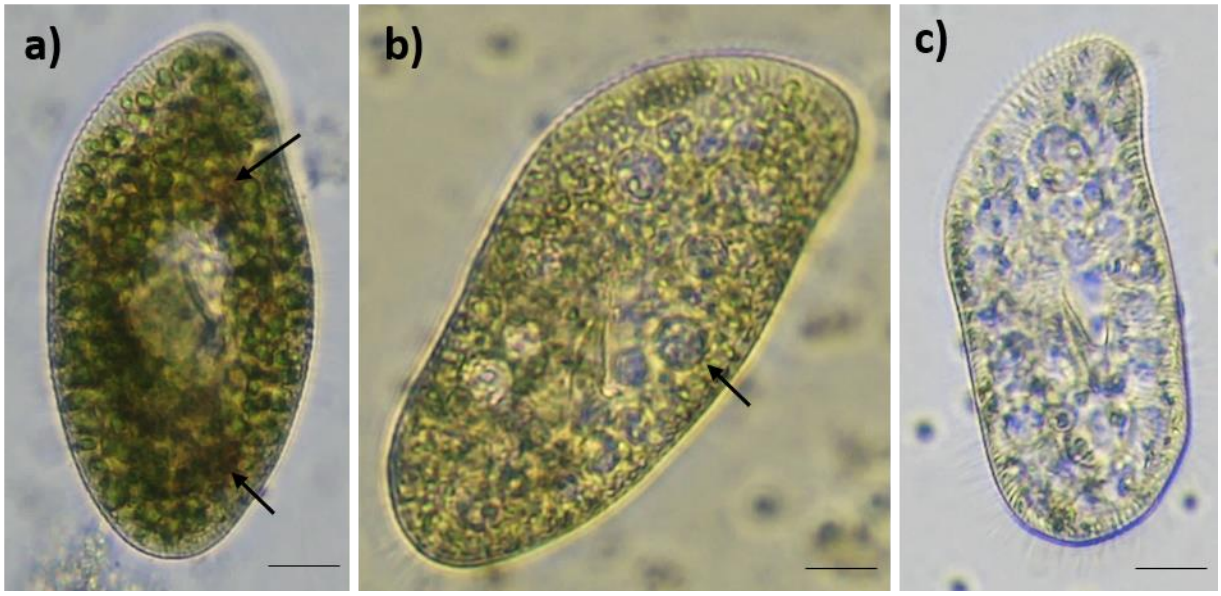

Figure 2. Host cell (P. bursaria) after long exposure to glucose (75mM). a) 48h after exposure to glucose. Some brown algae are apparent digestive vacuoles (arrow) **b)** Host cellafter 7 days of exposure to glucose (75mM). The host has no symbionts and form several digestive vacuoles **c)** Aposymbiotic host *P. bursaria* obteined after exposure to paraquat (herbicide)**.** Scale bar: 20µm.

In Chapter II, we investigated the possible heterogeneity of the symbiont population and the possible link with the **spatial localization of symbiotic microalgae inside a multicellular host.**

We compared the effect of 'top' – 'bottom' spatial distribution of symbiotic microalgae and assess the high-resolution morphometry. Our FIB-SEM 3D modeling revealed heterogeneity within the symbiotic population differentially distributed in the host tissue. Similarly, we observed higher starch volume per cell at the bottom region of the coral tissue. We need to further investigate the physiological status of symbiotic cells respect to each condition and environmental and microenvironmental measurements are necessary. While differences related to spatial localization in corals have previously been reported (Titlyanov et al. 2001), the subcellular morphological differences were unknown. Morphometrics showed different starch volume content between symbiotic microalgae localized at the 'top' and 'bottom' of the coral tissue *Favites abdita.* (Titlyanov et al. 2001) assessed the physiological characterization during photo acclimation in *Stylophora pistillata.* In this work they reported

differences in terms of symbiont cells densities (more dense cells) in low-exposure *versus* high-exposure to light in the coral tissue. This observation was consistent with our results; thus, we could hypothesize photo-acclimation in 'bottom' cells due to lower light exposure. Yet, we require more contextual information. The differences in terms of cell volume and carbon storage (starch) highlight the heterogeneity of symbiotic population within a host influenced by the spatial distribution and reflected in their carbon storage content. For instance, in corals photosymbiosis it is reported that ~90% of the photosynthetic carbon is transferred to the host (Falkowski 1980). The observation of cells in the 'bottom' of the host showing higher starch storage that cells in the 'top' could be link to how much of this carbon is being translocated to the host. To assess this, we would need NanoSIMS, for instance to track carbon in the host tissue overtime between both conditions.

A time-resolved experiment, following carbon storage dynamics of symbiotic microalgae respect to their spatial distribution (thus, different environment and microenvironment conditions) within a host would be necessary to characterize the carbon metabolism of symbiotic microalgae in corals. Finally, thanks to the nanoengineering develop in the laboratory of D. Wangpraseurt, we could develop combined conditions similar host microenvironment and assess the morphological transformation of symbiotic microalgae. Our results require more contextual information to better interpret our observations. We foresee a complementary analysis that will include characterization of light profiles inside host tissue through microsensors (expertise of our collaborator D. Wangpraseurt). In this work, samples where chemically fixed and not cryo-fixed using high pressure freezing. Thus, we faced challenges when assessing semi-automatic segmentation based on contrast. In the future, high-pressure freezing needs to be considered to improve the sample preparation and so the 3D reconstruction of different algal structures

In Chapter III, we focused on **the metabolic connectivity between host and algae and** particularly **investigated the sugar transporters expressed in symbiotic versus free-living forms.**

Several studies have delved into the exchange of energy-rich organic molecules to unravel the mechanisms governing photosymbiotic associations (Burriesci et al. 2012; Carabantes, Grosso-Becerra, and Thomé 2024; Davy et al. 2012; Hofmann and Kremer 1981). Symbiotic microalgae are maintained in a host microenvironment: the symbiosome. This host compartment houses symbiotic microalgae,

and is likely facilitating nutrient exchange and metabolic crosstalk between the host and symbiont. Thus, any transfer of organic molecules must occur through this selective barrier. Photosynthetic products, known as photosynthates, are a primary energy source in this relationship, with glucose and glycerol being key soluble sugars.

We identified different sugar transporters likely involved in the metabolic connectivity of the host and symbiotic microalgae. Some of the predicted genes up-regulated in symbiosis (Scheme 1.) in both the host and the microalgae have also been reported in other photosymbiosis: *Hydra-Chlorella*, from freshwater ecosystems (Hamada et al. 2018) and cnidarians (*Aiptasia* and *Cassiopea*) from marine ecosystems (Carabantes et al. 2024; Mashini et al. 2022; Sproles et al. 2018). We also observed up-regulated genes annotated as Aquaporins (AQPs), that we did not include initially as part of the sugar transportome as they belong to a large family of proteins involved in the transfer of different substrates including glycerol (Giovannetti et al. 2012; Hara-Chikuma and Verkman 2006). Finally, we also observed a gene identified as SWEET (Sugar Will Eventually be Exported Transporter: hexose and sucrose transporters), which was expressed in the symbiotic microalgae but not differentially regulated. Of note, this sugar transporter has been studied in different pathogen interactions and intercellular sugar translocation in plants (Chen 2014; Eom et al. 2015). Two sugar transporters not described in other photosymbiotic organisms were found to be up-regulated in our study: *Hexose H+ symporter* and *Putative Inositol transporter 2* in the symbiotic microalgae. Of note, MEX1 (maltose excess1), a maltose-specific transporter was not identified among up-regulated genes in the symbiotic microalgae, known to be associated with the chloroplast (Niittylä et al. 2004).

From the host side, we observed that only 9.1% of the sugar transport undergoes remodeling in symbiosis, in contrast to the microalga's sugar transport with an extensive remodeling of 50%. Three genes were up-regulated, the sugar transporters GLUT3 and two Phosphate transporter and receptor. Similar GLUT genes have been documented in other photosymbiotic hosts such as cnidarians (*Cassiopea andromeda*, anemone Aiptasia) (Carabantes et al., 2024).(Sproles et al., 2020) (Lehnert et al. 2014), and the freshwater hydra *Hydra viridissima* (Hamada et al. 2018) suggesting a conserved role of GLUT genes in transporting algal photosynthates. The identification of GLUT up-regulation in both *Hydra* and *P. bursaria* suggests a shared mechanism for transporting photosynthates across the symbiosome membranes in unicellular and multicellular photosymbiosis of freshwater ecosystems. In

addition, maltose has been proposed as a potential ligand for GLUT in cnidarians (Sproles et al. 2018). This disaccharide is known to be excreted by the symbiotic microalgae of *P. bursaria* under acidic conditions. Further analysis is needed to confirm the sugar substrate of GLUT in *P. bursaria* and an adequate internal localization, potentially within the symbiosome. The second upregulated gene of the host sugar transportome was annotated as Phosphate transporter and receptor. This transporter was previously described in *Saccharomyces cerevisiae,* involved in glucose sensing rather than glucose transport for hexose transport regulation (Ozcan 1998; Theodoris et al. 1994; Wykoff and O'Shea 2001) We further evaluated a localization prediction outlined in Scheme 1. We highlight the need for a more detailed analysis of the sugar transportome. For instance, immunofluorescence analysis could be used to identified subcellular localization of sugar transporters in photosymbioses. Yet, we need to develop antibodies specific for this type of organism systems. Additionally, we emphasize the need to improve differential gene expression analysis of the symbiotic microalgae by comparing it to the free-living form we obtained and characterized in this study. Gene annotation in this system posed challenges and was a significant constraint due to the abundance of unknown genes in these organisms. (Arriola et al. 2018a).

Moving towards functionality?

Symbiotic *Chlorella* microalgae and *Chlorella*-like species belonging to the Trebouxiophyceae class are notable for their ability to establish symbiotic relationships with diverse host cells (Pröschold et al. 2011) including lichens, diverse protists, and metazoan (Metz et al. 2019). Extensive research has been made on symbiotic *Chlorella* species brought to culture. The evidence consistently indicates that maltose and/or glucose are the primary carbon sources provided to the host. The preference for maltose release over alternative sugars is a noteworthy aspect to explore. For instance, it is known that in green microalgae and higher plants, maltose serves as a transient breakdown product of starch in chloroplasts (Arriola et al. 2018a; Busi et al. 2014). In Chapter I, we conducted a temporal analysis of carbon storage, focusing on starch and lipid droplets. Further experimental approaches are necessary to comprehensively characterize the sugar transporters identified in this study. This will involve employing RT-qPCR for quantitative analysis and RNAi to elucidate the effects of loss of function in the host organism, thereby revealing the molecular mechanisms underlying photosynthetic carbon

translocation. Future transcriptomic analyses could incorporate temporal resolution, allowing us to correlate our previous observations with metabolic connections and carbon exchange between the microalgae and the host. Furthermore, additional investigation of metabolic pathways associated with starch and lipid synthesis and degradation is required to complement our study. On the sugar transporter candidates validated by the molecular approaches above, functional characterization will also be necessary in order to identify the potential sugar substrates.

General perspectives

Photosymbiotic interactions are complex to study because of the involvement of two cell types and two metabolism. Some of the challenges encountered in this project were linked to the low-throughput 3D reconstruction. A major investment was made to obtained the semi-automatic segmentation of 3D reconstruction and morphometrics of around ~80 cells in this work. Currently, deep-learning is more advanced to improve the technical limitation we faced. Nonetheless, the large data set I built through my PhD project could be used to nourished an automated deep-learning source. FIB-SEM based 3D reconstruction we unveil the cellular remodeling taking place of microalgae in symbiosis. Of note, we assessed a temporal morphometrics quantification at a nanoscale of carbon storage compounds. These structures are well contrasted and semi-automatic segmentation can be simpler and faster to accomplish.

Cryo-preservation would be a next step to complement this study. We observed a volumetric dynamic of the pyrenoid thorough the day (increase in volume during the day) and different dynamics of starch plates and starch grains. Cryo-EM could allow us to access a very high resolution and native view of the structures and organization of major organelles (chloroplast) and protein complexes. For instance, the symbiosome is one of the major structures in the photosymbiotic systems facilitating, through membrane transporters, the metabolic connectivity between partners. Yet, structural information about this major membrane interface in symbiosis is needed. Our transcriptomic analysis revealed some of the potential sugar transporters involved in the host-microalgae metabolic crosstalk. The versatility of *P. bursaria* photosymbiosis could be a potential starting point to explore available "omics" tools.

Field work: hunting wild symbiotic associations

Symbiotic paramecium and other photosymbiotic cells from Pontet Lake

During my PhD project, we sampled in the alpine lake 'Pontet" (1920 m.s.l.), Haute-Alpes-France. These sampling allowed us to discovered a wild green *Paramecium*. Sequencing analysis confirmed the symbiotic microalgae as *M. conductrix.* Furthermore, other single-celled photosymbiosis were collected within the same lake, potentially in symbiosis with *M. conductrix.* Most of the protist observed in symbiosis were ciliates (Fig. 3). Lake ecosystems are natural environments where we could better characterize the dynamics across symbiosis with green microalgae of the class Trebouxiophyceae.

Additional effort can be made to bring to culture some of these symbiotic associations, as it is possible that our current culture representative (the green *Paramecium bursaria*) changed and adapted to the artificial culture conditions. In addition, cells could be collected for further microscopy characterization, thanks to the microscopy facilities in Grenoble. Furthermore, more investment is being deployed to study organisms in their natural condition. For instance, an initiative from EMBL (TREC expedition), deployed a mobile laboratory with equipment for sample preparation (cryo-EM, high pressure freezing). We could combine effort to characterize freshwater photosymbiosis across alpine lakes, as unique ecosystems.

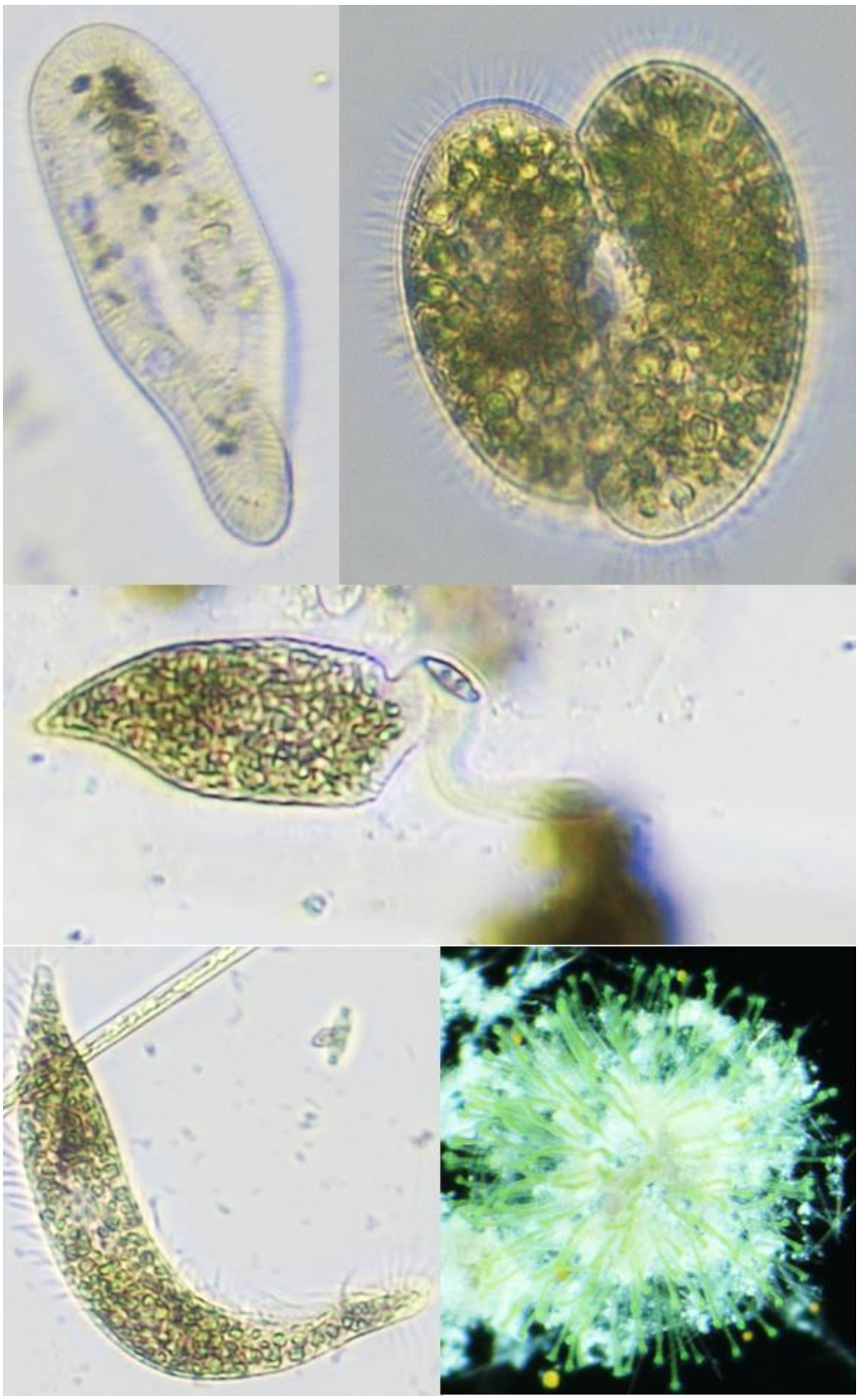

Figure 3. Alpine photosymbiotic ciliates collected in Pontet Lake, France. a) non-symbiotic paramecium. b) wild green paramecium in symbiosis with *M. conductrix* c) and d) unidentified ciliates likely in symbiosis with green microalgae e) ciliate colony in symbiosis with green microalgae

Acknowledgments

This project was made possible thanks to the funding provided by LabEx GRAL (ANR-10-LABX-49-01), supported by the University Grenoble Alpes graduate school (Ecoles Universitaires de Recherche) CBHEUR-GS (ANR-17-EURE-0003). I was hosted by the team Photosymbiosis-PCV. In the course of my project, I have collaborated with several institutes and scientists who contributed to this project: Anders Meibom and Stephane Escrig for their assistance with NanoSIMS analysis, EA-IRMS platform (Gael Guillou and Benoit Lebreton), Guy Schoehn and Christine Moriscot, as well as the electron microscope facility at IBS, whose operations are made possible by the collaborative support of various institutions including the Rhône-Alpes Region, Fondation Recherche Medicale (FRM), fonds FEDER, CNRS, CEA, University of Grenoble, EMBL, and GIS Infrastructures en Biologie Sante et Agronomie (IBISA). D. Wangpraseurt, thanks for letting me explore a marine symbiosis.

To Johan Decelle. I have been fascinated by symbiotic interactions for a long time and I have been dreaming of doing marine biology for as long as I can remember. Thanks to this PhD and the project we have shared for 3.5 years, I was able to get closer to my dream, and discover these mysterious plankton symbioses through EM, and wow! this blow my mind. I will always be grateful for that! I enjoyed every single concept/discussion/organisms I discovered. Thanks a lot for your investment in the writing of the article. They were long days, of learning, busy mornings that I appreciated. Someday, I hope, I'll be able to write with the talent you have. It was truly a pleasure. Also!! thanks for inviting me to enjoy one of the crazy TREC adventures. The work and scientific environment I saw, was something I will keep with me preciously.

Gilles Curien. Thanks for your involvement, feedback, and wonderful discussions and hypotheses about the metabolism of algae in symbiosis. I would like to thank your immense kindness and support, both scientifically and personally.

Thanks to the all the Photosymbiosis team (Daniel, Fabien, Ananya, Caroline), for their enthusiasm and the scientific moments shared (also to the new members I shared my last PhD road Gaelle, Laia and Catrinel :D). Special thanks to F. Chevalier, D. Yee and Ananya R. Thanks for sharing the daily challenges of my lab work, science and personal life. I was very lucky to have you around.

Deep thanks to the teams I shared labs too. Team CytomorphoLab, Photosynthesis. Thanks for sharing all the laboratory challenges we confront daily with a big smile. I would not have succeeded anything without your warming friendship: JhoJho, Mathilde, Chri-Chri, Sandrine. Thanks to the incredible women scientists that supported me without hesitation, where accessible and are a great example to follow: Alex (cytomorpholab), Christel, Gabrielle, and Florence (Thanks for following me until the PhD defense, what a pleasure!).

To the Vincent family. Have no words but I am sure I was very lucky to meet you. Thanks for all the glaciers and mountains, I conquered with you. Thank you for witnessing and supporting me in my process of overstepping my own personal limits. You are all unique. Thanks to all the amazing people I encounter in my long days of segmentation and sample prep: PH, Benoit, Thomas. Thanks, Yours, Patrice for lighting my lab work at PFNC and during Covid. Thanks to all my dear friends in Europe, and Bolivia. Ferchu, Carlotita, Elenu, Jhojho, Ximena, Salseros, Forroseiros, And etc etc. To my family. Thanks for letting me flight away, free. For letting me dream and keep on dreaming elsewhere. To my younger self, to your resilience that kept on giving.

Résumé

La symbiose a joué un rôle essentiel dans l'évolution des plastes et des mitochondries chez les eucaryotes, et fait encore partie intégrante des écosystèmes aujourd'hui. Parmi les relations symbiotiques, la photosymbiose - un partenariat impliquant une cellule photosynthétique - est très répandue dans les environnements aquatiques. Bien que notre compréhension de certains aspects de la photosymbiose se soit améliorée, l'influence du microenvironnement de l'hôte sur la morphologie et la physiologie des microalgues avant l'apport de carbone n'est toujours pas claire. En outre, des recherches supplémentaires sont nécessaires pour caractériser les composants moléculaires qui facilitent la connectivité métabolique entre les partenaires symbiotiques. Dans cette thèse, j'ai mené une étude sur le modèle photosymbiotique unicellulaire Paramecium bursaria (Chapitre I) et l'hôte photosymbiotique multicellulaire Favites abdita (Chapitre II), découvrant des différences morphologiques et physiologiques dans l'organisation cellulaire et le stockage du carbone. En outre, j'étudie les transporteurs de sucre potentiels impliqués dans la translocation du carbone par le biais d'une analyse transcriptomique.

Dans l'ensemble, nos résultats montrent que les microalgues symbiotiques subissent un remodelage subcellulaire impliquant principalement les organites liés à la photosynthèse (par exemple les chloroplastes et le pyrénoïde), ce qui entraîne une fixation plus élevée du carbone. Cette productivité élevée est liée à la demande énergétique de l'hôte. Une caractérisation temporelle a dévoilé la production et le renouvellement du carbone dans la symbiose : le carbone photosynthétique est accumulé dans des composés de stockage (p. ex. gouttelettes d'amidon et de lipides) avant d'être transféré à l'hôte.

Cette étude permet de mieux comprendre le métabolisme du carbone chez les microalgues symbiotiques et les processus potentiels de l'hôte qui génèrent l'énergie du carbone dans la photosymbiose. En outre, notre évaluation morphométrique de la photosymbiose multicellulaire a révélé une hétérogénéité entre les cellules symbiotiques d'un même hôte. D'autres études sont nécessaires pour explorer comment le microenvironnement de l'hôte affecte la distribution des microalgues dans les tissus de l'hôte. Enfin, les acteurs moléculaires impliqués dans la translocation du carbone dans la photosymbiose ont été analysés. Notre travail a révélé l'existence de transporteurs moléculaires de sucres communs aux photosymbioses unicellulaires et multicellulaires. Les associations photosymbiotiques sont dynamiques, la résolution temporelle est donc cruciale pour mieux comprendre les mécanismes moléculaires et physiologiques qui sous-tendent le stockage et la translocation du carbone.

Abstract

Symbiosis has been pivotal in the evolution of plastids and mitochondria in eukaryotes, remaining integral to ecosystems today. Among symbiotic relationships, photosymbiosis—a partnership involving a photosynthetic cell—is widespread in aquatic environments. While our understanding of some aspects of photosymbiosis has improved, the influence of the host microenvironment on the morphology and physiology of microalgae before carbon delivery remains unclear. Additionally, further investigation is needed to characterize the molecular components facilitating metabolic connectivity between symbiotic partners. In this thesis, I conducted a study on the single-celled photosymbiotic model *Paramecium bursaria* (Chapter I) and the multicellular photosymbiotic host *Favites abdita* (Chapter II), uncovering morphological and physiological differences in cellular organization and carbon storage. Additionally, I study potential sugar transporters involved in carbon translocation through transcriptomic analysis.

Overall, our results showed that symbiotic microalgae undergo subcellular remodeling involving principally photosynthetic-related organelles (e.g. chloroplasts and pyrenoid) leading to higher carbon fixation. This high productivity is linked to the host's energetic demands. A temporal characterization unveiled the carbon production and carbon turnover in symbiosis: photosynthetic carbon is accumulated in storage compounds (e.g. starch and lipid droplets) before being transferred to the host. This study provides insights into carbon metabolism in symbiotic microalgae and potential host processes that engineer carbon energy in photosymbiosis. Furthermore, our morphometric assessment in multicellular photosymbiosis revealed heterogeneity among symbiotic cells within a single host. Further investigations are needed to explore how the host microenvironment affects microalgae distribution within host tissues. Finally, the molecular players involved in the carbon translocation in photosymbiosis were analyzed. Our work revealed shared molecular sugar membrane transporters across unicellular and multicellular photosymbiosis. Photosymbiotic associations are dynamics, thus temporal resolution is crucial to better understand the molecular and physiological mechanisms underlying carbon storage and carbon translocation.

References

Abida, Heni, Lina-Juana Dolch, Coline Meï, Valeria Villanova, Melissa Conte, Maryse A. Block, Giovanni Finazzi, Olivier Bastien, Leïla Tirichine, Chris Bowler, Fabrice Rébeillé, Dimitris Petroutsos, Juliette Jouhet, and Eric Maréchal. 2015. "Membrane Glycerolipid Remodeling Triggered by Nitrogen and Phosphorus Starvation in *Phaeodactylum Tricornutum*." *Plant Physiology* 167(1):118–36. doi: 10.1104/pp.114.252395.

Abramson, Bradley W., Benjamin Kachel, David M. Kramer, and Daniel C. Ducat. 2016. "Increased Photochemical Efficiency in Cyanobacteria via an Engineered Sucrose Sink." *Plant and Cell Physiology* 57(12):2451–60. doi: 10.1093/pcp/pcw169.

Adams, Melanie S., Barbara Demmig-Adams, Ruiqi Li, Daniel Zarate, and Jingchun Li. 2020. "Coral Reef Productivity and Diversity—Contributions from Enhanced Photosynthesis via Demand for Carbohydrate from the Host." *Marine Ecology* 41(6). doi: 10.1111/maec.12618.

Albers, D., W. Reisser, and W. Wiessner. 1982. "STUDIES ON THE NITROGEN SUPPLY OF ENDOSYMBIOTIC CHLORELLAE IN GREEN PARAMECIUM BURSARIA."

Andersen, Christian P. 2003. "Source–Sink Balance and Carbon Allocation below Ground in Plants Exposed to Ozone." *New Phytologist* 157(2):213–28. doi: 10.1046/j.1469-8137.2003.00674.x.

Anthony, K. R. N., and O. Hoegh-Guldberg. 2003. "Variation in Coral Photosynthesis, Respiration and Growth Characteristics in Contrasting Light Microhabitats: An Analogue to Plants in Forest Gaps and Understoreys?" *Functional Ecology* 17(2):246–59. doi: 10.1046/j.1365-2435.2003.00731.x.

Armstrong, Eric J., Jinae N. Roa, Jonathon H. Stillman, and Martin Tresguerres. 2018. "Symbiont Photosynthesis in Giant Clams Is Promoted by V-Type H+-ATPase from Host Cells." *The Journal of Experimental Biology* 221(Pt 18). doi: 10.1242/jeb.177220.

Arriola, Matthew B., Natarajan Velmurugan, Ying Zhang, Mary H. Plunkett, Hanna Hondzo, and Brett M. Barney. 2018a. "Genome Sequences of *Chlorella Sorokiniana* UTEX 1602 and *Micractinium Conductrix* SAG 241.80: Implications to Maltose Excretion by a Green Alga." *The Plant Journal* 93(3):566–86. doi: 10.1111/tpj.13789.

Arriola, Matthew B., Natarajan Velmurugan, Ying Zhang, Mary H. Plunkett, Hanna Hondzo, and Brett M. Barney. 2018b. "Genome Sequences of *Chlorella Sorokiniana* UTEX 1602 and *Micractinium Conductrix* SAG 241.80: Implications to Maltose Excretion by a Green Alga." *The Plant Journal* 93(3):566–86. doi: 10.1111/tpj.13789.

Augustin, Robert, Joan Riley, and Kelle H. Moley. 2005. "GLUT8 Contains a [DE]XXXL[LI] Sorting Motif and Localizes to a Late Endosomal/Lysosomal Compartment." *Traffic* 6(12):1196–1212. doi: 10.1111/j.1600-0854.2005.00354.x.

Ball, Steven G., Léon Dirick, André Decq, Jean-Claude Martiat, and RenéF. Matagne. 1990. "Physiology of Starch Storage in the Monocellular Alga Chlamydomonas Reinhardtii." *Plant Science* 66(1):1–9. doi: 10.1016/0168-9452(90)90162-H.

Barott, Katie L., Alexander A. Venn, Sidney O. Perez, Sylvie Tambutté, and Martin Tresguerres. 2015. "Coral Host Cells Acidify Symbiotic Algal Microenvironment to Promote Photosynthesis." *Proceedings of the National Academy of Sciences* 112(2):607–12. doi: 10.1073/pnas.1413483112.

Bennett, Adam E., Kedar Narayan, Dan Shi, Lisa M. Hartnell, Karine Gousset, Haifeng He, Bradley C. Lowekamp, Terry S. Yoo, Donald Bliss, Eric O. Freed, and Sriram Subramaniam. 2009. "Ion-Abrasion Scanning Electron Microscopy Reveals Surface-Connected Tubular Conduits in HIV-Infected Macrophages" edited by T. J. Hope. *PLoS Pathogens* 5(9):e1000591. doi: 10.1371/journal.ppat.1000591.

Bezrutczyk, Margaret, Thomas Hartwig, Marc Horschman, Si Nian Char, Jinliang Yang, Bing Yang, Wolf B. Frommer, and Davide Sosso. 2018. "Impaired Phloem Loading in Zmsweet13a, b, c Sucrose Transporter Triple Knock-out Mutants in Zea Mays." *New Phytologist* 218(2):594–603.

Bhattacharya, Debashish, Hwan Su Yoon, and Jeremiah D. Hackett. 2004. "Photosynthetic Eukaryotes Unite: Endosymbiosis Connects the Dots." *BioEssays* 26(1):50–60. doi: 10.1002/bies.10376.

Biard, Tristan, Lars Stemmann, Marc Picheral, Nicolas Mayot, Pieter Vandromme, Helena Hauss, Gabriel Gorsky, Lionel Guidi, Rainer Kiko, and Fabrice Not. 2016. "In Situ Imaging Reveals the Biomass of Giant Protists in the Global Ocean." *Nature* 532(7600):504–7. doi: 10.1038/nature17652.

Brandt, Karl. 1881. *Über Das Zusammenleben von Algen Und Tieren*. Junge.

Brierley, Andrew S. 2017. "Plankton." *Current Biology* 27(11):R478–83. doi: 10.1016/j.cub.2017.02.045.

Brown, Jack A., and P. James Nielsen. 1974. "Transfer of Photosynthetically Produced Carbohydrate from Endosymbiotic Chlorellae to *Paramecium Bursaria* *." *The Journal of Protozoology* 21(4):569–70. doi: 10.1111/j.1550-7408.1974.tb03702.x.

Bukhov, N. G. 2004. "Dynamic Light Regulation of Photosynthesis (A Review)." *Russian Journal of Plant Physiology* 51(6):742–53. doi: 10.1023/B:RUPP.0000047822.66925.bf.

Burns, John A., Ryan Kerney, and Solange Duhamel. 2020. "Heterotrophic Carbon Fixation in a Salamander-Alga Symbiosis." *Frontiers in Microbiology* 11:1815. doi: 10.3389/fmicb.2020.01815.

Burriesci, Matthew S., Theodore K. Raab, and John R. Pringle. 2012. "Evidence That Glucose Is the Major Transferred Metabolite in Dinoflagellate–Cnidarian Symbiosis." *Journal of Experimental Biology* 215(19):3467–77. doi: 10.1242/jeb.070946.

Busi, María V., Julieta Barchiesi, Mariana Martín, and Diego F. Gomez-Casati. 2014. "Starch Metabolism in Green Algae." *Starch - Stärke* 66(1–2):28–40. doi: 10.1002/star.201200211.

Carabantes, Natalia, María Victoria Grosso-Becerra, and Patricia E. Thomé. 2024. "Expression of Glucose (GLUT) and Glycerol (GLP) Transporters in Symbiotic and Bleached Cassiopea Xamachana (Bigelow, 1892) Jellyfish." *Marine Biology* 171(2):54. doi: 10.1007/s00227-023-04374-2.

Carbó, Roxana, and Emma Rodríguez. 2023. "Relevance of Sugar Transport across the Cell Membrane." *International Journal of Molecular Sciences* 24(7):6085. doi: 10.3390/ijms24076085.

Caspari, Thomas, Andreas Will, Miroslava Opekarová, Norbert Sauer, and Widmar Tanner. 1994. "Hexose/H+ Symporters in Lower and Higher Plants." *Journal of Experimental Biology* 196(1):483–91. doi: 10.1242/jeb.196.1.483.

Chen, Li-Qing. 2014. "SWEET Sugar Transporters for Phloem Transport and Pathogen Nutrition." *New Phytologist* 201(4):1150–55.

Chen, Li-Qing, Bi-Huei Hou, Sylvie Lalonde, Hitomi Takanaga, Mara L. Hartung, Xiao-Qing Qu, Woei-Jiun Guo, Jung-Gun Kim, William Underwood, Bhavna Chaudhuri, Diane Chermak, Ginny Antony, Frank F. White, Shauna C. Somerville, Mary Beth Mudgett, and Wolf B. Frommer. 2010. "Sugar Transporters for Intercellular Exchange and Nutrition of Pathogens." *Nature* 468(7323):527–32. doi: 10.1038/nature09606.

Cheng, Yu-Hsuan, Chien-Fu Jeff Liu, Yen-Hsin Yu, Yu-Ting Jhou, Masahiro Fujishima, Isheng Jason Tsai, and Jun-Yi Leu. 2020. "Genome Plasticity in Paramecium Bursaria Revealed by Population Genomics." *BMC Biology* 18(1):180. doi: 10.1186/s12915-020-00912-2.

Cooksey, Keith E., James B. Guckert, Scott A. Williams, and Patrik R. Callis. 1987. "Fluorometric Determination of the Neutral Lipid Content of Microalgal Cells Using Nile Red." *Journal of Microbiological Methods* 6(6):333–45. doi: 10.1016/0167-7012(87)90019-4.

Cruz, Sónia, and Paulo Cartaxana. 2022. "Kleptoplasty: Getting Away with Stolen Chloroplasts." *PLOS Biology* 20(11):e3001857. doi: 10.1371/journal.pbio.3001857.

Davy, Simon K., Denis Allemand, and Virginia M. Weis. 2012. "Cell Biology of Cnidarian-Dinoflagellate Symbiosis." *Microbiology and Molecular Biology Reviews* 76(2):229–61. doi: 10.1128/MMBR.05014-11.

Davy, Simon K., and Clayton B. Cook. 2001. "The Influence of 'Host Release Factor' on Carbon Release by Zooxanthellae Isolated from Fed and Starved Aiptasia Pallida (Verrill)." *Comparative Biochemistry and Physiology Part A: Molecular & Integrative Physiology* 129(2–3):487–94. doi: 10.1016/S1095-6433(01)00285-9.

Decelle, Johan, Sébastien Colin, and Rachel A. Foster. 2015. "Photosymbiosis in Marine Planktonic Protists." Pp. 465–500 in *Marine Protists*, edited by S. Ohtsuka, T. Suzaki, T. Horiguchi, N. Suzuki, and F. Not. Tokyo: Springer Japan.

Decelle, Johan, Ian Probert, Lucie Bittner, Yves Desdevises, Sébastien Colin, Colomban De Vargas, Martí Galí, Rafel Simó, and Fabrice Not. 2012. "An Original Mode of Symbiosis in Open Ocean Plankton." *Proceedings of the National Academy of Sciences* 109(44):18000–5. doi: 10.1073/pnas.1212303109.

Decelle, Johan, Hryhoriy Stryhanyuk, Benoit Gallet, Giulia Veronesi, Matthias Schmidt, Sergio Balzano, Sophie Marro, Clarisse Uwizeye, Pierre-Henri Jouneau, Josselin Lupette, Juliette Jouhet, Eric Maréchal, Yannick Schwab, Nicole L. Schieber, Rémi Tucoulou, Hans Richnow, Giovanni Finazzi, and Niculina Musat. 2019. "Algal Remodeling in a Ubiquitous Planktonic Photosymbiosis." *Current Biology* 29(6):968-978.e4. doi: 10.1016/j.cub.2019.01.073.

Decelle, Johan, Giulia Veronesi, Charlotte LeKieffre, Benoit Gallet, Fabien Chevalier, Hryhoriy Stryhanyuk, Sophie Marro, Stéphane Ravanel, Rémi Tucoulou, Nicole Schieber, Giovanni Finazzi, Yannick Schwab, and Niculina Musat. 2021a. "Subcellular Architecture and Metabolic Connection in the Planktonic Photosymbiosis between Collodaria (Radiolarians) and Their Microalgae." *Environmental Microbiology* 1462-2920.15766. doi: 10.1111/1462-2920.15766.

Decelle, Johan, Giulia Veronesi, Charlotte LeKieffre, Benoit Gallet, Fabien Chevalier, Hryhoriy Stryhanyuk, Sophie Marro, Stéphane Ravanel, Rémi Tucoulou, Nicole Schieber, Giovanni Finazzi, Yannick Schwab, and Niculina Musat. 2021b. "Subcellular Architecture and Metabolic Connection in the Planktonic Photosymbiosis between Collodaria (Radiolarians) and Their Microalgae." *Environmental Microbiology* 23(11):6569–86. doi: 10.1111/1462-2920.15766.

Demmig-Adams, Barbara, Tyson A. Burch, Jared J. Stewart, Evan L. Savage, and William W. Adams. 2017. "Algal Glycerol Accumulation and Release as a Sink for Photosynthetic Electron Transport." *Algal Research* 21:161–68. doi: 10.1016/j.algal.2016.11.017.

Deshmukh, Rupesh K., Humira Sonah, and Richard R. Bélanger. 2016. "Plant Aquaporins: Genome-Wide Identification, Transcriptomics, Proteomics, and Advanced Analytical Tools." *Frontiers in Plant Science* 7. doi: 10.3389/fpls.2016.01896.

Díaz Hernández, Diana Patricia, and Luis Carlos Burgos Herrera. 2002. "¿Cómo se transporta la glucosa a través de la membrana celular?" *Iatreia*. doi: 10.17533/udea.iatreia.3957.

Dolan, John. 1992. "Mixotrophy in Ciliates: A Review of Chlorella Symbiosis and Chloroplast Retention." *Marine Microbial Food Webs* 6:133–53.

Dorling, M., P. J. McAuley, and H. Hodge. 1997a. "Effect of pH on Growth and Carbon Metabolism of Maltose-Releasing *Chlorella* (Chlorophyta)." *European Journal of Phycology* 32(1):19–24. doi: 10.1080/09541449710001719335.

Dorling, M., P. J. McAuley, and H. Hodge. 1997b. "Effect of pH on Growth and Carbon Metabolism of Maltose-Releasing *Chlorella* (Chlorophyta)." *European Journal of Phycology* 32(1):19–24. doi: 10.1080/09541449710001719335.

Dubinsky, Zvy, and Paul Falkowski. 2011. "Light as a Source of Information and Energy in Zooxanthellate Corals." Pp. 107–18 in *Coral Reefs: An Ecosystem in Transition*, edited by Z. Dubinsky and N. Stambler. Dordrecht: Springer Netherlands.

Dunn, Simon R., Mathieu Pernice, Kathryn Green, Ove Hoegh-Guldberg, and Sophie G. Dove. 2012. "Thermal Stress Promotes Host Mitochondrial Degradation in Symbiotic Cnidarians: Are the Batteries of the Reef Going to Run Out?" edited by M. Polymenis. *PLoS ONE* 7(7):e39024. doi: 10.1371/journal.pone.0039024.

Dziallas, Claudia, Martin Allgaier, Michael T. Monaghan, and Hans-Peter Grossart. 2012. "Act Together—Implications of Symbioses in Aquatic Ciliates." *Frontiers in Microbiology* 3. doi: 10.3389/fmicb.2012.00288.

Engel, Benjamin D., Miroslava Schaffer, Luis Kuhn Cuellar, Elizabeth Villa, Jürgen M. Plitzko, and Wolfgang Baumeister. 2015. "Native Architecture of the Chlamydomonas Chloroplast Revealed by in Situ Cryo-Electron Tomography." *eLife* 4:e04889. doi: 10.7554/eLife.04889.

Enríquez, Susana, Eugenio R. Méndez, and Roberto Iglesias -Prieto. 2005. "Multiple Scattering on Coral Skeletons Enhances Light Absorption by Symbiotic Algae." *Limnology and Oceanography* 50(4):1025–32. doi: 10.4319/lo.2005.50.4.1025.

Eom, Joon-Seob, Li-Qing Chen, Davide Sosso, Benjamin T. Julius, IW Lin, Xiao-Qing Qu, David M. Braun, and Wolf B. Frommer. 2015. "SWEETs, Transporters for Intracellular and Intercellular Sugar Translocation." *Current Opinion in Plant Biology* 25:53–62.

Falkowski, Paul G., ed. 1980. *Primary Productivity in the Sea*. Boston, MA: Springer US.

Falkowski, Paul G., Zvy Dubinsky, Leonard Muscatine, and James W. Porter. 1984. "Light and the Bioenergetics of a Symbiotic Coral." *BioScience* 34(11):705–9. doi: 10.2307/1309663.

Falkowski, Paul G., Paul L. Jokiel, and Robert A. Kinzie. 1990. "Irradiance and Corals." *Ecosystems of the World* 25:89–107.

Findinier, Justin, Sylvain Laurent, Thierry Duchêne, Xavier Roussel, Christine Lancelon-Pin, Stéphan Cuiné, Jean-Luc Putaux, Yonghua Li-Beisson, Christophe D'Hulst, Fabrice Wattebled, and David Dauvillée. 2019. "Deletion of BSG1 in Chlamydomonas Reinhardtii Leads to Abnormal

Starch Granule Size and Morphology." *Scientific Reports* 9(1):1990. doi: 10.1038/s41598-019-39506-6.

Flori, Serena, Pierre-Henri Jouneau, Benjamin Bailleul, Benoit Gallet, Leandro F. Estrozi, Christine Moriscot, Olivier Bastien, Simona Eicke, Alexander Schober, Carolina Río Bártulos, Eric Maréchal, Peter G. Kroth, Dimitris Petroutsos, Samuel Zeeman, Cécile Breyton, Guy Schoehn, Denis Falconet, and Giovanni Finazzi. 2017. "Plastid Thylakoid Architecture Optimizes Photosynthesis in Diatoms." *Nature Communications* 8(1):15885. doi: 10.1038/ncomms15885.

Foissner, Wilhelm, Helmut Berger, and Jochen Schaumburg. 1999. *Identification and Ecology of Limnetic Plankton Ciliates*. München: Bayerisches Landesamt für Wasserwirtschaft.

Fujishima, Masahiro, ed. 2009. *Endosymbionts in Paramecium*. Vol. 12. Berlin, Heidelberg: Springer Berlin Heidelberg.

Gast, Rebecca J., and David A. Caron. 2001. "Photosymbiotic Associations in Planktonic Foraminifera and Radiolaria." *Hydrobiologia* 461(1/3):1–7. doi: 10.1023/A:1012710909023.

Geddes, Patrick. 1878. "Sur La Fonction de La Chlorophylle Avec Les Planaires Vertes." *CR Séances Acad Sci Paris* 87:1095–97.

Gibbin, Emma, Guilhem Banc-Prandi, Maoz Fine, Arnaud Comment, and Anders Meibom. 2020. "A Method to Disentangle and Quantify Host Anabolic Turnover in Photosymbiotic Holobionts with Subcellular Resolution." *Communications Biology* 3(1):14. doi: 10.1038/s42003-019-0742-6.

Giovannetti, Marco, Raffaella Balestrini, Veronica Volpe, Mike Guether, Daniel Straub, Alex Costa, Uwe Ludewig, and Paola Bonfante. 2012. "Two Putative-Aquaporin Genes Are Differentially Expressed during Arbuscular Mycorrhizal Symbiosis in Lotus Japonicus." *BMC Plant Biology* 12(1):186. doi: 10.1186/1471-2229-12-186.

Glynn, Peter W. 1996. "Coral Reef Bleaching: Facts, Hypotheses and Implications." *Global Change Biology* 2(6):495–509. doi: 10.1111/j.1365-2486.1996.tb00063.x.

Gorman, D. S., and R. P. Levine. 1965. "Cytochrome f and Plastocyanin: Their Sequence in the Photosynthetic Electron Transport Chain of Chlamydomonas Reinhardi." *Proceedings of the National Academy of Sciences* 54(6):1665–69. doi: 10.1073/pnas.54.6.1665.

Graf, Alexander, and Alison M. Smith. 2011. "Starch and the Clock: The Dark Side of Plant Productivity." *Trends in Plant Science* 16(3):169–75. doi: 10.1016/j.tplants.2010.12.003.

Grajales, Alejandro, and Estefanía Rodríguez. 2014. "Morphological Revision of the Genus Aiptasia and the Family Aiptasiidae (Cnidaria, Actiniaria, Metridioidea)." *Zootaxa* 3826(1):55. doi: 10.11646/zootaxa.3826.1.2.

Grube, Martin, Joseph Seckbach, and Lucia Muggia, eds. 2017. *Algal and Cyanobacteria Symbioses*. New Jersey London Singapore Beijing Shanghai Hong Kong Taipei Chennai Tokyo: World Scientific.

Gu, Fukang, Ling Chen, Bing Ni, and Xumei Zhang. 2002. "A Comparative Study on the Electron Microscopic Enzymo-Cytochemistry of Paramecium Bursaria from Light and Dark Cultures." *European Journal of Protistology* 38(3):267–78. doi: 10.1078/0932-4739-00875.

Hamada, Mayuko, Katja Schröder, Jay Bathia, Ulrich Kürn, Sebastian Fraune, Mariia Khalturina, Konstantin Khalturin, Chuya Shinzato, Nori Satoh, and Thomas CG Bosch. 2018. "Metabolic Co-Dependence Drives the Evolutionarily Ancient Hydra–Chlorella Symbiosis" edited by P. G. Falkowski. *eLife* 7:e35122. doi: 10.7554/eLife.35122.

Hara-Chikuma, M., and A. S. Verkman. 2006. "Physiological Roles of Glycerol-Transporting Aquaporins: The Aquaglyceroporins." *Cellular and Molecular Life Sciences* 63(12):1386–92. doi: 10.1007/s00018-006-6028-4.

Hausmann, Klaus, and Richard D. Allen. 2010. "Electron Microscopy of Paramecium (Ciliata)." Pp. 143–73 in *Methods in Cell Biology*. Vol. 96. Elsevier.

He, Ming, Jinfeng Wang, Xinpeng Fan, Xiaohui Liu, Wenyu Shi, Ning Huang, Fangqing Zhao, and Miao Miao. 2019. "Genetic Basis for the Establishment of Endosymbiosis in Paramecium." *The ISME Journal* 13(5):1360–69. doi: 10.1038/s41396-018-0341-4.

He, Shan, Victoria L. Crans, and Martin C. Jonikas. 2023. "The Pyrenoid: The Eukaryotic CO2-Concentrating Organelle." *The Plant Cell* 35(9):3236–59. doi: 10.1093/plcell/koad157.

Hennion, Nils, Mickael Durand, Cécile Vriet, Joan Doidy, Laurence Maurousset, Rémi Lemoine, and Nathalie Pourtau. 2019. "Sugars En Route to the Roots. Transport, Metabolism and Storage within Plant Roots and towards Microorganisms of the Rhizosphere." *Physiologia Plantarum* 165(1):44–57.

Heymann, Jurgen A. W., Mike Hayles, Ingo Gestmann, Lucille A. Giannuzzi, Ben Lich, and Sriram Subramaniam. 2006. "Site-Specific 3D Imaging of Cells and Tissues with a Dual Beam Microscope." *Journal of Structural Biology* 155(1):63–73. doi: 10.1016/j.jsb.2006.03.006.

Hildebrand, Mark, Sang Kim, Dan Shi, Keana Scott, and Sriram Subramaniam. 2009. "3D Imaging of Diatoms with Ion-Abrasion Scanning Electron Microscopy." *Journal of Structural Biology* 166(3):316–28. doi: 10.1016/j.jsb.2009.02.014.

Hoegh-Guldberg, Ove. 1999. "Climate Change, Coral Bleaching and the Future of the World's Coral Reefs." *Marine and Freshwater Research*. doi: 10.1071/MF99078.

Hofmann, D. K., and B. P. Kremer. 1981. "Carbon Metabolism and Strobilation in Cassiopea Andromedea (Cnidaria: Scyphozoa): Significance of Endosymbiotic Dinoflagellates." *Marine Biology* 65(1):25–33. doi: 10.1007/BF00397064.

Hoshina, Ryo, and Nobutaka Imamura. 2008. "Multiple Origins of the Symbioses in Paramecium Bursaria." *Protist* 159(1):53–63. doi: 10.1016/j.protis.2007.08.002.

Hoshina, Ryo, Emi Sato, Aika Shibata, Yuko Fujiwara, Yasushi Kusuoka, and Nobutaka Imamura. 2013. "Cytological, Genetic, and Biochemical Characteristics of an Unusual non-C Hlorella Photobiont of S Tentor Polymorphus Collected from an Artificial Pond Close to the Shore of L Ake B Iwa, J Apan." *Phycological Research* 61(1):7–14.

Hoshina, Ryo, Yuuji Tsukii, Terue Harumoto, and Toshinobu Suzaki. 2021. "Characterization of a Green Stentor with Symbiotic Algae Growing in an Extremely Oligotrophic Environment and Storing Large Amounts of Starch Granules in Its Cytoplasm." *Scientific Reports* 11(1):2865. doi: 10.1038/s41598-021-82416-9.

Hughes, Terry P., Michele L. Barnes, David R. Bellwood, Joshua E. Cinner, Graeme S. Cumming, Jeremy B. C. Jackson, Joanie Kleypas, Ingrid A. Van De Leemput, Janice M. Lough, Tiffany H. Morrison, Stephen R. Palumbi, Egbert H. Van Nes, and Marten Scheffer. 2017. "Coral Reefs in the Anthropocene." *Nature* 546(7656):82–90. doi: 10.1038/nature22901.

Hughes, Terry P., James T. Kerry, Mariana Álvarez-Noriega, Jorge G. Álvarez-Romero, Kristen D. Anderson, Andrew H. Baird, Russell C. Babcock, Maria Beger, David R. Bellwood, Ray Berkelmans, Tom C. Bridge, Ian R. Butler, Maria Byrne, Neal E. Cantin, Steeve Comeau, Sean R. Connolly, Graeme S. Cumming, Steven J. Dalton, Guillermo Diaz-Pulido, C. Mark Eakin,

Will F. Figueira, James P. Gilmour, Hugo B. Harrison, Scott F. Heron, Andrew S. Hoey, Jean-Paul A. Hobbs, Mia O. Hoogenboom, Emma V. Kennedy, Chao-yang Kuo, Janice M. Lough, Ryan J. Lowe, Gang Liu, Malcolm T. McCulloch, Hamish A. Malcolm, Michael J. McWilliam, John M. Pandolfi, Rachel J. Pears, Morgan S. Pratchett, Verena Schoepf, Tristan Simpson, William J. Skirving, Brigitte Sommer, Gergely Torda, David R. Wachenfeld, Bette L. Willis, and Shaun K. Wilson. 2017. "Global Warming and Recurrent Mass Bleaching of Corals." *Nature* 543(7645):373–77. doi: 10.1038/nature21707.

Itakura, Alan K., Kher Xing Chan, Nicky Atkinson, Leif Pallesen, Lianyong Wang, Gregory Reeves, Weronika Patena, Oliver Caspari, Robyn Roth, Ursula Goodenough, Alistair J. McCormick, Howard Griffiths, and Martin C. Jonikas. 2019. "A Rubisco-Binding Protein Is Required for Normal Pyrenoid Number and Starch Sheath Morphology in *Chlamydomonas Reinhardtii*." *Proceedings of the National Academy of Sciences* 116(37):18445–54. doi: 10.1073/pnas.1904587116.

Jacobovitz, Marie R., Elizabeth A. Hambleton, and Annika Guse. 2023. "Unlocking the Complex Cell Biology of Coral–Dinoflagellate Symbiosis: A Model Systems Approach." *Annual Review of Genetics* 57(1):411–34. doi: 10.1146/annurev-genet-072320-125436.

Johnson, Matthew D. 2011. "The Acquisition of Phototrophy: Adaptive Strategies of Hosting Endosymbionts and Organelles." *Photosynthesis Research* 107(1):117–32. doi: 10.1007/s11120-010-9546-8.

Joost, H. G., Sonja Wandel, and Annette Schürmann. 2009. "Structure-Function Relationship of Glucose Transporters Catalyzing Facilitated Diffusion." *Experimental and Clinical Endocrinology & Diabetes* 102(06):434–38. doi: 10.1055/s-0029-1211315.

Jouhet, Juliette, Mie Shimojima, Koichiro Awai, and Eric Maréchal. 2022. "Editorial: Lipids in Cyanobacteria, Algae, and Plants—From Biology to Biotechnology." *Frontiers in Plant Science* 12:834384. doi: 10.3389/fpls.2021.834384.

Kadono, T., T. Kawano, H. Hosoya, and T. Kosaka. 2004. "Flow Cytometric Studies of the Host-Regulated Cell Cycle in Algae Symbiotic with Green Paramecium." *Protoplasma* 223(2–4):133–41. doi: 10.1007/s00709-004-0046-6.

Kamako, Shin-ichiro, Ryo Hoshina, Seiko Ueno, and Nobutaka Imamura. 2005. "Establishment of Axenic Endosymbiotic Strains of Japanese Paramecium Bursaria and the Utilization of Carbohydrate and Nitrogen Compounds by the Isolated Algae." *European Journal of Protistology* 41(3):193–202. doi: 10.1016/j.ejop.2005.04.001.

Karajan, Bella P., Andrey E. Vishnyakov, Marina V. Tavrovskaya, and Sergey I. Vasyanin. 2007. "Infection of Algae-Free Climacostomum Virens with Symbiotic Chlorella Sp. Isolated from Algae-Containing C. Virens." *European Journal of Protistology* 43(2):141–46. doi: 10.1016/j.ejop.2007.01.001.

Karakashian, M. W. 1975. "Symbiosis in Paramecium Bursaria." *Symposia of the Society for Experimental Biology* (29):145–73.

Karakashian, Stephen J., and Marlene W. Karakashian. 1965. "EVOLUTION AND SYMBIOSIS IN THE GENUS *CHLORELLA* AND RELATED ALGAE." *Evolution* 19(3):368–77. doi: 10.1111/j.1558-5646.1965.tb01728.x.

Kaschuk, Glaciela, Thomas W. Kuyper, Peter A. Leffelaar, Mariangela Hungria, and Ken E. Giller. 2009. "Are the Rates of Photosynthesis Stimulated by the Carbon Sink Strength of Rhizobial

and Arbuscular Mycorrhizal Symbioses?" *Soil Biology and Biochemistry* 41(6):1233–44. doi: 10.1016/j.soilbio.2009.03.005.

Katsu-Kimura, Yumiko, Fumio Nakaya, Shoji A. Baba, and Yoshihiro Mogami. 2009. "Substantial Energy Expenditure for Locomotion in Ciliates Verified by Means of Simultaneous Measurement of Oxygen Consumption Rate and Swimming Speed." *Journal of Experimental Biology* 212(12):1819–24. doi: 10.1242/jeb.028894.

Kerney, Ryan, Eunsoo Kim, Roger P. Hangarter, Aaron A. Heiss, Cory D. Bishop, and Brian K. Hall. 2011. "Intracellular Invasion of Green Algae in a Salamander Host." *Proceedings of the National Academy of Sciences* 108(16):6497–6502. doi: 10.1073/pnas.1018259108.

Kersting, Michael C., and Phillip E. Ryals. 2004. "Sodium-dependent Transport of [^{3} H](1 D) *Chiro* - Inositol by *Tetrahymena*." *Journal of Eukaryotic Microbiology* 51(3):307–11. doi: 10.1111/j.1550-7408.2004.tb00571.x.

Kessler, E., G. Kauer, and M. Rahat. 1991. "Excretion of Sugars by *Chlorella* Species Capable and Incapable of Symbiosis with *Hydra Viridis*." *Botanica Acta* 104(1):58–63. doi: 10.1111/j.1438-8677.1991.tb00194.x.

Kimball, R. F., T. O. Caspersson, G. Svensson, and L. Carlson. 1959. "Quantitative Cytochemical Studies on Paramecium Aurelia." *Experimental Cell Research* 17(1):160–72. doi: 10.1016/0014-4827(59)90161-2.

Kodama, Y., and M. Fujishima. 2016. "Differences in Infectivity between Endosymbiotic *Chlorella Variabilis* Cultivated Outside Host *Paramecium Bursaria* for 50 Years and Those Immediately Isolated from Host Cells after One Year of Reendosymbiosis." *Biology Open* 5(1):55–61. doi: 10.1242/bio.013946.

Kodama, Yuuki, and Masahiro Fujishima. 2005. "Symbiotic Chlorella Sp. of the Ciliate Paramecium Bursaria Do Not Prevent Acidification and Lysosomal Fusion of Host Digestive Vacuoles during Infection." *Protoplasma* 225(3–4):191–203. doi: 10.1007/s00709-005-0087-5.

Kodama, Yuuki, and Masahiro Fujishima. 2007. "Infectivity of Chlorella Species for the Ciliate Paramecium Bursaria Is Not Based on Sugar Residues of Their Cell Wall Components, but on Their Ability to Localize beneath the Host Cell Membrane after Escaping from the Host Digestive Vacuole in the Early Infection Process." *Protoplasma* 231(1–2):55–63. doi: 10.1007/s00709-006-0241-8.

Kodama, Yuuki, and Masahiro Fujishima. 2008. "Cycloheximide Induces Synchronous Swelling of Perialgal Vacuoles Enclosing Symbiotic Chlorella Vulgaris and Digestion of the Algae in the Ciliate Paramecium Bursaria." *Protist* 159(3):483–94. doi: transcriptom.

Kodama, Yuuki, and Masahiro Fujishima. 2012. "Cell Division and Density of Symbiotic *Chlorella Variabilis* of the Ciliate *Paramecium Bursaria* Is Controlled by the Host's Nutritional Conditions during Early Infection Process." *Environmental Microbiology* 14(10):2800–2811. doi: 10.1111/j.1462-2920.2012.02793.x.

Kodama, Yuuki, and Shoya Miyazaki. 2021. "Autolysis of Chlorella Variabilis in Starving Paramecium Bursaria Help the Host Cell Survive Against Starvation Stress." *Current Microbiology* 78(2):558–65. doi: 10.1007/s00284-020-02304-9.

Kong, Fantao, Ismael Torres Romero, Jaruswan Warakanont, and Yonghua Li-Beisson. 2018. "Lipid Catabolism in Microalgae." *New Phytologist* 218(4):1340–48. doi: 10.1111/nph.15047.

Kopp, Christophe, Isabelle Domart-Coulon, Stephane Escrig, Bruno M. Humbel, Michel Hignette, and Anders Meibom. 2015. "Subcellular Investigation of Photosynthesis-Driven Carbon Assimilation in the Symbiotic Reef Coral Pocillopora Damicornis." 6(1):9.

Krapp, Anne, and Mark Stitt. 1995. "An Evaluation of Direct and Indirect Mechanisms for the ?Sink-Regulation? Of Photosynthesis in Spinach: Changes in Gas Exchange, Carbohydrates, Metabolites, Enzyme Activities and Steady-State Transcript Levels after Cold-Girdling Source Leaves." *Planta* 195(3). doi: 10.1007/BF00202587.

Krienitz, Lothar, Volker A. R. Huss, and Christina Bock. 2015. "Chlorella: 125 Years of the Green Survivalist." *Trends in Plant Science* 20(2):67–69. doi: 10.1016/j.tplants.2014.11.005.

Krueger, Thomas, Julia Bodin, Noa Horwitz, Céline Loussert-Fonta, Adrian Sakr, Stéphane Escrig, Maoz Fine, and Anders Meibom. 2018. "Temperature and Feeding Induce Tissue Level Changes in Autotrophic and Heterotrophic Nutrient Allocation in the Coral Symbiosis – A NanoSIMS Study." *Scientific Reports* 8(1):12710. doi: 10.1038/s41598-018-31094-1.

Kuba, Jakub, John Mitchels, Miloš Hovorka, Philipp Erdmann, Lukáš Berka, Robert Kirmse, Julia König, Jan De Bock, Bernhard Goetze, and Alexander Rigort. 2021. "Advanced Cryo-tomography Workflow Developments – Correlative Microscopy, Milling Automation and Cryo-lift-out." *Journal of Microscopy* 281(2):112–24. doi: 10.1111/jmi.12939.

Kuchitsu, K., M. Tsuzuki, and S. Miyachi. 1988. "Characterization of the Pyrenoid Isolated from Unicellular Green algaChlamydomonas Reinhardtii: Particulate Form of RuBisCO Protein." *Protoplasma* 144(1):17–24. doi: 10.1007/BF01320276.

Leggat, William, Elessa M. Marendy, Brett Baillie, Spencer M. Whitney, Martha Ludwig, Murray R. Badger, and David Yellowlees. 2002. "Dinoflagellate Symbioses: Strategies and Adaptations for the Acquisition and Fixation of Inorganic Carbon." *Functional Plant Biology* 29(3):309. doi: 10.1071/PP01202.

Lehnert, Erik M., Morgan E. Mouchka, Matthew S. Burriesci, Natalya D. Gallo, Jodi A. Schwarz, and John R. Pringle. 2014. "Extensive Differences in Gene Expression Between Symbiotic and Aposymbiotic Cnidarians." *G3 Genes|Genomes|Genetics* 4(2):277–95. doi: 10.1534/g3.113.009084.

LeKieffre, Charlotte, Howard J. Spero, Ann D. Russell, Jennifer S. Fehrenbacher, Emmanuelle Geslin, and Anders Meibom. 2018. "Assimilation, Translocation, and Utilization of Carbon between Photosynthetic Symbiotic Dinoflagellates and Their Planktic Foraminifera Host." *Marine Biology* 165(6):104. doi: 10.1007/s00227-018-3362-7.

Lemonnier, Pauline, Cécile Gaillard, Florian Veillet, Jérémy Verbeke, Rémi Lemoine, Pierre Coutos-Thévenot, and Sylvain La Camera. 2014. "Expression of Arabidopsis Sugar Transport Protein STP13 Differentially Affects Glucose Transport Activity and Basal Resistance to Botrytis Cinerea." *Plant Molecular Biology* 85(4–5):473–84. doi: 10.1007/s11103-014-0198-5.

León-Saiki, G. Mitsue, Ilse M. Remmers, Dirk E. Martens, Packo P. Lamers, René H. Wijffels, and Douwe van der Veen. 2017. "The Role of Starch as Transient Energy Buffer in Synchronized Microalgal Growth in Acutodesmus Obliquus." *Algal Research* 25:160–67. doi: 10.1016/j.algal.2017.05.018.

Lizák, Beáta, András Szarka, Yejin Kim, Kyu-sung Choi, Csilla E. Németh, Paola Marcolongo, Angelo Benedetti, Gábor Bánhegyi, and Éva Margittai. 2019. "Glucose Transport and Transporters in

the Endomembranes." *International Journal of Molecular Sciences* 20(23):5898. doi: 10.3390/ijms20235898.

López-García, Purificación, Laura Eme, and David Moreira. 2017. "Symbiosis in Eukaryotic Evolution." *Journal of Theoretical Biology* 434:20–33. doi: 10.1016/j.jtbi.2017.02.031.

Lowe, Christopher D., Ewan J. Minter, Duncan D. Cameron, and Michael A. Brockhurst. 2016. "Shining a Light on Exploitative Host Control in a Photosynthetic Endosymbiosis." *Current Biology* 26(2):207–11. doi: 10.1016/j.cub.2015.11.052.

Manck-Götzenberger, Jasmin, and Natalia Requena. 2016. "Arbuscular Mycorrhiza Symbiosis Induces a Major Transcriptional Reprogramming of the Potato SWEET Sugar Transporter Family." *Frontiers in Plant Science* 7. doi: 10.3389/fpls.2016.00487.

Maor-Landaw, Keren, Marion Eisenhut, Giada Tortorelli, Allison Van De Meene, Samantha Kurz, Gabriela Segal, Madeleine J. H. Van Oppen, Andreas P. M. Weber, and Geoffrey I. McFadden. 2023. "A Candidate Transporter Allowing Symbiotic Dinoflagellates to Feed Their Coral Hosts." *ISME Communications* 3(1):7. doi: 10.1038/s43705-023-00218-8.

Margulis, L. 1996. "Archaeal-Eubacterial Mergers in the Origin of Eukarya: Phylogenetic Classification of Life." *Proceedings of the National Academy of Sciences* 93(3):1071–76. doi: 10.1073/pnas.93.3.1071.

Margulis, L., and D. Sagan. 2008. *Acquiring Genomes: A Theory Of The Origin Of Species*. Basic Books.

Margulis, Lynn. 1998. "Symbiotic Planet: A New Look of Evolution."

Mashini, Amirhossein Gheitanchi, Clinton A. Oakley, Arthur R. Grossman, Virginia M. Weis, and Simon K. Davy. 2022. "Immunolocalization of Metabolite Transporter Proteins in a Model Cnidarian-Dinoflagellate Symbiosis" edited by L. Villanueva. *Applied and Environmental Microbiology* 88(12):e00412-22. doi: 10.1128/aem.00412-22.

Matsuzaki, Motomichi, Osami Misumi, Tadasu Shin-i, Shinichiro Maruyama, Manabu Takahara, Shin-ya Miyagishima, Toshiyuki Mori, Keiji Nishida, Fumi Yagisawa, Keishin Nishida, Yamato Yoshida, Yoshiki Nishimura, Shunsuke Nakao, Tamaki Kobayashi, Yu Momoyama, Tetsuya Higashiyama, Ayumi Minoda, Masako Sano, Hisayo Nomoto, Kazuko Oishi, Hiroko Hayashi, Fumiko Ohta, Satoko Nishizaka, Shinobu Haga, Sachiko Miura, Tomomi Morishita, Yukihiro Kabeya, Kimihiro Terasawa, Yutaka Suzuki, Yasuyuki Ishii, Shuichi Asakawa, Hiroyoshi Takano, Niji Ohta, Haruko Kuroiwa, Kan Tanaka, Nobuyoshi Shimizu, Sumio Sugano, Naoki Sato, Hisayoshi Nozaki, Naotake Ogasawara, Yuji Kohara, and Tsuneyoshi Kuroiwa. 2004. "Genome Sequence of the Ultrasmall Unicellular Red Alga Cyanidioschyzon Merolae 10D." *Nature* 428(6983):653–57. doi: 10.1038/nature02398.

Matthews, Jennifer L., Clinton A. Oakley, Adrian Lutz, Katie E. Hillyer, Ute Roessner, Arthur R. Grossman, Virginia M. Weis, and Simon K. Davy. 2018. "Partner Switching and Metabolic Flux in a Model Cnidarian–Dinoflagellate Symbiosis." *Proceedings of the Royal Society B: Biological Sciences* 285(1892):20182336. doi: 10.1098/rspb.2018.2336.

Matzke, Bettina, Elisabeth Schwarzmeier, and Eckhard Loos. 1990. "Maltose Excretion by the Symbiotic Chlorella of the Heliozoan Acanthocystis Turfacea." *Planta* 181(4):593–98.

McAuley, P. J. 1986. "Glucose Uptake by Symbiotic Chlorella in the Green-Hydra Symbiosis." *Planta* 168(4):523–29. doi: 10.1007/BF00392272.

McDonald, Kent L., and Manfred Auer. 2006. "High-Pressure Freezing, Cellular Tomography, and Structural Cell Biology." *BioTechniques* 41(2):137–43. doi: 10.2144/000112226.

McKenna, Victoria, John M. Archibald, Roxanne Beinart, Michael N. Dawson, Ute Hentschel, Patrick J. Keeling, Jose V. Lopez, José M. Martín-Durán, Jillian M. Petersen, Julia D. Sigwart, Oleg Simakov, Kelly R. Sutherland, Michael Sweet, Nick Talbot, Anne W. Thompson, Sara Bender, Peter W. Harrison, Jeena Rajan, Guy Cochrane, Matthew Berriman, Mara K. N. Lawniczak, and Mark Blaxter. 2021. "The Aquatic Symbiosis Genomics Project: Probing the Evolution of Symbiosis across the Tree of Life." *Wellcome Open Research* 6:254. doi: 10.12688/wellcomeopenres.17222.1.

Metz, Sebastian, David Singer, Isabelle Domaizon, Fernando Unrein, and Enrique Lara. 2019. "Global Distribution of Trebouxiophyceae Diversity Explored by High-throughput Sequencing and Phylogenetic Approaches." *Environmental Microbiology* 21(10):3885–95. doi: 10.1111/1462-2920.14738.

Meyer, Moritz T., Charles Whittaker, and Howard Griffiths. 2017. "The Algal Pyrenoid: Key Unanswered Questions." *Journal of Experimental Botany* 68(14):3739–49. doi: 10.1093/jxb/erx178.

Mohd Noor, Siti N., David A. Day, and Penelope M. Smith. 2015. "The Symbiosome Membrane." Pp. 683–94 in *Biological Nitrogen Fixation*, edited by F. J. De Bruijn. Wiley.

Moog, Daniel, Stefan A. Rensing, John M. Archibald, Uwe G. Maier, and Kristian K. Ullrich. 2015. "Localization and Evolution of Putative Triose Phosphate Translocators in the Diatom *Phaeodactylum Tricornutum*." *Genome Biology and Evolution* 7(11):2955–69. doi: 10.1093/gbe/evv190.

Moor, Hans. 1987. "Theory and Practice of High Pressure Freezing." Pp. 175–91 in *Cryotechniques in Biological Electron Microscopy*, edited by R. A. Steinbrecht and K. Zierold. Berlin, Heidelberg: Springer Berlin Heidelberg.

Moreira, David, Hervé Le Guyader, and Hervé Philippe. 2000. "The Origin of Red Algae and the Evolution of Chloroplasts." *Nature* 405(6782):69–72. doi: 10.1038/35011054.

Możdżeń, Katarzyna, Patrycja Z. Leśnicka, Tomasz Burnecki, Sylwia Śliwińska-Wilczewska, Andrzej Skoczowski, and Magdalena Greczek-Stachura. 2018. "Photosynthetic Efficiency of Endosymbiotic Algae of *Paramecium Bursaria* Originating from Locations with Cold and Warm Climates." *Oceanological and Hydrobiological Studies* 47(2):202–10. doi: 10.1515/ohs-2018-0019.

Muller-Parker, Gisèle, Kit W. Lee, and Clayton B. Cook. 1996. "CHANGES IN THE ULTRASTRUCTURE OF SYMBIOTIC ZOOXANTHELLAE (*SYMBIODINIUM* SP., DINOPHYCEAE) IN FED AND STARVED SEA ANEMONES MAINTAINED UNDER HIGH AND LOW LIGHT [1]." *Journal of Phycology* 32(6):987–94. doi: 10.1111/j.0022-3646.1996.00987.x.

Muscatine, L. 1990. "The Role of Symbiotic Algae in Carbon and Energy Flux in Reef Corals." *Coral Reefs*.

Muscatine, Leonard, Stephen J. Karakashian, and Marlene W. Karakashian. 1967. "Soluble Extracellular Products of Algae Symbiotic with a Ciliate, a Sponge and a Mutant Hydra." *Comparative Biochemistry and Physiology* 20(1):1–12. doi: 10.1016/0010-406X(67)90720-7.

Narayan, Kedar, and Sriram Subramaniam. 2015. "Focused Ion Beams in Biology." *Nature Methods* 12(11):1021–31. doi: 10.1038/nmeth.3623.

Niittylä, Totte, Gaëlle Messerli, Martine Trevisan, Jychian Chen, Alison M. Smith, and Samuel C. Zeeman. 2004. "A Previously Unknown Maltose Transporter Essential for Starch Degradation in Leaves." *Science* 303(5654):87–89. doi: 10.1126/science.1091811.

Nitschke, Matthew R., Sabrina L. Rosset, Clinton A. Oakley, Stephanie G. Gardner, Emma F. Camp, David J. Suggett, and Simon K. Davy. 2022. "The Diversity and Ecology of Symbiodiniaceae: A Traits-Based Review." Pp. 55–127 in *Advances in Marine Biology*. Vol. 92. Elsevier.

Nowack, Eva C. M., and Michael Melkonian. 2010. "Endosymbiotic Associations within Protists." *Philosophical Transactions of the Royal Society B: Biological Sciences* 365(1541):699–712. doi: 10.1098/rstb.2009.0188.

Ogura, Atsushi, Ryuhei Minei, Ryo Hoshina, Rina Higuchi, Lin Chen, Yuki Akizuki, Yasunobu Terabayashi, Satoshi Kira, Masanari Kitagawa, and Toshinobu Suzaki. 2022. *Multi-Omics Analysis of the Symbiotic Green Algae, Chlorella Variabilis, Revealing the Genetic Basis of the Obligate Endosymbiotic Lifestyle*. *preprint*. In Review. doi: 10.21203/rs.3.rs-713024/v2.

Ozcan, S. 1998. "Glucose Sensing and Signaling by Two Glucose Receptors in the Yeast Saccharomyces Cerevisiae." *The EMBO Journal* 17(9):2566–73. doi: 10.1093/emboj/17.9.2566.

Picelli, Simone, Omid R. Faridani, Åsa K. Björklund, Gösta Winberg, Sven Sagasser, and Rickard Sandberg. 2014. "Full-Length RNA-Seq from Single Cells Using Smart-Seq2." *Nature Protocols* 9(1):171–81. doi: 10.1038/nprot.2014.006.

Pröschold, Thomas, Tatyana Darienko, Paul C. Silva, Werner Reisser, and Lothar Krienitz. 2011. "The Systematics of Zoochlorella Revisited Employing an Integrative Approach." *Environmental Microbiology* 13(2):350–64. doi: 10.1111/j.1462-2920.2010.02333.x.

Puerta, M. V. S. 2004. "The Complete Mitochondrial Genome Sequence of the Haptophyte Emiliania Huxleyi and Its Relation to Heterokonts (Supplement)." *DNA Research* 11(1):67–68. doi: 10.1093/dnares/11.1.67.

Queimalinos, C. 1999. "Symbiotic Association of the Ciliate Ophrydium Naumanni with Chlorella Causing a Deep Chlorophyll a Maximum in an Oligotrophic South Andes Lake." *Journal of Plankton Research* 21(1):167–78. doi: 10.1093/plankt/21.1.167.

Quevarec, Loïc, Gaël Brasseur, Denise Aragnol, and Christophe Robaglia. 2023. "Tracking the Early Events of Photosymbiosis Evolution." *Trends in Plant Science* S1360138523003643. doi: 10.1016/j.tplants.2023.11.005.

Quispe, Cristian F., Olivia Sonderman, Maya Khasin, Wayne R. Riekhof, James L. Van Etten, and Kenneth W. Nickerson. 2016. "Comparative Genomics, Transcriptomics, and Physiology Distinguish Symbiotic from Free-Living Chlorella Strains." *Algal Research* 18:332–40. doi: 10.1016/j.algal.2016.06.001.

Rajević, Nives, Goran Kovačević, Mirjana Kalafatić, Sven B. Gould, William F. Martin, and Damjan Franjević. 2015. "Algal Endosymbionts in European Hydra Strains Reflect Multiple Origins of the Zoochlorella Symbiosis." *Molecular Phylogenetics and Evolution* 93:55–62. doi: 10.1016/j.ympev.2015.07.014.

Ran, Wenyi, Haitao Wang, Yinghui Liu, Man Qi, Qi Xiang, Changhong Yao, Yongkui Zhang, and Xianqiu Lan. 2019. "Storage of Starch and Lipids in Microalgae: Biosynthesis and Manipulation by Nutrients." *Bioresource Technology* 291:121894. doi: 10.1016/j.biortech.2019.121894.

Rautian, Maria S., and Alexey A. Potekhin. 2002. "Electrokaryotypes of Macronuclei of Several *Paramecium* Species." *Journal of Eukaryotic Microbiology* 49(4):296–304. doi: 10.1111/j.1550-7408.2002.tb00372.x.

Reisser, W., and W. Wiessner. 1984. "Autotrophic Eukaryotic Freshwater Symbionts." Pp. 59–74 in *Cellular Interactions*, edited by H. F. Linskens and J. Heslop-Harrison. Berlin, Heidelberg: Springer Berlin Heidelberg.

Reisser, Werner. 1980. "The Metabolic Interactions Between Paramecium Bursaria Ehrbg. and Chlorella Spec. in the Paramecium Bursaria-Symbiosis." 3.

Roberty, Stéphane, Virginia M. Weis, Simon K. Davy, and Christian R. Voolstra. 2024. "Editorial: Aiptasia: A Model System in Coral Symbiosis Research." *Frontiers in Marine Science* 11:1370814. doi: 10.3389/fmars.2024.1370814.

Rohde, Klaus, ed. 2005. *Marine Parasitology*. CSIRO Publishing.

Sanders, William B. 2001. "Lichens: The Interface between Mycology and Plant Morphology." *BioScience* 51(12):1025. doi: 10.1641/0006-3568(2001)051[1025:LTIBMA]2.0.CO;2.

Sapp, Jan. 2004. "The Dynamics of Symbiosis: An Historical Overview." 82:11.

SchluBler, A., and E. Schnepf. 1992. "Photosynthesis Dependent Acidification of Perialgal Vacuoles in theParamedum Bursaria/Chlorella Symbiosis: Visualization by Monensin." *Protoplasma* 166(3–4):218–22. doi: 10.1007/BF01322784.

Schneider, Sabine, Alexander Schneidereit, Patrick Udvardi, Ulrich Hammes, Monika Gramann, Petra Dietrich, and Norbert Sauer. 2007. "Arabidopsis INOSITOL TRANSPORTER2 Mediates H^+ Symport of Different Inositol Epimers and Derivatives across the Plasma Membrane." *Plant Physiology* 145(4):1395–1407. doi: 10.1104/pp.107.109033.

Schüßler, Arthur, and E. Schnepf. 1992. "Photosynthesis Dependent Acidification of Perialgal Vacuoles in the Paramedum Bursaria/Chlorella Symbiosis: Visualization by Monensin." *Protoplasma* 166:218–22.

Shaked, Y., and C. De Vargas. 2006. "Pelagic Photosymbiosis: rDNA Assessment of Diversity and Evolution of Dinoflagellate Symbionts and Planktonic Foraminiferal Hosts." *Marine Ecology Progress Series* 325:59–71. doi: 10.3354/meps325059.

Shibata, Aika, Fumio Takahashi, Nobutaka Imamura, and Masahiro Kasahara. 2021. "Characteristics of Maltose Transport System in the Endosymbiont *Chlorella Variabilis* of *Paramecium Bursaria*." *Phycological Research* pre.12461. doi: 10.1111/pre.12461.

Skelton, James, and Mac Strand. 2013. "Trophic Ecology of a Freshwater Sponge (Spongilla Lacustris) Revealed by Stable Isotope Analysis." *Hydrobiologia* 709(1):227–35. doi: 10.1007/s10750-013-1452-6.

Song, Chihong, Kazuyoshi Murata, and Toshinobu Suzaki. 2017. "Intracellular Symbiosis of Algae with Possible Involvement of Mitochondrial Dynamics." *Scientific Reports* 7(1):1–11. doi: 10.1038/s41598-017-01331-0.

Sørensen, Megan E. S., A. Jamie Wood, Ewan J. A. Minter, Chris D. Lowe, Duncan D. Cameron, and Michael A. Brockhurst. 2020. "Comparison of Independent Evolutionary Origins Reveals Both Convergence and Divergence in the Metabolic Mechanisms of Symbiosis." *Current Biology* 30(2):328-334.e4. doi: 10.1016/j.cub.2019.11.053.

Spanner, Christian, Tatyana Darienko, Sabine Filker, Bettina Sonntag, and Thomas Pröschold. 2022. "Morphological Diversity and Molecular Phylogeny of Five Paramecium Bursaria (Alveolata,

Ciliophora, Oligohymenophorea) Syngens and the Identification of Their Green Algal Endosymbionts." *Scientific Reports* 12(1):18089. doi: 10.1038/s41598-022-22284-z.

Sproles, Ashley E., Nathan L. Kirk, Sheila A. Kitchen, Clinton A. Oakley, Arthur R. Grossman, Virginia M. Weis, and Simon K. Davy. 2018. "Phylogenetic Characterization of Transporter Proteins in the Cnidarian-Dinoflagellate Symbiosis." *Molecular Phylogenetics and Evolution* 120:307–20. doi: 10.1016/j.ympev.2017.12.007.

Sproles, Ashley E., Clinton A. Oakley, Thomas Krueger, Arthur R. Grossman, Virginia M. Weis, Anders Meibom, and Simon K. Davy. 2020. "Sub-cellular Imaging Shows Reduced Photosynthetic Carbon and Increased Nitrogen Assimilation by the Non-native Endosymbiont *Durusdinium Trenchii* in the Model Cnidarian Aiptasia." *Environmental Microbiology* 22(9):3741–53. doi: 10.1111/1462-2920.15142.

Stibitz, Thomas B., Patrick J. Keeling, and Debashish Bhattacharya. 2000. "Symbiotic Origin of a Novel Actin Gene in the Cryptophyte Pyrenomonas Helgolandii." *Molecular Biology and Evolution* 17(11):1731–38. doi: 10.1093/oxfordjournals.molbev.a026271.

Stoecker, Dk, Md Johnson, C. deVargas, and F. Not. 2009. "Acquired Phototrophy in Aquatic Protists." *Aquatic Microbial Ecology* 57:279–310. doi: 10.3354/ame01340.

Sueoka, N. 1960. "MITOTIC REPLICATION OF DEOXYRIBONUCLEIC ACID IN CHLAMYDOMONAS REINHARDI." *Proceedings of the National Academy of Sciences* 46(1):83–91. doi: 10.1073/pnas.46.1.83.

Sugiyama, Akifumi, Yuka Saida, Mayuko Yoshimizu, Kojiro Takanashi, Davide Sosso, Wolf B. Frommer, and Kazufumi Yazaki. 2017. "Molecular Characterization of LjSWEET3, a Sugar Transporter in Nodules of Lotus Japonicus." *Plant and Cell Physiology* 58(2):298–306.

Sukumaran, Swapna Thacheril, and Keerthi. TR Keerthi., eds. 2023. *Conservation and Sustainable Utilization of Bioresources*. Singapore: Springer.

Takahashi, Toshiyuki. 2016. "Simultaneous Evaluation of Life Cycle Dynamics between a Host Paramecium and the Endosymbionts of Paramecium Bursaria Using Capillary Flow Cytometry." *Scientific Reports* 6(1):31638. doi: 10.1038/srep31638.

Takahashi, Toshiyuki. 2017. "Life Cycle Analysis of Endosymbiotic Algae in an Endosymbiotic Situation with Paramecium Bursaria Using Capillary Flow Cytometry." *Energies* 10(9):1413. doi: 10.3390/en10091413.

Takeda, Hiroshi, Tamami Sekiguchi, Sumi Nunokawa, and Itaru Usuki. 1998. "Species-Specificity of Chlorella for Establishment of Symbiotic Association with Paramecium Bursaria — Does Infectivity Depend upon Sugar Components of the Cell Wall?" *European Journal of Protistology* 34(2):133–37. doi: 10.1016/S0932-4739(98)80023-0.

Tanaka, Miho, Maki Murata-Hori, Takashi Kadono, Takashi Yamada, Toshikazu Kosaka, and Hiroshi Hosoya. 2002. "Complete Elimination of Endosymbiotic Algae from Paramecium Bursaria and Its Confirmation by Diagnostic PCR."

Tanner, Widmar. 2000. "The Chlorella Hexose/H+-Symporters." Pp. 101–41 in *International Review of Cytology*. Vol. 200. Elsevier.

Theodoris, G., N. M. Fong, D. M. Coons, and L. F. Bisson. 1994. "High-Copy Suppression of Glucose Transport Defects by HXT4 and Regulatory Elements in the Promoters of the HXT Genes in Saccharomyces Cerevisiae." *Genetics* 137(4):957–66. doi: 10.1093/genetics/137.4.957.

Thorens, Bernard, and Mike Mueckler. 2010. "Glucose Transporters in the 21st Century." *American Journal of Physiology-Endocrinology and Metabolism* 298(2):E141–45. doi: 10.1152/ajpendo.00712.2009.

Thrall, Peter H., Michael E. Hochberg, Jeremy J. Burdon, and James D. Bever. 2007. "Coevolution of Symbiotic Mutualists and Parasites in a Community Context." *Trends in Ecology & Evolution* 22(3):120–26. doi: 10.1016/j.tree.2006.11.007.

Titlyanov, E. A., T. V. Titlyanova, K. Yamazato, and R. Van Woesik. 2001. "Photo-Acclimation Dynamics of the Coral Stylophora Pistillata to Low and Extremely Low Light." *Journal of Experimental Marine Biology and Ecology* 263(2):211–25. doi: 10.1016/S0022-0981(01)00309-4.

Toyokawa, Chihana, Takashi Yamano, and Hideya Fukuzawa. 2020. "Pyrenoid Starch Sheath Is Required for LCIB Localization and the CO_2-Concentrating Mechanism in Green Algae." *Plant Physiology* 182(4):1883–93. doi: 10.1104/pp.19.01587.

Tresguerres, Martin. 2016. "Novel and Potential Physiological Roles of Vacuolar-Type H+-ATPase in Marine Organisms." *Journal of Experimental Biology* 219(14):2088–97. doi: 10.1242/jeb.128389.

Uwizeye, Clarisse. 2021. "Cytoklepty in the Plankton: A Host Strategy to Optimize the Bioenergetic Machinery of Endosymbiotic Algae." 37.

Uwizeye, Clarisse, Johan Decelle, Pierre-Henri Jouneau, Serena Flori, Benoit Gallet, Jean-Baptiste Keck, Davide Dal Bo, Christine Moriscot, Claire Seydoux, Fabien Chevalier, Nicole L. Schieber, Rachel Templin, Guillaume Allorent, Florence Courtois, Gilles Curien, Yannick Schwab, Guy Schoehn, Samuel C. Zeeman, Denis Falconet, and Giovanni Finazzi. 2021. "Morphological Bases of Phytoplankton Energy Management and Physiological Responses Unveiled by 3D Subcellular Imaging." *Nature Communications* 12(1):1049. doi: 10.1038/s41467-021-21314-0.

Uwizeye, Clarisse, Johan Decelle, Pierre-Henri Jouneau, Benoit Gallet, Jean-Baptiste Keck, Christine Moriscot, Fabien Chevalier, Nicole L. Schieber, Rachel Templin, Gilles Curien, Yannick Schwab, Guy Schoehn, Samuel C. Zeeman, Denis Falconet, and Giovanni Finazzi. 2020. *In-Cell Quantitative Structural Imaging of Phytoplankton Using 3D Electron Microscopy*. *preprint*. Plant Biology. doi: 10.1101/2020.05.19.104166.

Valentine, Megan S., and Judith Van Houten. 2022. "Ion Channels of Cilia: *Paramecium* as a Model." *Journal of Eukaryotic Microbiology* 69(5):e12884. doi: 10.1111/jeu.12884.

Vander Heiden, Matthew G., Lewis C. Cantley, and Craig B. Thompson. 2009. "Understanding the Warburg Effect: The Metabolic Requirements of Cell Proliferation." *Science* 324(5930):1029–33.

Wang, J. T., and A. E. Douglas. 1997. "Nutrients, Signals, and Photosynthate Release by Symbiotic Algae (The Impact of Taurine on the Dinoflagellate Alga Symbiodinium from the Sea Anemone Aiptasia Pulchella)." *Plant Physiology* 114(2):631–36. doi: 10.1104/pp.114.2.631.

Wang, Yongqin, Yuguo Xiao, Yu Zhang, Chenglin Chai, Gang Wei, Xiaoli Wei, Honglin Xu, Mei Wang, Pieter B. F. Ouwerkerk, and Zhen Zhu. 2008. "Molecular Cloning, Functional Characterization and Expression Analysis of a Novel Monosaccharide Transporter Gene OsMST6 from Rice (Oryza Sativa L.)." *Planta* 228(4):525–35. doi: 10.1007/s00425-008-0755-8.

Wangpraseurt, Daniel, Anthony W. D. Larkum, Peter J. Ralph, and Michael Kühl. 2012. "Light Gradients and Optical Microniches in Coral Tissues." *Frontiers in Microbiology* 3. doi: 10.3389/fmicb.2012.00316.

Wangpraseurt, Daniel, Lubos Polerecky, Anthony W. D. Larkum, Peter J. Ralph, Daniel A. Nielsen, Mathieu Pernice, and Michael Kühl. 2014. "The in Situ Light Microenvironment of Corals." *Limnology and Oceanography* 59(3):917–26. doi: 10.4319/lo.2014.59.3.0917.

Wangpraseurt, Daniel, Miriam Weber, Hans Røy, Lubos Polerecky, Dirk De Beer, Suharsono, and Maggy M. Nugues. 2012. "In Situ Oxygen Dynamics in Coral-Algal Interactions" edited by S. J. Goldstien. *PLoS ONE* 7(2):e31192. doi: 10.1371/journal.pone.0031192.

Weber, Andreas P. M., and Nicole Linka. 2011. "Connecting the Plastid: Transporters of the Plastid Envelope and Their Role in Linking Plastidial with Cytosolic Metabolism." *Annual Review of Plant Biology* 62(1):53–77. doi: 10.1146/annurev-arplant-042110-103903.

Wolfowicz, Iliona, Sebastian Baumgarten, Philipp A. Voss, Elizabeth A. Hambleton, Christian R. Voolstra, Masayuki Hatta, and Annika Guse. 2016. "Aiptasia Sp. Larvae as a Model to Reveal Mechanisms of Symbiont Selection in Cnidarians." *Scientific Reports* 6(1):32366. doi: 10.1038/srep32366.

Wong, Poh Ying, Yuen Hing Lai, Soopna Puspanadan, Rozi Nuraika Ramli, Vuanghao Lim, and Chee Keong Lee. 2019. "Extraction of Starch from Marine Microalgae, Chlorella Salina: Efficiency and Recovery." *International Journal of Environmental Research* 13(2):283–93. doi: 10.1007/s41742-019-00173-0.

Wykoff, Dennis D., and Erin K. O'Shea. 2001. "Phosphate Transport and Sensing in *Saccharomyces Cerevisiae*." *Genetics* 159(4):1491–99. doi: 10.1093/genetics/159.4.1491.

Yee, Daniel P., Ty J. Samo, Raffaela M. Abbriano, Bethany Shimasaki, Maria Vernet, Xavier Mayali, Peter K. Weber, B. Greg Mitchell, Mark Hildebrand, Johan Decelle, and Martin Tresguerres. 2023. "The V-Type ATPase Enhances Photosynthesis in Marine Phytoplankton and Further Links Phagocytosis to Symbiogenesis." *Current Biology* 33(12):2541-2547.e5. doi: 10.1016/j.cub.2023.05.020.

Yellowlees, David, T. Alwyn V. Rees, and William Leggat. 2008. "Metabolic Interactions between Algal Symbionts and Invertebrate Hosts." *Plant, Cell & Environment* 31(5):679–94. doi: 10.1111/j.1365-3040.2008.01802.x.

Zhao, Jingjing, Xiaoping Yu, Xuping Shentu, and Danting Li. 2024. "The Application and Development of Electron Microscopy for Three-Dimensional Reconstruction in Life Science: A Review." *Cell and Tissue Research*. doi: 10.1007/s00441-024-03878-7.

Ziesenisz, Egmont, Werner Reisser, and Wolfgang Wiessner. 1981. "Evidence of de Novo Synthesis of Maltose Excreted by the Endosymbiotic Chlorella from Paramecium Bursaria." *Planta* 153(5):481–85. doi: 10.1007/BF00394991.

Zimorski, Verena, Chuan Ku, William F. Martin, and Sven B. Gould. 2014. "Endosymbiotic Theory for Organelle Origins." *Current Opinion in Microbiology* 22:38–48. doi: 10.1016/j.mib.2014.09.008.